INFORMATION TO USERS

This manuscript has been reproduced from the microfilm master. UMI films the text directly from the original or copy submitted. Thus, some thesis and dissertation copies are in typewriter face, while others may be from any type of computer printer.

The quality of this reproduction is dependent upon the quality of the copy submitted. Broken or indistinct print, colored or poor quality illustrations and photographs, print bleedthrough, substandard margins, and improper alignment can adversely affect reproduction.

In the unlikely event that the author did not send UMI a complete manuscript and there are missing pages, these will be noted. Also, if unauthorized copyright material had to be removed, a note will indicate the deletion.

Oversize materials (e.g., maps, drawings, charts) are reproduced by sectioning the original, beginning at the upper left-hand corner and continuing from left to right in equal sections with small overlaps. Each original is also photographed in one exposure and is included in reduced form at the back of the book.

Photographs included in the original manuscript have been reproduced xerographically in this copy. Higher quality 6" x 9" black and white photographic prints are available for any photographs or illustrations appearing in this copy for an additional charge. Contact UMI directly to order.

UMI

A Bell & Howell Information Company
300 North Zeeb Road, Ann Arbor MI 48106-1346 USA
313/761-4700 800/521-0600

Theoretical and Experimental Investigations of Dynamic Automatic Gain Control in Multi-Channel EDFA Cascades and its Implication on WDM Multi-Access Lightwave Networks Performance

by

Gengxian Luo

A dissertation submitted to the Graduate Faculty in Engineering in partial fulfillment of the requirements for the degree of Doctor of Philosophy, The City University of New York.

1997

This manuscript has been read and accepted for the Graduate Faculty in Engineering in satisfaction of the dissertation requirement for the degree of Doctor of Philosophy.

06/10/97
Data

Chair of Examining Committee - Prof. Mohamed A. Ali

6/16/97
Data

Executive Officer - Prof. Gerard G. Lowen

Prof. Samir A. Ahmed

Prof. Ibrahim W. Habib

Prof. Leonid Roytman

Dr. Jonathan Nagel

Dr. John L. Zyskind

Supervisory Committee

THE CITY UNIVERSITY OF NEW YORK

The City University of New York

ABSTRACT

Theoretical and Experimental Investigations of Dynamic Automatic Gain Control in Multi-Channel EDFA Cascades and its Implication on WDM Multi-Access Lightwave Networks Performance

By: Gengxian Luo

Thesis mentor: Prof. Mohamed A. Ali

This thesis presents a detailed experimental and theoretical analysis of gain dynamics of an all-optically stabilized multi-channel EDFA and the impact on WDM networks performances. Specifically, this thesis analyzes and examines the critical factors such as, lasing wavelength, amplifier operating point, gain recovery time, relaxation oscillation frequency of the feedback loop, cavity structure, cavity length and losses, signal(s) and laser power, lasing direction, switching speeds, and the number of channels dropped/added, that affect the transient power excursions in the surviving channel. We show that any degradation at the first EDFA has a cumulative effect at the output of all subsequent EDFA's in the chain. This has the important implication that the length of the chain is a function of the design parameters of the first EDFA in the chain.

The main objective of this work is to protect surviving channels against such impairments, by minimizing the impact of variations in the number of wavelength channels in operation, and of rapid changes in their signal power levels. The basic requirement is that the quality of service for any given channel passing through an optical amplifier shall not be adversely impacted by anything that happens to any of other channels passing through the same amplifier. This requirement applies both to amplifiers in WDM repeaters network elements, and to amplifiers included in other network elements. We will consider means of adjusting the flattened-gain amplifier's total output power to maintain constant per-channel output power with a minimally degraded SNR, regardless of the number of channels present. This will require that the amplifier's control system be aware of the number of channels present. This information could be passed on a telemetry channel or derived through measurement at the amplifier.

This thesis is divided into two overlapping phases, experimental and theoretical. First, we consider the applicability of laser automatic gain control (AGC) to control fast power transients in WDM optical networks and reports the first high resolution measurements of transients in such gain controlled EDFA's. Second, we will implement a dynamic simulation tool for modeling the behavior of single amplifier and amplifier chains, with and without stabilization. We will develop an approximate rate equation model for a homogeneously broadened 3-level multi-excited-mode laser system, where relaxation-oscillations characteristic parameters,

i.e., threshold pumping rate, pumping factor, damping rate, and oscillation frequency will be derived based on 4-level laser system model. The experimental results are then compared with those predicted using the dynamic simulation tool.

We will show the degradations imposed by each of these factors on the transient power excursions of the surviving channel and explore the limitations that any of these degradations can impose on the stabilization techniques.

We will devise, compare, and demonstrate several active techniques, such as, link control, pump control, and a passive all-optical gain control technique, for stabilizing the per-channel output power both for single amplifier and cascades of amplifiers. Our primary concern and focus will be on the passive technique, since, as this thesis will show, this technique is simple, inexpensive, and robust, requiring neither monitoring of the amplifier output nor any active feedback.

The overall objective is to investigate numerically and experimentally the optimum configuration of an EDFA with laser AGC for WDM applications as a function of all the relevant performance parameters such as, lasing wavelength, amplifier operating point, cavity length and losses, power, and laser propagation directions. We will devise and examine several different approaches to reduce and/or eliminate the spiking amplitudes associated with relaxation-oscillations.

Another critical performance criterion is to ensure sufficient gain flatness to permit amplifiers to be cascaded while maintaining acceptable inter channel power

variations and signal-to-noise ratios at all wavelengths. Since gain flatness depends on the signal input power levels, stabilizing the amplifier gain is a must. What is needed is a multi-channel equalized and stabilized gain amplifier.

Acknowledgments

I would like to express cordial thanks to my mentor Prof. Mohamed A. Ali for his allowing me to conduct my thesis at Bell Labs, continuous encouragement, thesis advice, financial support, and understandings during my pursuing degree.

I sincerely acknowledge my mentors Drs. John L. Zyskind and Jim W. Sulhoff of Bell Labs for accepting me to work in their group, direct thesis advice, financial support, a long time understanding and patient, a wealth of helpful, stimulating, and fruitful discussions.

I am greatly indebted to Dr. Jonathan Nagel of AT&T Labs-research for many helpful discussions and assistance in computer simulation, to Drs. Yan Sun and Atul K. Srivastava of Bell Labs for many helpful discussions, to Drs. Robert Jopson and Jerry Chen of Bell Labs for their a lot of help and suggestions during my stay in Bell Labs/Crawford Hill Laboratory, and to Dwight Richards for his assistance in computer simulation.

I am also very grateful to a lot of my friends, Guobao Zheng, Mingliang Zou, Hongmei Jian, Yu Zheng, Fei Wang, Gong Su, Yan Hong, Jiali Li, Zhiwei Zang, Canhai Lai, Hong Cui, Jinwen Xu, ..., for their kind help and concern during the difficult time of my life.

I wish to extend my thanks to my current boss A. A. Akinpelu, my current mentor L. L. Andrews, and my friend Garrick G. Metivier, of AT&T, for their understanding and support of the fulfillment of my thesis during my employment at AT&T.

I also wish to acknowledge the financial support from ARPA/AFSOR (Grant No. F49620-941) and a NSF Faculty Early Career Development Award.

Finally, I would like to express sincere thanks to my parents for their a long time understanding, support, concern and encouragement.

Table of Contents

List of Tables

Lists of Figures

Chapter 1
Introduction

1.1 Introduction

Driven by the emerging explosion of information exchange and the prospect of introducing broad-band integrated services digital network (B-ISDN), the capacity requirements of future telecommunication networks will be demanding. Various estimates predict an increase in the traffic demands by the turn of the century by a factor of 10, or even more. In today's information infrastructure, the increased transport capacity requirements of telecommunication networks are met by the use of fiber-optics as a single-channel, point-to-point transmission links, with all networking and services functions done electronically. To upgrade such an infrastructure, a core transport network is required to handle both narrow-band and broad-band services together in an efficient manner. This calls for not only high-capacity channels but also transport channels with sufficient granularity to handle signals at all levels in the network. Electronics switching systems are seen to have a capacity limit in the region of a few tens of Gb/sec. While it will no doubt be possible to increase this limit through the further development of high-speed electronic technology, there will be an increase price to pay.

The fundamental limitation of existing conventional single-channel TDM networks is that the entire throughput is bounded by the transmission rate that can

be supported by electronics at any one of the end-stations. To solve this electronic bottleneck, and to advance the communication link toward exploiting the huge optical fiber capacity, a multi-channel transmission scheme is needed, with each channel running at about the capacity of electronics, i.e., several to few tens of Gb/s. Multi-channel networks can be implemented using optical fibers through wavelength-division multiplexing (WDM), subcarrier multiplexing (SCM), time-division multiplexing (TDM), code-division multiple access (CDMA), or a combination of these techniques. WDM can support concurrent transmission on a single optical fiber, with the potential of relieving electronic bottleneck and allowing the bandwidth to grow linearly with the number of wavelengths deployed. Unlike single-channel TDM systems, WDM systems effectively use the large built-in bandwidth in installed fibers while maintaining the same or greater degrees of system performance, robustness, reliability, operations, and maintenance as current transport systems. With WDM, each channel is transmitted on a unique optical carrier wavelength. WDM optical networks using wavelength routing are considered to be the most promising candidates for the next generation of wide-area backbone networks.

The use of WDM technology provides a powerful mechanism to overcome these technological bottlenecks while preserving the important survivability feature. This is particularly true when transmission and wavelength assignment are performed in a manner that does not require each terminal to detect and process

all wavelengths traveling through transmission path. The transparency and independence of the WDM channels permit vastly dissimilar bit rates to pass between different pairs of nodes, allowing network connectivity and transmission rates to be tailored and upgraded flexibly according to prevailing traffic patterns and evolving service demands. This has resulted in a rapidly growing interest in the study of all-optical WDM networks which provide both switching and transmission within the optical domain. The prospects for creating such networks are being investigated in several consortia activities and research programs around the world. The principle goal for these programs is to create the possibility of a "future proof" network in which the optical signals flowing through the network are uninterrupted by electronics from source to destination, and in which the character of the individual signals is determined by the terminal equipment which is attached to the network at the source and destination.

The possibility of such WDM networks has arisen because of the realization of optical amplification, particularly with the development of Erbium-doped fiber amplifiers (EDFAs). The advent of EDFAs has revolutionized the field of optical communications in two ways: First their large optical gain allows long-haul unregenerate systems with optical repeaters spaced more than 100 km. Second, their large bandwidth permits to increase the capacity by an order of magnitude by WDM several high bit-rate channels. Furthermore, EDFAs can simultaneously accommodate multiple optical channels without significant crosstalk, due to their

slow gain dynamics, and therefore have greatly accelerated the pace at which WDM systems are being developed and deployed. In this context, Erbium-doped fiber amplifiers (EDFAs) are expected to be extensively used as power boosters, repeaters and preamplifiers because of their advantageous properties, e. g., high saturation output power, polarization independence, compatibility with fiber networks, high gain and low insertion loss. In conjunction with WDM techniques, EDFAs promise to offer significant economic performance advantages for a network through improved capacity, reliability, and transparency.

Although EDFAs are the key technology enabling the realization of transparent WDM repeaters, and despite their unsurpassed performance, however, a number of significant technological challenges remain. These challenges grow increasingly severe as the network grows in complexity and reach, particularly, in a large reconfigurable network where dynamic reconfiguration exacerbates the difficulties and imposes stringent demands on their WDM amplifiers. One of the most significant remaining problem of these technological challenges, that is the focus of this thesis, is "Transient Cross-Saturation" or "gain dynamics"

1.2 Transient Cross-Saturation or "gain dynamics"

The number of wavelength channels passing through an EDFA in a multiwavelength network will vary as a result of network reconfiguration, network growth to larger number of channels, or component failures which can

cause one or more channel to drop out. Because these amplifiers are operating near saturation, and since the total output power of a saturated EDFA is very nearly constant, independent of the number of channels, the gain experienced by each channel will therefore depend on the number of channels present. This will induce transients in the gain at other wavelengths, via transient cross-saturation in the amplifier [1]. Cross-saturation in the network's EDFAs will induce power transients in the surviving channels, the speed of which is proportional to the number of amplifiers in the network. For large networks, as this work will show, surviving channels power transients can be large and extremely fast. Such fast power transients constitute a major issue for reconfigurable optical networks in which channels are added or dropped. Dropping channels can give rise to surviving channel errors since the power of the surviving channels may surpass the thresholds for nonlinear effects such as Self-Phase Modulation (SPM). Addition of channels can cause errors by depressing the power of the surviving channels below the receiver sensitivity.

Stated differently, a power fluctuation in a dropped/added wavelength channel may cause a receiver in a client Network Element (NE) to receive a signal with too little or too much optical power. This, in turn, could cause the client NE to declare a loss of signal, or to declare a degraded signal (e. g., unacceptable BER or SNR performance). Since such errors bursts in surviving channels are unacceptable to service providers, EDFAs will not be used in multiwavelength

optical networks unless these fast transients are controlled. Fast dynamic gain control is therefore required for amplifiers constituting the nodes and repeaters of a WDM routed network. This is most easily accomplished by requiring that the amplifier output a constant power per channel. However, that in turn raises monitoring and control issues. While typical time scales for gain changes in a single amplifier, as this work will show, are tens of microseconds, the time constant for a chain of N amplifiers is 1/N times shorter than that of a single amplifier [1]. Thus long chains of amplifiers will require faster control to limit the undesirable power excursions, so that long chains of amplifiers present a greater gain stabilization challenge.

1.3 Thesis Statement

This thesis presents a detailed experimental and theoretical analysis of gain dynamics of all-optically stabilized multi-channel EDFA and the impact on WDM networks performances. Rather than following the conventional scheme of measuring the unwanted power excursions of the surviving channel [2-8], the work reported here focus on analyzing the detailed transient response of the surviving channel and the relaxation oscillations of the compensating (lasing) signal. Specifically, this thesis analyzes and examines the critical factors such as, lasing wavelength, amplifier operating point, gain recovery time, relaxation

oscillation frequency of the feedback loop, cavity length and losses, power, switching speeds, and the number of channels dropped/added, that affect the transient power excursions in the surviving channel. We show that any degradation at the first EDFA has a cumulative effect at the output of all subsequent EDFA's in the chain. This has the important implication that the length of the chain is a function of the design parameters of the first EDFA in the chain.

The main objective of this work is to protect surviving channels against such impairments, by minimizing the impact of variations in the number of wavelength channels in operation, and of rapid changes in their signal power levels. The basic requirement is that the quality of service for any given channel passing through an optical amplifier shall not be adversely impacted by anything that happens to any of other channels passing through the same amplifier. This requirement applies both to amplifiers in WDM repeaters network elements, and to amplifiers included in other network elements. We will consider means of adjusting the flattened-gain amplifier's total output power to maintain constant per-channel output power with a minimally degraded SNR, regardless of the number of channels present. This will require that the amplifier's control system be aware of the number of channels present. This information could be passed on a telemetry channel or derived through measurement at the amplifier.

This thesis is divided into two overlapping phases, experimental and theoretical. First, we consider the applicability of laser automatic gain control (AGC) to control fast power transients in WDM optical networks and reports the first high resolution measurements of transients in such gain controlled EDFA's [9]. Second, we will implement a dynamic simulation tool for modeling the behavior of single amplifier and amplifier chains, with and without stabilization. We will develop an approximate rate equation model for a homogeneously broadened 3-level multi-excited-mode laser system, where relaxation-oscillations characteristic parameters, i.e., threshold pumping rate, pumping factor, damping rate, and oscillation frequency will be derived based on 4-level laser system model. The experimental results are then compared with those predicted using the dynamic simulation tool.

We will show the degradations imposed by each of these factors on the transient power excursions of the surviving channel and explore the limitations that any of these degradations can impose on the stabilization techniques. It is shown that these power excursions have two contributions: a static contribution owing to the spectral hole burning (SHB), and a dynamic contribution owing to the relaxation oscillations in the laser. Furthermore, it is shown that so long as the lasing wavelength is not close from the spectral band occupied by signal wavelengths, the static power excursions related to SHB is the dominant effect. There is a trade-off in selecting the lasing control wavelength to minimize impairments from SHB and relaxation oscillations; a lasing wavelength cannot be chosen, which avoids

both impairments. The experimental results are found to be in a good agreement with those predicted using the dynamic simulation tool.

Some of the critical questions that have to be answered, in order to help us identify and evaluate different options for implementing surviving channels protection, during the course of this work are:

- What scenarios cause the problem, and is recovery necessary for all of them ?
- What parameters must be controlled to solve the problem ?
- How quickly the problem must be solved ?

  This will depend on the type and timescale of the performance parameters for the service being transported. The ultimate performance criteria is instantaneous recovery (or may be the practical recovery time is within a bit period of a digital signal) ?
- Do standby "idle" channels, in which each network element is able to replace any missing channel with a dummy signal of the same wavelength and power, may be used to maintain the amplifiers at the proper operating point, need to be inserted ?

  This requires each network element with the ability to transmit dummy signals on any and all of the channel wavelengths simultaneously. How economical is this approach ?

  A simpler, more economical and equally effective solution is to lower the amplifier pump power to maintain the amplifier operating point. Is this a simpler

and more economical approach ? may be ?

- How fast can devices detect and react to changes ?
- How much changes of per-channel output power may be acceptable ?

This thesis will attempt to answer these critical questions, by devising, comparing, and demonstrating several active techniques, such as, link control, pump control, and a passive all-optical gain control technique, for stabilizing the per-channel output power both for single amplifier and cascades of amplifiers. Our primary concern and focus will be on the passive technique, since, as this thesis will show, this technique is simple, inexpensive, and robust, requiring neither monitoring of the amplifier output nor any active feedback.

The overall objective is to investigate numerically and experimentally the optimum configuration of an EDFA with laser AGC for WDM applications as a function of all the relevant performance parameters such as, lasing wavelength, amplifier operating point, cavity length and losses, power, and laser propagation directions. We will devise and examine several different approaches to reduce and/or eliminate the spiking amplitudes associated with relaxation-oscillations.

Another critical performance criterion is to ensure sufficient gain flatness to permit amplifiers to be cascaded while maintaining acceptable inter channel power variations and signal-to-noise ratios at all wavelengths. Since gain flatness depends

on the signal input power levels, stabilizing the amplifier gain is a must. What is needed is a multi-channel equalized and stabilized gain amplifier.

References:

[1] J. L. Zyskind, Y. Sun, A.K. Srivastava, J.W. Sulhoff, A.J. Lucero, C.Wolf and R.W. Tkach, "Fast power transients in optically amplified multiwavelength optical networks", in OFC'96, Tech. Digest, San Jose, CA, USA, Postdeadline PD31-1 .

[2] M. Zirngibl, "Gain control in Erbium-Doped Fiber Amplifiers by an all-optical feedback loop", Electron. Lett., Vol. 27, pp. 560-561, 1991.

[3] E. Delevaque, T. Georges, J.F. Bayon, M.Monerie, P. Niay and P. Bernage, "Gain control in Erbium-doped Fiber amplifiers by lasing at 1480 nm with written on fiber ends", Electron. Lett., Vol. 29, pp.1112-1113, 1993.

[4] B. Landousies, T. Georges, E. Delevaque, R. Lebref, and M. Monerie, "Low power transient in multichannel equalized and stabilized gain amplifier using passive gain control", Electron. Lett., Vol. 32, pp. 1912-1913, 1996.

[5] A. K. Srivastava, Y. Sun, J. L. Zyskind, J. W. Sulhoff, C. Wolf, R. W. Tkach, "Fast Gain Control in Erbium-Doped Fiber Amplifier," in Optical Amplifier and Their Applications, Vol. V of 1996 Trends in Optics and Photonic Series (Optical Society of America, Washington, D. C., 1996.

[6] J. L. Zyskind, A. K. Srivastava, Y. Sun, J. C. Ellison, G. W. Newsome, R. W. Tkach, A. R. Chraplyvy, J. W. Sulhoff, T. A. Strasser, J. R. Pedrazzani and C. Wolf, " Fast link control protection for surviving channels in multiwavelength optical networks," in Proceedings of European Conference on Optical Communications ECOC'96, Oslo, 1996 Post-deadline paper.

[7] F. Shehadeh, R. S. Vodhanel, C. Gibbons, and M. Ali, "Comparison of gain control techniques to stabilize EDFA's for WDM networks," in OFC'96, Tech. Digest, San Jose, CA, USA, WM8, pp.190-191.

[8] Janet Lehr Jackel and Dwight Richards, "All-optical stabilization of multi-wavelength EDFA chains: a network-level approach", in LEOS'96, Boston, MA, USA, Post-deadline paper, PDP2.2.

[9] G. Luo, J.L. Zyskind, Y. Sun, A.K. Srivastava, J.W. Sulhoff, and M.A. Ali, "Relaxation-oscillations and spectral hole burning in laser automatic gain control of EDFA's", in OFC'97, Tech. Digest, Dallas, Texas, USA, WF4, pp.130-131.

Chapter 2
Basic Characteristics of Optical Doped-Fiber Amplifiers

2.1 Introduction

The origin of optical fiber amplifiers may date back to the early of 1960's, when E. Snitzer reported the first fiber action with a neodymium doped alkali-silicate glass fiber although it was a multi-mode fiber and the pumping was side-pumping [1]. A variety of host glasses and doped lasing elements were then investigated. Fiber laser or amplifiers, however, were not used in optical fiber communications for a long period of time, partly because the development of transmission systems with high-performance silica-based optical fibers and semiconductor lasers was so rapid in the 1970's and after, and partly because the key technology for practical fiber amplifiers was not mature. Until optical fiber amplifiers were put into practice, optical fiber transmission systems were using one system configuration in which digitized optical signals from a light source were launched out from a transmitter, and then connected by spans of transmission optical fiber interspersed with optoelectronic regenerators, and then the output from the fiber was detected by a detector which generated the electrical signals again. In these conventional systems, the optical fibers are merely a transmission medium; the optoelectronic regenerators corrected attenuation, dispersion and other transmission degradations of the signal by detecting the attenuated and distorted data pulses, electronically reconstituting them and then transmitting the

regenerated data into the next transmission span [2]. In the late 1980's optical fiber amplifiers appeared again as a promising active device for fiber communications [3]. The EDFA is an optical amplifier that faithfully amplifies lightwave signals purely in the optical domain, which covers a wide gain band around 1550 nm which overlaps with the low-loss wavelength region of the silica-based optical fibers. EDFA's have several potential functions in optical fiber transmission systems. They can be used as power amplifiers to boost transmitter power, as repeaters or in-line amplifiers to increase system reach or as pre-amplifiers to enhance receiver sensitivity. The most far-reaching impact of EDFA's has resulted from their use as repeaters in place of conventional optoelectronic regenerators to compensate transmission loss and extend the span between digital terminals. Used as a repeater, the optical amplifier offers the possibility of transforming the optical transmission line into a transparent optical pipeline that will support signals independent of their modulation format or their channel data rate. The EDFA is also featured by its high gain for a small signal, a high conversion efficiency from pumping power to signal due to its three-level structure, and a low noise figure. These excellent characteristics are backed by key technologies which have been developed: the stable doping of rare-earths into silica-based fibers without an increase of the extrinsic transmission loss, high-power pumping laser diodes with appropriate source wavelengths of 1480 nm or 980 nm, Wavelength Division Multiplexing (WDM) technology for efficiently combining the signal pump powers, and so on. The EDFA offers wide application, such as long-haul fiber transmission of multi-Gb/s and multi-thousand kilometers or cable television

broadcasting using optical fibers, because the direct amplification of optical signals simplifies the system configuration and the system becomes free from the bit rate. Optical amplifiers (EDFA's) have wide bandwidth (BW), which could be up to 35 nm (~ 4,000 GHz). This feature is suitable for the simultaneous amplification of several input lights with a different wavelength in WDM or OFDM (Optical Frequency-Division Multiplexing) transmission. Therefore, optical amplifiers can support the use of WDM whereby signals of different wavelength are combined and transmitted together on the same transmission fiber, with the potential of relieving electronic bottleneck and allowing the BW to grow linearly with the number of wavelengths deployed. Unlike single-channel TDM (Time-Division Multiplexing) systems, WDM systems effectively use the large built-in BW in installed fibers while maintaining the same or greater degrees of system performance, robustness, reliability, operations, and maintenance as current transport systems. With WDM, each channel is transmitted on an unique optical carrier wavelength. WDM optical networks using wavelength routing are considered to be the most promising candidates for the next generation of wide-area backbone networks. Although EDFA's are considered to be highly matured, the growth of WDM transmission and the prospect of multiwavelength optical networking require further improvement of the performance of EDFA's, which is still a challenge toward realization of the ultimately large-capacity optical fiber transmission based on WDM. Such issues include amplifier noises, amplifier spectral gain nonuniformity, and channel cross saturation which do limit the performance of optically amplified transmission systems and networks. Transmission impairments,

such as those from optical nonlinearities, dispersion and polarization effects accumulate in amplified systems and have greater impact [4].

2.2 Basics of Optical Doped-Fiber Amplifiers

This Section briefly reviews main characteristics of EDFA's. These characteristics are essentially related to the amplifier gain, saturation, and noise properties; *all three are generally couple together*. Ideally, the EDFA should yield the highest gain possible (given the pump power available), while having the highest saturation output power and lowest noise possible. The combined EDFA characteristics of gain, saturation power and noise are often referred to in the literature as the EDFA performance. The spectroscope of EDFA`s play a fundamental role in the analysis and physical understanding of optical fiber amplifiers. All the important device characteristics of EDFA's, i.e., gain spectrum, gain versus pump power and pump wavelength, output saturation power, power conversion efficiency, and noise figure are fundamentally related to spectroscopic properties.

2.2.1 Configurations

The basic EDFA device architectures, shown in Fig.2.1, include an erbium-doped fiber spliced into the signal transmission path of an optical fiber communication system and a source of pump light. The pump light either co-propagates or counter-propagates or bi-propagates with the signal light. More advanced EDFA architectures may be found out in [6]. It is the atomic level scheme of the Er ion (Fig.2.2) that gives the EDFA its

nearly ideal properties for optical communications. Light from the pump supplies energy to elevate the erbium ions to the $^4I_{13/2}$ first excited state. The excitation energy of this state corresponds to wavelength near the minimum optical loss of silica optical fibers (~1550 nm). Optical input signals propagating through the EDFA with wavelength between roughly 1525 and 1565 nm stimulate emission in excited erbium ions and are thereby amplified.

2.2.2 Gain and Gain Spectrum

Device gain is the fundamental characteristic of an amplifier, which is defined as the ratio of output signal power to input signal power,

$$G(\lambda) \equiv \frac{P_{sig}^{out}}{P_{sig}^{in}} = \int_0^L g(\lambda, z)dz \qquad (2.1.a)$$

and is obtained by integrating the gain coefficient $g(\lambda)$ over the length L of the erbium-doped fiber. Since it is a ratio of optical power, G is often expressed in decibels as $G(dB)=10\log_{10}(G)$. The (signal, local) gain coefficient, also called differential gain [7]--sees the definition of Equ.(2.2.a): defined as the local growth of optical power and normally expressed in units of dB/m, is the sum of the emission coefficient $g^*(\lambda) = \Gamma_s n_{Er} \sigma_e(\lambda)$ and the absorption coefficient $\alpha(\lambda) = \Gamma_s n_{Er} \sigma_a(\lambda)$ weighted by the *fractional* populations N_2 and N_1, respectively, of the first excited and ground states of erbium

$$g(\lambda,z) \equiv \frac{1}{P(\lambda,z)} \cdot \frac{dP(\lambda,z)}{dz} = g^*(\lambda) \cdot N_2(z) - \alpha(\lambda) \cdot N_1(z)$$

(2.2.a)

where Γ_s is the overlap integral between the optical mode and the erbium ions, n_{Er} is the concentration of Er ions in the core, and $\sigma_e(\lambda)$ and $\sigma_a(\lambda)$ are, respectively, the signal absorption and emission cross sections as functions of wavelength. Note that the (2.2.a) can be derived from the propagation equations in which the ASE terms have been deleted, Equ. (21) in [11], where the homogeneous broadening assumption, of course, is still sustained. The spectra for the fully inverted gain coefficient $g^*(\lambda) = \Gamma_s n_{Er} \sigma_e(\lambda)$ and the small signal absorption coefficient $\alpha(\lambda) = \Gamma_s n_{Er} \sigma_a(\lambda)$ are shown in Fig.2.3 for an erbium doped fiber with aluminum and germanium codoping in the core. The gain coefficient of the EDFA at high pump power can be expressed as follows [8]

$$g \approx g^* \frac{1}{1 + \frac{P_p^{th}}{P_p} \frac{P_s}{P_{sat}}} \qquad (2.2.b)$$

where P_p^{th} is the pump threshold power, P_p the pump power, P_{sat} the intrinsic saturation power, and P_s the signal power. It is noted that Equ. (2.2.b) describes the saturation behavior of a two-level optical amplifier with a saturation power dependent on the pump power.

Note that if the passive loss coefficient $k(\lambda)$ (dB/m) due to absorption and scattering [9], or the other passive loss (excess loss) $K(\lambda)$ (dB) of, such as, filters and components [10], must be taken into account, the expression (2.1.a) should be changed as follows

$$G(\lambda) \equiv \frac{P_{sig}^{out}}{P_{sig}^{in}} = \int_0^L (g(\lambda, z) - k(\lambda)) \cdot dz \qquad (2.1.b)$$

$$G(\lambda) \equiv \frac{P_{sig}^{out}}{P_{sig}^{in}} = \int_0^L g(\lambda, z) dz - K(\lambda) \qquad (2.1.c)$$

Erbium-doped fiber amplifiers can be modeled accurately using rate equations for the populations of the atomic levels and the photon fluxes [11,12]. The other chapters in this thesis will also discuss modeling issues where the system consisting of one laser channel and many of signal channels will be addressed.

Another issue related to the gain coefficient expression (2.2.a) is the so-called gain spectrum. The gain BW of the EDFA extends from about 1525 to 1565 nm as a result of the Stark splitting experienced by the high angular momentum ground and first excited states of the erbium ions in the local electrical fields in the glass matrix. The gain spectrum, which is determined by the distribution and the thermal population of the sublevels, is not flat and its shape changes with the level of inversion. Substituting Equ. (2.2.a) into Equ. (1.1.a) and then taking the metastable population averaged along the whole length of the amplifier [11],

$$G(\lambda) \equiv \frac{P_{sig}^{out}}{P_{sig}^{in}} = \exp\left(\bar{g}(\lambda) \cdot L\right) \tag{2.3}$$

where

$$\bar{g}(\lambda) = g^*(\lambda) \cdot \bar{N}_2 - \alpha(\lambda) \cdot \bar{N}_1 = \left(g^*(\lambda) + \alpha(\lambda)\right) \cdot \bar{N}_2 - \alpha(\lambda) \tag{2.4}$$

Here the horizontal bars indicate taking the average over the length of the entire erbium-doped fiber and we have used the fact that $N_1+N_2=1$. $\bar{g}^*(\lambda)$ is called the average gain coefficient, and thus the gain spectrum for an amplifier or whole system of amplifiers is equal to the spectrum of the $\bar{g}^*(\lambda)$ scaled for the total length of erbium-doped fiber in the amplifier or system. Equ. (2.4) indicates that the average gain coefficient, unlike the gain coefficient expression (2.2.a), does not describe the local behavior again, but the aggregate behavior of a complete amplifier or even a complete amplifier system. When an amplifier with a doped fiber length L is operated at a constant average inversion of erbium ions, the amplifier gives the constant gain.

Gain coefficient spectra for different values of inversion are shown in Fig.2.4 for an erbium-doped fiber with Al and Ge co-doping. For an amplifier, or even for a complete system, the gain divided by the total length of EDF determines the average inversion and the gain spectrum. Obviously, if the operating wavelengths and operating inversion are not chosen with care, the gain spectrum can be highly nonuniform. For a proper choice of the average inversion the gain is quite flat for wavelengths near 1550 nm (also see chapter 8)

The above calculation of gain spectra as a function of inversion, or degree of saturation, assumes that the stimulated laser transitions are homogeneously broadened. This is not strictly true but it is a good approximation. Low temperature measurements indicate that homogeneous and inhomogeneous linewidths are comparable [13,14]. Room temperature spectral hole burning, a signature of inhomogeneous saturation, has been observed but it is even weaker [15] than would be expected from the extrapolated homogeneous and inhomogeneous linewidths, presumably as a result of the rapid thermal redistribution among the sublevels of the Stark split manifolds of the first excited state.

For applications such as WDM system and multiwavelength networks, amplifiers with flat gain over a substantial spectral range are desired. Depending on the degree of flatness required and the spectral range, flat amplifier gain can be achieved by designing the amplifiers to operate at the appropriate inversion level and/or by incorporating gain flattening filters into the amplifiers.

The gain spectra are strongly dependent on the composition of the erbium-doped core. Erbium-doped silica fibers with Al co-doping are capable of flatter and broader gain spectra than other choices of co-dopants such as germanium or phosphorous (which is necessary in Er:Yb co-doped fibers to promote efficient energy transfer from the Yb to the Er ions). Additionally, gain spectra with even greater optical bandwidth (around 30

nm [10]) are produced by erbium-doped fluoride fiber [16], but some concern over productivity and/or reliability of the fluoride-based fiber still remains [17].

2.2.3 Output Power and Saturation

The output power is approximately proportional to the pump power when total signal levels are high and the amplifier is saturated as shown in Fig. 2.5.

This is a characteristic of the three level erbium laser system as can be understood by reference to the Er energy level scheme (Fig.2.1); when the amplifier is saturated, pump absorption from the ground state is almost balanced by signal induced, stimulated emission from the first excited state induced by the signal. The higher the pump power is, the higher the signal power at which this balance occurs. This can be verified by using the rate equations describing the populations of the erbium energy levels and the light intensity to calculate the gain coefficient and analyze its saturation characteristics[19]. The signal power at which the gain coefficient is reduced to half its small signal value is

$$P_{sat} = \frac{h\upsilon_s A_c}{(\sigma_{es} + \sigma_{as})\Gamma_s \tau_{sp}} \left[1 + \frac{\sigma_{as} \cdot P_p}{\sigma_{es} \cdot P_p^{th}} \right] \qquad (2.5)$$

where σ_{es} and σ_{as} are the emission and absorption cross section, respectively, at the signal wavelength, A_c is the core area, τ_{sp} is the first excited state spontaneous lifetime and P_p is the pump power. The pump threshold for transparency, i.e., the

pump power below which the small signal gain coefficient is negative, corresponding to absorption, and above which it is positive, corresponding to gain, is

$$P_p^{th} = \frac{\sigma_{ap}}{\sigma_{es}} \frac{h\upsilon_p A_c}{\Gamma_p \tau_{sp} \sigma_{ap}} \tag{2.6}$$

Here $h\upsilon_p$ is the pump photon, Γ_p is the pump mode confinement factor and σ_{ap} is pump absorption cross section. Equ. (2.5) shows that if $P_p >> P_p^{th}$ then P_{sat} is proportional to $\frac{P_p}{P_p^{th}}$.

Equs. (2.5) and (2.6) are local in character describing the behavior of the gain coefficient at a particular value of z. The gain characteristics of the complete amplifier are found by solving the rate equation at each point along the length of the EDF and integrating the gain coefficient as indicated in Equ.(2.1.a). As the saturation behavior is typically determined primarily near the output end of the amplifier where the signal power is largest, this local description generally provides a good qualitative understanding of the saturation behavior.

In a typical saturation curve, P_{sat} refers to the output power at the 3 dB gain compression point, and is closely related to the maximum output power that the amplifier can produce, and depends on pump laser power. The large saturated output power occurs at high input signals that cause a high rate of stimulated emission accompanied by gain compression [20,21]. In power amplifiers, the optical conversion

efficiency describing the energy transfer between pump and signal quantifies the ability of the amplifier to produce high output signal power [20, 21]. More detail discussions about conversion efficiency sees [6].

2.2.4 Noise Figure

Any amplifier or attenuator always adds fluctuations or noise to the various physical parameters that characterize the input and output light, and thus the amplification of the EDFA is inescapably accompanied by a background of amplified spontaneous emission (ASE)--the gain is accompanied by broadband ASE. ASE arises when light emitted by spontaneous decay of excited erbium ions is captured by the optical waveguid and then amplified in the EDFA. Without an input signal, the energy in the erbium ions is converted to ASE which is the noise source within the amplifier. If a signal stimulates the erbium ions to emit photons, then most of the energy is used for amplification, and only a small fraction remains for the ASE. The input signal supersedes the noise at the wavelength of interest (the signal hides the ASE at its center wavelength), and while this ASE background in turn adds noise which degrades amplified signals. Interplay between signal gain and ASE noise has central importance for optical amplifiers in WDM lightwave systems. The noise figure (NF), defined as the signal-to-noise ratio at the output divided by that corresponding to the shot noise of the signal at the input, is a measure of the degradation of the signal by noise added by the amplifier. The NF will always be greater than one. This is because the amplifier always adds noise during signal amplification process and the signal to

noise ratio at the output is always lower than that at the input although both output signal and noise are amplified, the total output noise powers are not just shot noise, unlike the input signal defined as a shot noise limited in the calculation of NF--in this sense, the multiplication of output noise is larger than that output signal, resulting in larger than one of NF. Note that the definition of NF is with reference to the input signal with Poisson statistics (i.e., shot noise only), and thus only if all of input signal statistics meet the Poisson distribution the comparisons of NF do make a sense--for actual cases there exists some deviation [p.362, 5]. NF is often expressed in dB as $NF(dB)=10\log_{10}(NF)$. The dominant contribution to the noise figure of a well designed, high gain amplifier are signal-spontaneous beat noise and signal shot noise (provided that the input noise is shot-noise limited, i.e., a coherent input signal), and are given by

$$NF \equiv \frac{(SNR)_{in}}{(SNR)_{out}} \approx \frac{(P_{in}^{s} / h\upsilon B)}{(P_{out}^{s} / P_{ASE})} + \frac{1}{G} = \frac{P_{ASE}}{h\upsilon B \cdot G} + \frac{1}{G} = 2n_{sp}\frac{(G-1)}{G} + \frac{1}{G} \approx 2n_{sp} \tag{2.7}$$

where n_{sp} is the spontaneous emission factor, can be determined (calculated) from (has been used for the above expression)

$$n_{sp} = \frac{P_{ASE}}{h\upsilon_{s} \cdot B \cdot (G-1)} \tag{2.8.1}$$

Here P_{ASE} is the ASE power in one polarization in BW B (this is one half of the total power in BW B of the ASE which, in the absence of polarization hole burning, is unpolarized) and $h\upsilon_{s}$ is the photon energy. Combining Equs. (2.7) and (2.8.1) shows

that the signal-spontaneous beat noise contribution to the noise figure is proportional to P_{ASE} and can be viewed as resulting from the addition of ASE by the amplifier. Note that for uniform pumping laser medium [p.76, 5], the n_{sp} can be defined as

$$n_{sp} = \frac{\sigma_e N_2}{(\sigma_e N_2 - \sigma_a N_1)} \qquad (2.8.2)$$

The closer n_{sp} is to 1 (i.e., the better the inversion), the lower the noise figure. Because erbium-doped amplifiers can be very efficiently inverted (i.e., $N_2 - N_1 \approx 1$), the NF can approach 3 dB (with zero input signal coupling loss), which is the quantum limit for 980 nm pumped optical amplifiers, 4.1 dB for 1480 nm pumped amplifiers. The NF is also influenced by the EDFA pump configuration, with configurations that result in full inversion at the amplifier input having lower noise figures. In EDFA's with gain greater than 30 dB, the NF is limited by internal Rayleigh backscattering [22].

2.2.5 Response Characteristics (Gain Dynamics)

The response characteristics of EDFA's here refer to whether the EDFA can amplify a randomly modulated signal waveform without patterning effects or waveform distortion. Response to a modulated lightwave is attributed to the temporal behavior of the population inversion (in other words, the gain coefficient) when the optical signal is coupled into the device. The population inversion (gain coefficient) declines as the light input increases and its speed of response is governed by the effective upper level lifetime. As a result, the gain dynamics of EDFA's are slow due to the very long lifetime of the $^4I_{13/2}$ metastable first excited state (~10 ms) and thus the EDFA has a

low-pass frequency response to the transfer of noise from the pump to signals being amplified in the amplifier [23]. Therefore, when the data rate is high enough the modulation of signals does not cause significant gain modulation of the amplifier even in very deeply saturated amplifiers [24]. It is the inherent slow gain dynamics that EDFA's can be used in WDM transmission system since EDFA's gain is homogeneously dominated at room temperature. The corner frequency for the amplifier can be as low as a hundred Hz and increase with pump and signal power, but generally remain less than 10 KHz. Even for intensity modulated signals with relatively low data rate, the amplifiers do not introduce significant inter-symbol interference, crosstalk (in the case of multi-channel signals) or nonlinear distortions due to intermodulation.

References:

[1] E. Snitzer, Phys. Rev. Lett., 7 (1961) 444.

[2] See, for example, P.S. Henry, R.A. Linke, and A.H. Gnauck, "Introduction to Lightwave Systems", in *Optical Communications Systems*, ed. S.E. Miller and I.P. Kaminow, Academic Press (1988) 781.

[3] R.J. Mears, L. Reekie, I.M. Jauncey, and D.N. Payne, Electron. Lett., 23 (1987) 1026.

[4] See, for example, John Zyskind, "Performance issues in optically amplified systems and networks", OFC'97, Dallas, Texas, 1997 OSA Technical Digest Series, TuP1.

[5] E. Desurvire, Erbium-Doped Fiber Amplifiers: Principles and Applications, John Wiley & Sons, Inc., New York (1994).

[6] See, for example, J. -M. P Delavaux, J.A. Nagel, "Multi-stage erbium-doped fiber amplifier designs", J. Lightwave Technol. 13 (1995) 703; S. Seikai, K. Kusunoki, and S. Shimokado, "Experimental studies on wavelength division bidirectional optical amplifiers using an Er^{3+}-doped fiber", J. Lightwave Technol. 12 (1994) 849.

[7] K. Bertilsson and P.A. Andrekson, "Modeling of noise in erbium-doped fiber amplifiers in the saturated regime", J. Lightwave Technol. 12 (1994) 1198.

[8] E. Desurvire, "Erbium-doped fiber amplifiers: basic physics and characteristics", ed. M.J.F. DiGonnet, in *Rare-earth-doped fibers and devices* (Marcel Dekker, New York, 1992)

[9] M. Saruwatari, "Optical Amplifiers and their Applications", Chapt.2, John Wiley & Sons, ed. S. Shimada and H. Ishio, 1994.

[10] P.F. Wysocki, R.E. Tench, M. Andrejco, D. DiGiovanni, and I. Jayawardene, "Options for gain-flattened erbium-doped fiber amplifiers", OFC'97, Dallas, Texas, OSA Technical Digest Series, 6 (1997) 127, WF2.

[11] C.R. Giles and E. Desurvire, "Modeling erbium-doped fiber amplifiers", IEEE J. Lightwave Technol., 9 (1991) 271.

[12] A.A.M. Saleh, R.M. Jopson, J.D. Evankow and J. Aspell, "Modeling of gain in erbium-doped fiber amplifiers", IEEE Photonics Technol. Lett., 2 (1990) 714.

[13] E. Desurvire, J.L. Zyskind and J.R. Simpson, "Spectral gain hole-burning at 1.53 um in erbium-doped fiber amplifiers", IEEE Photonics Technol. Lett., 2 (1990) 246.

[14] J.L. Zyskind, E. Desurvire, J.W. Sulhoff and D. DiGiovanni, "Determination of homogeneous linewidth by spectral gain hole-burning in an erbium-doped fiber amplifier with GeO_2-SiO_2 core", IEEE Photonics Technol. Lett., 2 (1990) 869.

[15] A.K. Srivastava, J.L. Zkskind, J.W. Sulhoff, J.D. Evankow, Jr., M.A. Mills, "Room temperature spectral hole-burning in erbium-doped fiber amplifiers", OFC'96, San Jose, California, TuG7, OSA Technical Digest Series.

[16] D. Ronarch, et al., "30 dB optical net gain at 1.543 um in Er^{3+} doped fluoride fibre pumped around 1.48 um", Electron. Lett., 27 (1991) 908.

[17] M. Nishimura, "gain-flattened erbium-doped fiber amplifiers for WDM transmission", OFC'97, Dallas, Texas, OSA Technical Digest Series, 6 (1997) 127, WF1.

[18] E. Desurvire, C.R. Giles, J.R. Simpson and J.L. Zyskind, "Efficient erbium-doped fiber amplifier at a 1.53 um wavelength with a high output saturation power", Optics Lett., 14(1989) 1266.

[19] J.L. Zyskind, "Advances in Erbium-doped fiber amplifiers for optical communications", in: M.J. Digonnet (Ed.) *Fiber Laser Sources and Amplifiers II*, SPIE Proceedings, No. 1373, Bellingham, WA: SPIE, pp. 80-92.

[20] J.L. Zyskind and J.W. Sulhoff, "Length dependence of saturation power in erbium-doped fiber amplifiers", in Proc. SPIE, Boston, MA, 1581 (1991) 251.

[21] R.G. Smart, J.L. Zyakind, J.W. Sulhoff, and D.J. DiGiovanni, "Dependence of performance of saturation in-line erbium-doped fiber amplifiers on pump wavelength around 1480 nm", OFC'93, San Jose, CA, OSA Technical Digest Series, ThF5.

[22] M.N. Zervas and R. Laming, "Performance limits of erbium-doped fibre amplifiers due to internal rayleigh back-scattering", OFC'93, San Jose, CA, OSA Technical Digest Series, ThF1.

[23] R.I. Laming, L. Reekie, P.R. Morkel, and D.N. Payne, "Multichannel crosstalk and pump noise characterisation of Er^{3+}-doped fiber amplifier pumped at 980 nm", Electron. Lett., 25 (1988) 455.

[24] E. Desurvire, C.R. Giles, and J.R. Simpson "Gain saturation effects in high-speed, multichannel erbium-doped fiber amplifiers at λ=1.53 nm", IEEE J. Lightwave Technol. 7 (1989) 2095.

[25] J.L. Zyskind, Y. Sun, A.K. Srivastava, J.W. Sulhoff, A.J. Lucero, C. Wolf and R.W. Tkach, "Fast power transients in optically amplified multiwavelength optical networks", OFC'96, San Jose, CA, OSA Technical Digest Series, Postdeadline paper PD31.

Chapter 3
Experimental Investigations of an EDFA with Static and Dynamic Laser AGC

3.1 Introduction

Laser gain-controlled EDFAs, in which automatic gain control is achieved by introducing lasing at a particular wavelength in the optical amplifier [1], are very attractive for their application in multiwavelength optical networks. A number of experimental demonstrations using this passive automatic gain control scheme have been reported [1-15]. Two kinds of basic amplifier configurations, ring and linear cavity, respectively, shown in Fig.3.1, can be used to achieve such passive automatic gain control schemes. Laser gain-controlled amplifier design involves determining laser wavelength, cavity loss, amplifier length (or average inversion) for a given required signal gain.

Several schemes have been demonstrated to control the unwanted power excursions of surviving channels in EDFA's . These include gain clamping by an all-optical ring (feedback) [1-3, 6, 8, 10, 12-14]/linear [4, 5,7 -9, 11] cavity, fast pump control [16] and by insertion of a compensating signal [17-19]. Most of these schemes have focused on achieving a common goal; the maximum value of the power excursions of the surviving channel should be within a fraction of a dB from the original steady state value of that channel when the network is operating in the normal mode of operation

(no loss/addition of any other channels) without regard to the detailed transient response analysis of both the surviving and compensating signals.

This chapter presents a detailed experimental analysis of the gain dynamics of all-optically stabilized multi-channel EDFA and the impact on WDM networks performances. Rather than following the conventional scheme of measuring the unwanted power excursions of the surviving channel [1-14], the work reported in this chapter focus on analyzing the detailed transient response of the surviving channel and the relaxation oscillations of the compensating (lasing) signal. Specifically, the main objective of these experiments is to analyze and examine the critical factors such as, lasing wavelength, amplifier operating point, gain recovery time, relaxation oscillation frequency of the feedback loop, and the number of channels dropped/added, that affect the transient power excursions in the surviving channel. We consider the applicability of laser automatic gain control (AGC) to control fast power transients in WDM optical networks and reports the first high resolution measurements of transients in such gain controlled EDFA's [15].

We will show the degradations imposed by each of these factors on the transient power excursions of the surviving channel and explore the limitations that any of these degradations can impose on the stabilization techniques. It is shown that these power excursions have two contributions: a static contribution owing to the spectral hole burning (SHB), and a dynamic contribution owing to the relaxation oscillations in the laser. Furthermore, it is shown that so long as the lasing wavelength is not close from

the spectral band occupied by signal wavelengths, the static power excursions related to SHB is the dominant effect. There is a trade-off in selecting the lasing control wavelength to minimize impairments from SHB and relaxation oscillations; a lasing wavelength cannot be chosen, which avoids both impairments.

3.2 Experimental Configuration

The all-optical stabilization scheme used here assumes the basic configuration of laser-gain controlled EDFAs, in which automatic gain control is achieved by placing the amplifier in a ring laser cavity to clamp its gain. The experimental setup for the power transient measurements is shown in Fig.3.2. Two DFB lasers, at 1557.8 nm (laser A) and 1552.3 nm (laser B), each amplified by a booster EDFA, were used to simulate the power of 8 input channels with -18 dBm input each to the EDFA configuration under test. The signal at 1552.3-nm is taken as surviving channel. To form a feedback loop, two 50:50 wavelength insensitive couplers (WIC's), a tunable 1-nm bandpass optical filter with wavelength tunability from 1520.9 to 1565 nm, and a variable attenuator are employed as shown in Fig.3.2. Three optical isolators shown in Fig.3.2 force laser light to co-propagate with the signal to lower the noise figure penalty associated with laser AGC. An acousto-optic modulator (AOM) is incorporated in the path of signal A to simulate adding and dropping of 4 of the 8 WDM channels. The modulation rate is 910 Hz.

The EDFA configuration under test consists of a dual-stage EDFA, counter-pumped with 90 mW of pump power at 980-nm in stage 1 and co-pumped with 90 mW at 980-

nm in stage 2. The small signal gain (internal gain) at 1552.3 nm for this 2-stage amplifier without AGC is 38.4dB.

3.3 Experimental Results and Discussion

A. Choice of Feedback (Lasing) Wavelength

It is possible to achieve the same steady state signal gain in an all-optical gain controlled EDFA configuration using different lasing wavelengths. The steady state behavior in terms of output powers may be the same; but the transients are somewhat wavelength dependent. As an illustrative example, Fig. 3.3 shows a typical case of transient response of both the surviving and lasing (compensating) signals output power, when four out of eight signals are dropped/added, respectively. As can be seen from the Fig.3.3, both the surviving and compensating signals are subjected to initial power excursions and relaxation oscillations before steady state is reestablished. The frequency and damping constants of these oscillations are directly related to the laser characteristics such as power, lasing wavelength, and cavity length and losses. It can also be seen from the Fig3.3 that the relaxation oscillations of the compensating signal lag that of the surviving signal slightly in time phase, but the frequency of oscillations are identical. Dropping of a channel perturbs both the gain of the compensating signal and that of the surviving signal as the average inversion of the EDFA attempts to increase. The input of the compensating signal builds up in time to saturate the amplifier to its original level and thus keep the inversion fixed. The dynamics of

this process causes both signals to over and undershoot their steady state values, correcting each other as they evolve in time.

Fig. 3.4 shows transient response of the surviving signal output power, for three different lasing wavelengths, when the 1557.8-nm signal is modulated on and off, corresponding to the worst case scenario: addition and loss of 7 of the 8 WDM channels. For a given lasing wavelength (λ_1), the attenuator loss in the feedback loop is adjusted to maintain the same output power for the surviving channel. The gain experienced by the surviving signal is about 23 dB (amplifier is operating in about 15 dB gain compression).

At λ_1 = 1534-nm, Fig.3.4a, the laser AGC suppresses transients in the surviving channel, but not completely. The steady-state value of the surviving signal with and without the 1557.8-nm signal present differs by as much as 0.62 dB; this failure of the laser AGC arises from spectral hole burning, i.e., inhomogeneity of the erbium gain medium. The transition between these two gain levels requires on the order of hundreds of μs, reflecting the slow gain dynamics of the erbium gain medium. Note that the spikes arising due to relaxation oscillation in the laser do not undershoot and/or overshoot the steady-state values for lasing wavelengths near 1530-nm. This indicates that so long as the lasing wavelength is not close from the spectral band occupied by signal wavelengths, the static power excursions related to spectral hole burning is the dominant effect.

At λ_l = 1547-nm, as can be seen from Fig.3.4b, relaxation-oscillations, observed in the laser, give rise to fast oscillations in the surviving signal power resulting in transients which undershoot the lower gain level and overshoot the higher gain level. On the other hand, residual power excursions from SHB become smaller (The steady-state value of the surviving signal with and without the 1557.8-nm signal present now differs by only 0.31 dB). In this case, as λ_l approaches the signal wavelength, residual power excursions resulting from the static component due to the spectral hole burning, and the dynamic component due to the relaxation oscillations in the laser are both present.

At λ_l = 1555-nm, as can be seen from Fig.3.4c, relaxation-oscillations, observed in the laser, is the dominant component causing the residual power excursion in the surviving signal. On the other hand, residual power excursions from SHB are almost absent (almost no difference between the steady-state value of the surviving signal with and without the 1557.8-nm signal). As expected, the residual power excursions related to spectral hole burning resulting from inhomogeneity, becomes less significant as the lasing wavelength closely approaches the spectral band occupied by signal wavelengths. Furthermore, the dynamic power excursion (arising from relaxation oscillations in the laser) experienced by the surviving channel grow larger and larger (compare with Figs.3.4a and 3.4b). Note that both the frequency and amplitude of the relaxation oscillations are different for add or drop conditions. As can be seen form Fig. 3.4c, both the frequency and amplitude of the transient power excursions of the

surviving channel are lower in the case of adding channels versus that of dropping channels. This indicates that dropping of channels results in much more severe effects on the surviving channels.

In general, the frequency and damping constants of these oscillations are directly related to the laser system characteristics parameters such as power levels, lasing wavelength, and cavity length and losses. To explore these effects as a function of the lasing wavelength, we will define a gain recovery time, t_{rec}, as the time it takes the surviving signal to return to within a hundredth of a dB of its steady state value. Fig. 3.5 shows how t_{rec} varies for a discrete set of lasing wavelengths. As can be seen from the Fig.3.5, wavelengths that result in higher dynamic power excursions exhibit longer gain recovery times (lower oscillation frequency). These results are further illustrated in Fig.3.6, where the relaxation oscillation frequency of the feedback loop were measured for a discrete set of lasing wavelengths. As expected, wavelengths that result in higher dynamic power excursions exhibit lower oscillation frequency. These effects can be explained by the differences of differential gains of the surviving and compensating signals, for changes in the average inversion. This ratio is expressed as [20],

$$\frac{dg_s}{dg_c} = \frac{\sigma_e^s + \sigma_a^s}{\sigma_e^c + \sigma_a^c} \tag{3.1}$$

Where σ_e and σ_a are the EDFA's wavelength dependent emission and absorption cross-sections, respectively. For compensating wavelengths with larger denominators

on the RHS of (3.1), e.g. those compensating signals which are close from the 1530-nm gain peak, the differential gain for the signal as a result of changes in the average inversion is smaller, and thus smaller power excursions result. The simulation results presented in Chapter 5 will further clarify and confirm the validity of Eq. (3.1).

B. Number of Channels Dropped/Added

For a given attenuator loss, both the frequency and amplitude of the power excursions experienced by the surviving channels are a function of the number of channels in the system. Fig.3.7 shows an example of the dynamics of the surviving channel when 4 and 7 channels are switched, respectively. It can be seen that as the number of switched channels increases, both the frequency and amplitude of the power excursions experienced by the surviving channels increase. The speed at which the gain rises is proportional to the number of channels dropped, so as the number of dropped channels increases both the initial gain transient and the resulting signal oscillations are larger.

References:

[1] M. Zirngibl, "Gain control in Erbium-Doped Fibre Amplifiers by an all-optical feedback loop", Electron. Lett., 1991, 27, p.560.

[2] H. Okamura, "Automatic optical-loss compensation with Er-doped fibre amplifier", Electron. Lett., 1991, 27, p.2155.

[3] H. Okamura, "Automatic optical loss compensation with Erbium-Doped fiber amplifier", J. Lightwave Technol., 1992, 10, p.1110.

[4] E. Delevaque, T. Georges, J.F. Bayon, M.Monerie, P. Niay and P. Bernage, "Gain control in Erbium-doped fibre amplifiers by lasing at 1480nm with written on fibre ends", Electron. Lett., 1993, 29, p.1112 .

[5] J.F. Massicott, S.D. Willson, R.Wyatt, J.R. Armitage, R. Kashyap, D. Williams, and R.A. Lobbett, "1480nm pumped erbium doped fibre amplifier with all optical automatic gain control", Electron. Lett., 1994, 30, p.962.

[6] K. Motoshima, K. shimizu, K.Takano, T. Mizuochi, and T. KiTayama, "EDFA with dynamic gain compression for multiwavelength transmission systems", OFC'94, Tech. Dig., p.191.

[7] M. Fake, T.J. simmons, J. Massicott, R. Wyatt, "Optically stabilized EDFA for in-band WDM systems", OFC'95, Tech. dig., TuP3, p.79.

[8] A. Yu and M.J. O'Mahony, "Properties of gain controlled erbium doped fibre amplifiers by lasing", Electron. Lett., 1995, 31, p.1348; "Modelling of laser-controlled erbium-doped fiber amplifiers", OFC'96, San Jose, OSA Technical Digest, WK14, p.163.

[9] J. Massicott, C. Lebre, R. Wyatt, R. Kashyap, D. Williams, and A. Yu, "Low noise, all-optical gain controlled Er^{3+} doped fibre amplifier using asymmetric control laser cavity design", Electron. Lett., 1996, 32, p.816.

[10] E. Desurvire, "Erbium-Doped fiber amplifiers--principles and applications", (John Wiley & Sons, 1994), Chapt.5.

[11] R. Lebref, E. Delevaque, B. Landousies, H. Poignant, M. Guibert, T. Georges, "An advanced amplifier structure for WDM transmissions: The multichannel equalized and stabilized gain amplifier", Optical Amplifiers and their Applications Conf., Monterey, CA, Vol. 11, pp.81-84, 1996 OSA Tech. Dig. Series.

[12] H. Dai, J. Pan, C. Lin, "All-optical gain control of in-line EDFA for hybrid AM/digital WDM systems", in OFC'97, OSA Technical Digest, WF6, pp. 133-134,Dallas, Texas

[13] B. Landousies, T. Georges, E. Delevaque, R. Lebref, and M. Monerie, "Low power transient in multichannel equalized and stabilized gain amplifier using passive gain control", Electron. Lett., 1996, 32, p.1912.

[14] Joon Chung, Sang Yong Kim and Chang Joon Chae, "All-optical gain-clamped EDFAs with different feedback wavelengths for use in multiwavelength optical networks", Electron. Lett., 1996, 32, p.2159.

[15] G. Luo, J.L. Zyskind, Y. Sun, A.K. Srivastava, J.W. Sulhoff, and M.A. Ali, "Relaxation-oscillations and spectral hole burning in laser automatic gain control of EDFA's", in OFC'97, WF4, Dallas, Texas.

[16] A. K. Srivastava, Y. Sun, J. L. Zyskind, J. W. Sulhoff, C. Wolf, R. W. Tkach, "Fast Gain Control in Erbium-Doped Fiber Amplifier," in Optical Amplifier and Their Applications, Vol. V of 1996 Trends in Optics and Photonic Series (Optical Society of America, Washington, D. C., 1996.

[17] J. L. Zyskind, A. K. Srivastava, Y. Sun, J. C. Ellison, G. W. Newsome, R. W. Tkach, A. R. Chraplyvy, J. W. Sulhoff, T. A. Strasser, J. R. Pedrazzani and C. Wolf, " Fast link control protection for surviving channels in multiwavelength optical networks," in Proceedings of European Conference on Optical Communications ECOC'96, Oslo, 1996 Post-deadline paper.

[18] F. Shehadeh, R. S. Vodhanel, C. Gibbons, and M. Ali, "Comparison of gain control techniques to stabilize EDFA's for WDM networks," in OFC'96, Tech. Digest, San Jose, CA, USA, WM8, pp.190-191.

[19] Janet Lehr Jackel and Dwight Richards, "All-optical stabilization of multi-wavelength EDFA chains: a network-level approach", in LEOS'96, Boston, MA, USA, Post-deadline paper, PDP2.2.

[20] C.R. Giles and E. Desurvire, "Modeling erbium-doped fiber amplifiers", IEEE J. Lightwave Technol., 9(1991) 271.

Chapter 4
Analytical and Numerical Modeling of laser-Controlled EDFA's

4.1 Introduction

This chapter presents complete analytical and numerical modeling of EDFA's for steady-state case. The analytical model will be developed based on Saleh et al. model, the numerical model will be developed in terms of Giles' model, and both results will be compared.

4.2 Analytical Modeling

An analytical model (being capable of seeing physical insides through explicit or implicit solutions) is better than the numerical model (being capable of seeing physical insides just through the differential equations) from the point of view of reducing the computing time and clearly seeing through the physical relationship among different amplifier parameters. Analytical model provides the integrated solution of the pump/signal + noise equations. To date, there exists two such steady-state models: the first one [1] applies to the case of unsaturated amplification regime and provides the spectral gain and noise characteristics of the EDFA. In particular, the model also predicts the difference in amplified spontaneous emission (ASE) noise, or noise figure, between forward and backward pumping. The second model [2-5] applies to the saturated amplification regime, but excludes ASE noise. The model initially developed

by Peroni and Tamburrini [2] is restricted to a single signal wavelength. The model developed by Saleh et al.[3,4] represents a generalization of [2] to the multiwavelength case, with as many pump and signal channels in either propagation direction. Jopson and Saleh [4] extended [3]'s techniques to the treatment of an amplifier with self-saturation by dividing such a length of amplifier into sections short enough not to be self-saturated each. Additionally, [6] showed that the Saleh et al. model could in fact include the effect of ASE noise with reasonable accuracy, considering that noise can be described by equivalent input signals of $n_{sp} \approx 1-1.5$ photons per frequency bin, polarization state, and propagation direction. Thus, the Saleh et al. model can be regarded as the most versatile tool for a full analytical description of the EDFA characteristics. Finally, as a complemental study to [3], Pfeiffer and Bulow [7] took into account the transverse extension of mode fields and doping distribution.

We adopt Saleh et al.'s model since the amplifier that needs to be gain controlled is often an in-line amplifier, which operates in high saturated regime [8]. We first recall the required assumptions for Saleh's model: 1) There is no relevant excited-state absorption (i.e., the pump is in the 980 or 1480 nm band); 2) The Stark-split energy levels of the erbium ions are homogeneously broadened; 3) The amplifier is not self saturated by its own ASE noise (i.e., the amplifier's gain is less than about 25 dB); and 4) The area of the erbium-doped active regime is small compared to that of the optical mode at each wavelength of interest. Under these conditions, the analytical expression is directly written down [3] as follows (throughout this chapter, optical power, P, is

expressed in units of photons per unit time, i.e., the photon flux--the actual power normalized by the photon energy)

$$G_k = \exp\left\{-\alpha_k L + \frac{P_l^{IS}}{P_k^{IS}}\left[\ln(G_l) + \alpha_l L\right]\right\} \tag{4.1}$$

or

$$G_k = \exp\left\{-\alpha_k L + \frac{(g^*(\lambda_k) + \alpha(\lambda_k))}{(g^*(\lambda_l) + \alpha(\lambda_l))}\left[\ln\beta + \alpha_l L\right]\right\} \tag{4.2}$$

where $1/\beta$ is the loop attenuation, L the amplifier length, k the number of channels, the other parameters have common meanings. The physical process of clamping gain is that a portion of the ASE is coupled at the output of the amplifier, filtered at a selected wavelength, attenuated and finally re-injected at the input--the amplifier is thus in a ring-laser configuration (Fig.4.1). Lasing conditions are controlled by tuning the selected wavelength and varying the attenuation in the feedback loop. All the quantities in the exponential of (4.1) or (4.2) are constants independent of P_k^{in}, thus the gains at all signal channels are controlled through β, and are independent of the input power levels P_k^{in}. An increase of the total signal input power is automatically compensated by a decrease of the power in the feedback loop. The concept that one of assumptions for Saleh's model is the effect of ASE on the signal gain can be neglected should not be confused with the concept that part of ASE intensity is feedbacked to form the laser channel. The initial power of the ASE around the laser wavelength bin may be very small (only for initial starting of laser action), however, it becomes the different physical essential once the lasing along the feedback loop is built up.

Note that the Equs. (4.1) and (4.2) also apply to linear laser cavity cases [4,5,7-9,11, Chapter 3], where the initial laser action is caused by the reflection of Bragg grating reflectors located at two ends.

Equs.(4.1) and (4.2) reflect the homogeneous broadened property of the laser gain medium since the saturated gain at one wavelength can predict the gain at any other wavelengths. Both of these equations are explicit concise expressions, which thus leads us to be able to do as many basic mathematical calculations as possible. Having introduced the dB gain, $G_k(dB)=10\log_{10}(G_k)$, to (4.1),

$$G_k^{dB} = A\left\{-\alpha_k L + \frac{P_l^{IS}}{P_k^{IS}}\left[\frac{G_l^{dB}}{A} + \alpha_l L\right]\right\} \quad \text{(in dB)} \tag{4.3}$$

here $A\equiv(10\log_{10} e)=4.343$, G_l's dimensionless unit (exponential value) has also been converted to dB, G_l^{dB}. α_{kl}'s are not exponential values, but dB/m values. We can get the following results:

1) G_k^{dB} has a linear relationship with G_l^{dB}, which is a reflection of homogeneous broadening characteristics of laser gain medium, where "l" does not necessary represent the laser channel and could be any signal channel (the G_l^{dB} would be fixed, equal to the loop loss, if it expresses a laser channel);

2) Assuming that there exists a function relationship: $G_k^{dB} = f[G_l^{dB}]$ in terms of Equ. (4.3), then

$$\frac{\Delta(G_k^{dB})}{\Delta(G_l^{dB})} = \frac{P_l^{IS}}{P_k^{IS}} = \frac{g^*(\lambda_k) + \alpha(\lambda_k)}{g^*(\lambda_l) + \alpha(\lambda_l)} \neq 1 \qquad (\text{if } l \neq k) \qquad (4.4)$$

which discloses another property of homogeneous broadening characteristics of such a doped-fiber gain medium--the amount of gain suppression at different spectrum positions is different (independent of the specific gain compression degree--but there exists a limited gain compression range or the LHS of (4.4) will vary with the level of gain compression as such a limit is exceeded [9], amplifier length, and any other amplifier design parameters, just dependent on the glass composition and working temperature) which is a result of Stark splitting of two laser levels, $^4I_{15/2}$, $^4I_{13/2}$ (compared to case of single level laser transition); which also proves that the gain change at different channels will normally be different even if the gain spectrum was initially flat when the power load of an EDFA increases so that the gain is compressed [9]; and which shows that selecting the laser wavelength to be as close as possible to the peak of the sum of the absorption and emission cross-sections minimizes the amplifier sensitivity to loss change. Note that the concept of multi-channel gain tilt is, presently, also defined as (4.4)--the ratio of gain change at any channel to the gain change at a selected reference channel due to a certain number of recirculations of the optical channels through the line amplifier.

3) To evaluate the amplifier sensitivity to loop loss change from another quantity, we define the term "sensitivity" to describe the ratio of the per unit variation in G_k^{dB} to a small per unit variation in G_l^{dB}:

$$S_l^k = \frac{d(G_k^{dB})/G_k^{dB}}{d(G_l^{dB})/G_l^{dB}} = \frac{d\ln(G_k^{dB})}{d\ln(G_l^{dB})} \tag{4.5}$$

From this equation we can find the sensitivity of the G_k^{dB} to the loop loss β ($\equiv G_l^{dB}$):

$$\begin{aligned} S_l^k &= \frac{d(G_k^{dB})/G_k^{dB}}{d(G_l^{dB})/G_l^{dB}} = \frac{d(G_k^{dB})}{d(G_l^{dB})}\cdot\frac{G_l^{dB}}{G_k^{dB}} = \frac{G_l^{dB}}{G_l^{dB} + AL\left(\alpha_l - \frac{P_k^{IS}}{P_l^{IS}}\alpha_k\right)} \\ &= \frac{G_l^{dB}}{G_l^{dB} + AL\left(\alpha_l - \frac{(g_l^{\bullet}+\alpha_l)}{(g_k^{\bullet}+\alpha_k)}\alpha_k\right)} = \frac{G_l^{dB}/L}{G_l^{dB}/L + A\left(\frac{\alpha_l g_k^{\bullet} - \alpha_k g_l^{\bullet}}{\alpha_k + g_k^{\bullet}}\right)} \\ &= \frac{G_l^{dB}/L}{G_l^{dB}/L + A\alpha_l\left(\frac{g_k^{\bullet} - \alpha_k \exp\left(\left(\frac{hc}{\lambda_c} - \frac{hc}{\lambda}\right)\Big/kT\right)}{\alpha_k + g_k^{\bullet}}\right)} \end{aligned} \tag{4.6}$$

here the McCumber theory has been used for the last equality[10], where λ_c is a cross-over wavelength, fulfilling $\alpha(\lambda_c) = g^{\bullet}(\lambda_c)$. It shows that for minimizing the

amplifier sensitivity to loop loss change the loop loss should be selected as small as possible, i.e., the amplifier has an operating point (average population inversion) as low as possible; the lasing wavelength selected as close as the ASE peak (for EOO6 EDF, as λ_l=1527 nm the S_l^k approaches the minimum value)--but no monotone relation with the lasing wavelength unlike the result shown in (4.4) (the plotting of S_l^k versus lasing wavelength sees Fig. 4.2). These choices to the loop loss and lasing wavelength (assuming that the lasing wavelengths are shorter than the ASE peak wavelength) are opposite to the requirement of the fixed average population inversion (i.e., fixed the signal gain), where there is a combination between selecting the loop loss and lasing wavelength to be able to sustain the signal gain--a longer lasing wavelength should be combined with larger cavity loss, and vise verse; coincide with the requirement of the fixed average population inversion (the case when the lasing wavelengths longer than the ASE peak wavelength)-- a longer lasing wavelength should be combined with lower cavity loss, Fig. 4.4. Actually, Fig.4.4 can be explained from gain coefficient spectrum, Fig.2.4.

4) Following ref. [11], here we derive the analytical model of amplifier (with laser AGC) spectral properties. First of all, introducing the exponential gain coefficient, $g_k = \ln G_k$, then

$$g_k = \left\{ -\alpha_k L + \frac{(g_k^* + \alpha_k)}{(g_l^* + \alpha_l)} \left[\ln \beta + \alpha_l L \right] \right\} \tag{4.7}$$

For two wavelengths λ_i and λ_j, the ratio of the differential gains resulting from changes in a) β; b) EDF length L; c) α_i or λ_i ,

$$\text{a) } \frac{dg_i}{dg_j}=\frac{P_j^{IS}}{P_i^{IS}}=\frac{\alpha_i+g_i^*}{\alpha_j+g_j^*}=\frac{\Gamma_i(\sigma_i^a+\sigma_i^e)}{\Gamma_j(\sigma_j^a+\sigma_j^e)} \tag{4.8}$$

here $\frac{dg_k}{d\beta}=\frac{P_i^{IS}}{P_k^{IS}}\frac{1}{\beta}$ has been used. It is seen that (4.8) is the same as (28) in [11] since the change in β will lead to the change of the average population inversion, and thus the change of controlled G_k.

$$\text{b) } \frac{dg_i}{dg_j}=\frac{-\alpha_i+\frac{P_i^{IS}}{P_i^{IS}}\left(\alpha_i+\frac{1}{\beta}\frac{d\beta}{dL}\right)}{-\alpha_j+\frac{P_i^{IS}}{P_j^{IS}}\left(\alpha_i+\frac{1}{\beta}\frac{d\beta}{dL}\right)} \tag{4.9}$$

here assuming that β is dependent on L, and thus $\frac{dg_k}{dL}=-\alpha_k+\frac{P_i^{IS}}{P_k^{IS}}\left(\alpha_i+\frac{1}{\beta}\frac{d\beta}{dL}\right)$ has already been used.

c) The same as (4.8) since $\frac{dg_k}{d\alpha_i}=\frac{1}{P_k^{IS}}\left(\frac{dP_i^{IS}}{d\alpha_i}\ln\beta+LP_i^{IS}+\frac{dP_i^{IS}}{d\alpha_i}L\alpha_i\right)$. The same result would be obtained if the variation of gain was due to λ_i.

5) We have the same expression of quantum conversion efficiency (QCE) as [11], where $QCE \equiv \frac{P_s^{out} - P_s^{in}}{P_p^{in}}$ [12]. The general expression for PCE is as follows

$$(QCE)_k \equiv \frac{P_s^{out} - P_s^{in}}{P_{in}^P} \equiv \frac{P_k^{out} - P_k^{in}}{P_{in}^P} = \frac{P_k^{in}(G_k - 1)}{P_{in}^P}$$
$$= \frac{P_k^{in}}{P_{in}^P}\left[\exp\left(-\alpha_k L + \frac{P_l^{IS}}{P_k^{IS}}(\ln\beta + \alpha_l L)\right) - 1\right] \tag{4.10}$$

From the above equation, it is seen that the QCE will linearly increase with the increase of input signal power if the lasing works--that is like the small input signal case.

6) The calculation of average population inversion, $\bar{n}_2$:

Signal (the kth beam) gain may be expressed in terms of average inversion $\bar{n}_2$, i.e.,

$$G_k = \exp\left\{\left[(\alpha_k + g_k^*)\bar{n}_2 - \alpha_k\right]L\right\} \tag{4.11}$$

Combining with (4.1), we have

$$\bar{n}_2 = \frac{P_l^{IS}}{P_k^{IS}}\frac{\ln\beta + \alpha_l L}{L(g_k^* + \alpha_k)}$$
$$= \frac{\alpha_l}{\alpha_l + g_l^*} + \frac{\beta(dB)/L}{(10\log_{10} e)\cdot(\alpha_l + g_l^*)} \tag{4.12}$$

where for the last equality the definition of intrinsic saturation power of the l(k)th beam $P_{l,k}^s = \frac{A}{\Gamma_{l,k}(\sigma_{l,k}^e + \sigma_{l,k}^a)\tau}$ and $\Gamma_l = \Gamma_k$ have been used. (4.12) shows that the average population inversion is determined only by the parameters associated with lasing wavelength and the inversion is balanced by laser absorption and loop loss which are filling the metastable level, and stimulated emission by the laser acting to deplete it; and by the cavity loss per unit EDF length (loss density), not total cavity loss. The $\left(\frac{g_l^*}{\alpha_l}\right)$ and $(\alpha_l + g_l^*)$ against λ_1 curves [Fig.4.3] show that the large $\bar{n}_2$ favors short lasing wavelength (assuming that it is less than the ASE peak wavelength) since there are small values of both $\left(\frac{g_l^*}{\alpha_l}\right)$ and $(\alpha_l + g_l^*)$ for short wavelengths. As lasing wavelength is longer than the ASE peak wavelength, we plot $\bar{n}_2$ against lasing wavelength for various cavity loss/per unit length, β/L, Fig. 4.4, and find out that the larger $\bar{n}_2$ favors longer lasing wavelength (for the smaller cavity loss such as 0.2 dB/m, average population inversion increases as the lasing wavelength passes through the ASE peak; for the other larger cavity losses selected here, the average population inversion decreases first up to lasing wavelength around 1560 nm and then increases again). In fact, the relationship between the average population inversion and the lasing wavelength, cavity loss can be directly observed form (4.2)--small values of $(\alpha_l + g_l^*)$, corresponding to short lasing wavelength as it is shorter than ASE peak

wavelength or long wavelength as it is longer than ASE peak wavelength, will lead to large exponential values of RHS of (4.2) (the effect of $(\alpha_l L)$ less), i.e., large G_k, and thus high population inversion; large cavity loop loss will lead to large G_k, i.e., high population inversion.

Alternative way to derive the average population inversion is to start with the steady-state rate equation [3] for the fractional population of the upper level, i.e.,

$$n_2(z) = \frac{-\tau}{\rho A}\sum_{j=1}^{N}\mu_j\frac{\partial P_j(z)}{\partial z} \tag{4.13}$$

Taking the average along the amplifier length L to both sides of the above equation,

$$\begin{aligned}\bar{n}_2 &\equiv (1/L)\int_0^L n_2(z)\cdot dz = -(\frac{1}{L})\frac{\tau}{\rho A}\sum_{j=1}^{N}\mu_j\left(P_j(L)-P_j(0)\right)\\ &= (\frac{1}{L})\frac{\tau}{\rho A}\sum_{j=1}^{N}\left(P_j^{in}-P_j^{out}\right) = (\frac{1}{L})\frac{\tau}{\rho A}(\ln\beta+\alpha_l L)P_l^{IS}\\ &= \frac{\ln\beta+\alpha_l L}{L(g_l^{\bullet}+\alpha_l)} = \frac{\alpha_l}{\alpha_l+g_l^{\bullet}}+\frac{\beta(dB)}{(10\log_{10}e)\cdot L\cdot(\alpha_l+g_l^{\bullet})}\end{aligned} \tag{4.14}$$

Here ρ is a density of active atoms (erbium), i.e., n_t . (4.14) is identical to (4.12). Considering a special example[11]: A high pump power keeps the inversion be independent of the position of amplifier and then

$$\bar{n}_2 = \frac{\sigma_{ap}}{\sigma_{ap}+\sigma_{ap}} = \frac{\alpha_p}{\alpha_p+g_p^{\bullet}} \tag{4.15}$$

Let (4.14) be equal to (4.15), we get the following equation,

$$\frac{\alpha_l}{\alpha_l + g_l^*} + \frac{\beta(dB)}{(10\log_{10} e)\cdot L\cdot(\alpha_l + g_l^*)} = \frac{\alpha_p}{\alpha_p + g_p^*} \tag{4.16.1}$$

$$\frac{\alpha_l}{\alpha_l + g_l^*} + \frac{\beta(dB)/(10\log_{10} e\cdot L)}{(\alpha_l + g_l^*)} = \frac{\alpha_p}{\alpha_p + g_p^*}$$

(4.16.2)

It indicates that the pump power is totally absorbed/blanced by the laser power inside the feedback loop if the population inversion keeps unchanged along the whole amplifier length.

The average spontaneous factor $\bar{n}_{sp}$, ref [13] introducing the concept of the "average noise figure", can be obtained as follows

$$\bar{n}_{sp} = \frac{\sigma_e \bar{n}_2}{(\sigma_e \bar{n}_2 - \sigma_a \bar{n}_1)} = \frac{\sigma_e \bar{n}_2}{(\sigma_e + \sigma_a)\bar{n}_2 - \sigma_a} = \frac{g_k^* \bar{n}_2}{(g_k^* + \alpha)\bar{n}_2 - \alpha} \tag{4.17}$$

It shows that $\bar{n}_{sp}$ will decrease with the increase of $\bar{n}_2$. Note that we could not directly take the average to the definition of n_{sp} to get $\bar{n}_{sp}$ or it would not make a sense.

7) The calculation of critical input (output) power, $P_k^{in,c}$ ($P_k^{out,c}$): Provided that only one signal channel (the kth beam of signal) exists (of course, there is still pump beam), then [3]

$$G_k = \exp\left\{-\alpha_k L + \frac{1}{P_k^{IS}}[(P_p^{in} - P_p^{out}) + (P_k^{in} - P_k^{out})]\right\} \tag{4.18}$$

If $P_k^{in} \Rightarrow P_k^{in,c}$, then $G_k \Rightarrow G_k^c$, then

$$P_k^{in,c} = \frac{P_k^{IS}}{G_k^c - 1}\left[\frac{P_p^{in}(1-G_p^c)}{P_k^{IS}} - \ln G_k^c - \alpha_k \cdot L\right] \tag{4.19}$$

Thus, the critical output power $P_k^{out,c}(\equiv G_k^c \cdot P_k^{in,c})$,

$$P_k^{out,c} = \frac{G_k^c \cdot P_k^{IS}}{G_k^c - 1}\left[\frac{P_p^{in}(1-G_p^c)}{P_k^{IS}} - \ln G_k^c - \alpha_k \cdot L\right] \tag{4.20}$$

where the G_k^c is just the controlled signal gain G_k of the kth channel, and G_p^c is determined by (4.1) where G_t has been known. Eq. (4.20) shows that $P_k^{out,c}(\equiv G_k^c \cdot P_k^{in,c})$ ia proportional to the input pump power, which will be confirmed in next section. If there exist more than one channels (N channels), what is the corresponding result? First of all, assuming that all channels have the same input power each, and then [3]

$$\begin{aligned} G_k &= \exp\left\{-\alpha_k L + \frac{1}{P_k^{IS}}[(P_p^{in} - P_p^{out}) + \sum_{j=1}^{N}(P_j^{in} - P_j^{out})]\right\} \\ &= \exp\left\{-\alpha_k L + \frac{1}{P_k^{IS}}[(P_p^{in} - P_p^{out}) + \sum_{j=1}^{N} P_j^{in}(1-G_j)]\right\} \\ &= \exp\left\{-\alpha_k L + \frac{1}{P_k^{IS}}[(P_p^{in} - P_p^{out}) + P_k^{in} \cdot \sum_{j=1}^{N}(1-G_j)]\right\} \end{aligned} \tag{4.21}$$

Similar to (4.18)-(4.19), we have

$$P_k^{in,c} = \frac{P_k^{IS}}{\sum_{j=1}^{N}(G_j^c - 1)}\left[\frac{P_p^{in}(1-G_p^c)}{P_k^{IS}} - \ln G_k^c - \alpha_k \cdot L\right] \tag{4.22}$$

We may change (4.22) to the expression (4) in [14] using the necessary relations stated in [14], where the argument of average population inversion is replaced by G_k^c here. The second, if input power of each channel is different, we have

$$\begin{aligned} G_k &= \exp\left\{-\alpha_k L + \frac{1}{P_k^{IS}}[(P_p^{in} - P_p^{out}) + \sum_{j=1}^{N}(P_j^{in} - P_j^{out})]\right\} \\ &= \exp\left\{-\alpha_k L + \frac{1}{P_k^{IS}}[(P_p^{in} - P_p^{out}) + \sum_{j=1}^{N} P_j^{in}(1-G_j)]\right\} \\ &= \exp\left\{-\alpha_k L + \frac{1}{P_k^{IS}}[(P_p^{in} - P_p^{out}) + P_k^{in}(1-G_k) + \sum_{j\neq k}^{N} P_j^{in}(1-G_j)]\right\} \end{aligned}$$

(4.23)

and then

$$P_k^{in,c} = \frac{P_k^{IS}}{G_k^c - 1}\left[\frac{P_p^{in}(1-G_p^c)}{P_k^{IS}} + \frac{1}{P_k^{IS}}\sum_{j\neq k}^{N} P_j^{in}(1-G_j^c) - \ln G_k^c - \alpha_k \cdot L\right] \tag{4.24}$$

where P_j^{in} does not mean $P_j^{in,c}$, is a designed input signal power. (4.24) indicates that the critical input power varies with the channel.

8) The optimum amplifier length: the amplifier design with laser AGC involves determining laser wavelength, cavity loss, noise figure, PCE, and amplifier length for

given required signal gain. The optimum amplifier length for a) minimum noise figure, i.e, minimum $\overline{n}_{sp}$, b) maximum QCE, and c)maximum critical input power.

a) From (4.12), $\overline{n}_2$ will increase, i.e., $\overline{n}_{sp}$ will decrease, with the decrease of amplifier length L.

b)The analyses of $(QCE)_k$ versus L in (4.10) shows that if $\frac{g_k^*}{\alpha_k} > \frac{g_l^*}{\alpha_l}$ is met, the $(QCE)_k$ will increase with L, or vice verse. As a result, the optimum length of amplifier depends on the relative spectrum positions of lasing and signal(s) channel and thus for multi-channels case there maybe exist design tradeoff for different signal channels. Fig. 4.5 gives two opposite examples. Note that the relationship between $(QCE)_k$ and L is actually that between G_k and L in terms of (4.10).

c) The analyses of L against $P_k^{in,c}$ in (4.19) shows that the short amplifier length can cause large $P_k^{in,c}$ if the amplifier gain for signal and pump channels were sustained (it should be fixed since it is an amplifier with a constant gain). This conclusion is very obvious in physics. [14] plotted optimum amplifier length for maximum critical input power vs. pump power for different required signal gain.

Additionally, if the issue is: what is the optimum amplifier length L for which the EDFA gain is maximum? The derivation in (4.2) with respect to length L yields

$$\frac{\partial G_k}{\partial L} = \left\{ -\alpha_k + \frac{(g^*(\lambda_k) + \alpha(\lambda_k))}{(g^*(\lambda_l) + \alpha(\lambda_l))} \left(\alpha_l + \frac{1}{\beta} \frac{\partial \beta}{\partial L} \right) \right\} \cdot G_k \tag{4.25}$$

which gives the length optimization condition at wavelength λ_k,

$$-\alpha_k + \frac{(g^*(\lambda_k)+\alpha(\lambda_k))}{(g^*(\lambda_l)+\alpha(\lambda_l))}\left(\alpha_l + \frac{1}{\beta}\frac{\partial\beta}{\partial L}\right) = 0 \tag{4.26}$$

Equ. (4.2) also gives the gain coefficient expression as follows,

$$g_k(L) \equiv \frac{1}{P_k(L)}\frac{\partial P_k(L)}{\partial L} = \left\{-\alpha_k + \frac{(g^*(\lambda_k)+\alpha(\lambda_k))}{(g^*(\lambda_l)+\alpha(\lambda_l))}\left(\alpha_l + \frac{1}{\beta}\frac{\partial\beta}{\partial L}\right)\right\}. \tag{4.27}$$

which is identical to (4.25).

9) Analytical model makes possible a straightforward numerical evaluation of the EDFA spectral gain characteristics, including the gain spectrum compression, tilt (see chapter 7), ripple change under varying input signal power/wavelengths conditions, and the optimization and testing of gain-equalizing filters under various pumping and multiwavelength signal saturation regimes .

4.3 Numerical modeling

The previous section gave analytical expressions of the gain for an amplifier with laser AGC and the characteristics of such an amplifier can be seen intuitively, the signal gain being independent of the pump wavelength, power, and signal power, etc., for example. Additionally, it is easy to allow us to do a lot of analytical manipulations with respect to the analytical expression. However, such an analytical model can not deal with noise features, the effect of the lasing channel on the noise figure of the

amplifier can not be addressed. Also, some features predicted by the analytical model need to be confirmed by the full numerical integration of differential equations. This section will examine numerically the properties of an amplifier with laser AGC (cases of steady-state) in terms of Giles' [11] model. The EDFA configuration simulated here consists of a dual-stage EDFA, counter-pumped with 90 mW of pump power at 980-nm in stage 1 and copumped with 90 mW at 980-nm in stage 2. 1534 nm is selected as lasing wavelength; the compressed signal gain (@1552 nm) is 10 dB.

1) Fig.4.6 shows the working principle of laser AGC--the signal gain versus the input signal power. a) find out the small signal gain @ 1552 nm--run the program with only one signal (1552 nm) input to get saturation curve, i.e., the curve of signal gain vs. input signal power (the small signal gain @ 1552 nm is 36.9 dB for the 2-stages MONET amplifier structure without the ASE filter in between the 1st and 2nd stage); b) find out the P(1552nm,in) associated with 10 dB gain compression with two signal channels (1552 and 1558 nm) on for the case of 7 loss/restore out of 8 WDM channels; c) find out the cavity loss associated with 10 dB gain compression (for 1552nm), which is equal to the gain at some selected lasing wavelength; d) run the program with two signal channels input and lasing channel on and get the Fig.4.6. It shows that the signal gain is clamped to ~27 dB up to a maximum critical input signal power (1552 nm) of -19.0 dBm. Beyond this value, the laser oscillation stops and the amplifier response is linear, i.e., the transmission decreases linearly with the input signal [2,3, Chapt.3]. There is no obvious impact of the lasing channel power on noise figure of

the amplifier. Note that the NF of amplifier almost is almost constant as long as the input signal is less than the critical input power, $P^{in,c}$, and slowly increases as the P(s,in) approaches the critical input power and then increases relatively faster as the P(s,in) is beyond this value.

2) The signal gain vs. input pump power.

Fig.4.7 shows the signal (1552 nm) gain vs. input signal power for various input pump power levels (90, 120, 150, 180 mw, respectively). It was shown that the amplifier gain was clamped to ~27 dB, but the maximum critical input power increase with the pump power level [4,5, Chapt.3].

3) The signal gain vs. pump wavelength (980 or 1480 nm).

Fig.4.8 shows the plotting of signal gain vs. pump wavelength (980 or 1480 nm). It was seen that the signal gain did not vary with the pumping wavelength, which exactly agrees with the analytical prediction in section 4.2, and however, the maximum critical input power is larger for 980 nm pump than for 1480 nm pump [8, Chapt.3]. Additionally, the spontaneous emission factor is lower for 980 nm pump than that for 1480 nm pump. It indicates that 980 nm pump is better than 1480 nm pump in the sense here.

4) The maximum critical input power vs. pump power.

Based on Fig.4.7 we can get the curve of maximum critical input power vs. pump power, Fig.4.9, where pump power levels in both mw (linear unit) and dBm were shown. It was shown that there is an almost linear relationship between maximum critical input power and pump power.

5) Showing the amplifier gain sensitivity to cavity loss change--the signal gain vs. cavity loss for different lasing wavelengths (1505, 1534, and 1570 nm, respectively). The absorption and emission coefficients (in dB/m) of EOO6 for wavelength 1505, 1534, and 1570 are (0.76259, 0.439243), (1.259824,1.284824), and (0.281131,0.59273), respectively. First of all, finding out different loop losses associated with these three lasing wavelengths when the signal gain @ 1552 nm is depressed 10 dB: 3.84 dB (@1505 nm), 31.69 dB (@1534 nm), and 17.53 dB (@1570 nm), respectively; the signal (@1552 nm) gain variations as the loop loss is reduced 3 dB are: (18.1802 $\Rightarrow$ 2.47127)dB for lasing 1505 nm, (26.8245 $\Rightarrow$ 24.9115)dB for lasing 1534 nm, and (25.8857 $\Rightarrow$ 19.8635)dB for lasing 1570 nm. This indicates that the signal gain variations to the loop loss variations decrease with the increase of the sum of the absorption and emission coefficient and approaches minimum as such a sum of the absorption and emission coefficient is maximum, i.e., the lasing wavelength closes to the ASE peak. This result agrees with the analytical one (Eqs. (4.4) and (4.6)).

6) Showing asymmetric cavity design, i.e., *the loss at signal input end less than that at the output end,* to ensure minimum laser power at the signal input end of the amplifier and thus improve the noise figure of the amplifier, which was studied in linear cavity laser design [9, Chapt.3]. This conclusion was also confirmed by the ring laser cavity design, Fig.4.10. It gives us a guide for designing a low NF amplifier, a coupler with a low transmission loss in signal path (i.e., a high corresponding coupling loss in lasing path) should be selected as the input coupler such that the transmission loss of the output coupler should be high (i.e., the low corresponding coupling loss in lasing path) to sustain the total loop loss. For example, a 10:90% tab can be acted as an input coupler and while a 50:50% as an output coupler. It indicates that the effect arising from both input lasing intensity and the input transmission loss on the noise figure of the amplifier is the same. Note that this conclusion will also apply as the lasing wave counter-propagates with the signal.

7) Fig.4.11 shows the effects of forward-lasing and backward-lasing propagation on the NF of the amplifier. It is shown that although the signal gain-clamped is the same for both lasing directions, there exists large difference of the NF between forward and backward lasing direction as the signal gain is controlled very well (i.e., the input signal power < the maximum critical input power). Specifically, there is smaller value (almost half) of NF as the lasing wave co-propagates with the input signal wave compared to the counter-propagating case. Additionally, the trend of two NF curves shows obvious differences: for the backward-lasing , the NF is pretty large as the

P(s,in) is small and then decreases with the increase of P(s,in) and finally overlaps with that forward-lasing case; and while the NF almost stays in a constant value as the P(s,in) is small and then slowly increases. It indicates that the lasing intensity at the signal input end of the amplifier, for the backward-lasing, is very large such that it severely degrades the population inversion at the input end of the amplifier and then in turn degrades the NF of the amplifier. That is the reason in [15] where we used isolators to force the lasing wave to co-propagate with the input signal waves to reduce the impact of lasing wave on the NF of the amplifier. Fig.4.11 also clearly shows that the NF will be exactly the same after the lasing stops. Note that isolators along the feedback loop have been removed to compare co- and counter- lasing feedback cases.

4.4 Comparisons of linear and ring laser scheme

This section will address some comparisons between the linear (F-P, or called standing wave cavity) and ring laser scheme, shown in Fig.3.1, in terms of the analytical and numerical analyses shown previously.

Analytical relationship: Based on the laser principle--when lasing takes place, the optical wave round-trip net gain is equal to unity, i.e.,

$$l_c \exp\left\{r\left[\left(\alpha(\lambda)+g^*(\lambda)\right)\overline{n}_2-\alpha(\lambda)\right]L\right\}=1 \qquad (4.28)$$

where l_c is the total cavity loss, for instance, l_c would be (r_1r_2) for a linear cavity structure where r_1 and r_2 are the grating reflectivities at the input and output ends, respectively. (4.28) unifies both structures of linear and ring cavity, where r=2 for linear cavity, and while r=1 for ring cavity. Therefore, combining (4.28) with (4.1) (Gain is expressed in terms of lasing parameters) and (2.1) (Gain is expressed in terms of average population inversion), we can analytically discuss linear and ring lasing issue using the same set of expressions.

Numerical relationship: Here we used the same simulated parameters (i.e., the same losses arrangement, all isolators of a MONET 2-stages amplifiers have been removed) to find out the different effect of linear and ring laser configuration on the amplifier characteristics. Fig.4.12 shows that the gain and noise figure @ 1552 nm as a function of input signal power levels. As excepted, the signal gain was compressed in linear cavity configuration more than that in ring laser configuration. As a result, the noise figure (NF) was degraded in linear cavity configuration more severe than in ring laser configuration. This can be explained that all reflected lights from both cavity ends come back to the cavity for linear cavity design and while only one reflected light passes through the ring laser cavity and thus total laser intensity inside the linear laser cavity is larger than inside the ring laser cavity [15], resulting in more compression of the population inversion, and larger NF and maximum critical input signal power for a linear cavity design. Additionally, the relationship of NF versus the input signal power

for a linear cavity design was observed to be different from that one in a ring laser cavity design, which can be explained like that given in Fig.4.11.

References:

[1] E. Desurvire, Erbium-doped fiber amplifiers: Principles and Applications, pp. 36-40, 104-105.

[2] M. Peroni and M. Tamburrini, "Gain in erbium-doped fiber amplifiers: A simple solution for the rate equation", Optics Lett., 15 (1990) 842; see also ref. [1] pp. 40-43.

[3] A.A.M. Saleh, R.M. Jopson, J.D. Evankow, and J. Aspell, "Modelling of gain in erbium-doped fiber amplifiers", IEEE Photon. Technol. Lett., 2 (1990) 714; see also ref. [1] pp.43-46.

[4] R.M. Jopson and A.A.M. Saleh, "Modelingof gain noise in erbium doped fiber amplifiers", SPIE Fiber Laser Sources and Amplifiers III, 1581 (1991), 114.

[5] E. Desurvire, "An explicit analytical solution for the transcendental equation describing saturated erbium-doped fiber amplifiers", Optical Fiber Technology, 2 (1996) 367.

[6] Same as [1], see pp. 379-382; see also: T. Georges and E. Delevaque, "Analytic modeling of high-gain erbium-doped fiber amplifiers", Optics Lett., 17 (1992) 1113.

[7] Th. Pfeiffer and H. Bulow, "Analytical gain equation for erbium-doped fiber amplifiers including mode field profiles and dopant distribution", IEEE Photon. Technol. Lett., 4 (1992) 449.

[8] J.-M.P Delavaux and J.A. Nagel, "Multi-stage erbium-doped fiber amplifier designs", IEEE J. Lightwave Technol. 13 (1995) 703.

[9] J. Nilsson, W.H. Loh, S.T. Hwang, J.P. de Sandro, and S.J. Kim, "Simple gain-flattened erbium-doped fiber amplifier with a wide dynamic range", OFC'97, Dallas, Texas, OSA Technical Digest, WF3, p.129; and references therein.

[10] D.E. McCumber, "Theory of phononterminated optical masers", Phys. Rev., 134A (1964) 299; see also: J. Nilsson et al., "Analysis of AC Gain Tilt in Erbium-doped Fiber Amplifiers", 8 (1996) 515.

[11] C.R. Giles and E. Desurvire, "Modeling erbium-doped fiber amplifiers", IEEE J. Lightwave Technol., 9(1991) 271.

[12] Same as [1], p. 340.

[13] V.J. Mazurczyk and J.L. Zyskind, "Polarization dependent gain in erbium-doped-fiber amplifiers", IEEE Photon. Technol. Letts. 6 (1994) 616.

[14] A. Yu and M.J. O'Mahony, "Modelling of laser-controlled erbium-doped fiber amplifiers", OFC'96, San Jose, OSA Technical Digest, WK14, p.163.

[15] S. Li, H. Ding, and K.T. Chan, "Erbium-doped fibre lasers for dual wavelength operation", Electron. Lett., 33, p.52 (1997).

Chapter 5
Modeling of an Amplifier with Dynamic Laser AGC

5.1 Introduction

Chapter 4 has dealt with the issue of static-state (ss) amplifier with laser AGC based on analytical and numerical calculations. The ss problems apply to those associated with the low frequencies fluctuations (<a few KHz) of the input signal and/or pump intensity and/or local loss. This is determined by the EDFA's slow gain saturation and recovery time. A recent report [1] showed that, despite the slow gain dynamics of individual EDFA's, the power transients for such systems can be very fast. Times for 1 dB power excursion are expected to be as short as 100 ns for chains of 100 amplifiers when seven of eight channels are dropped. As a result, the characteristics of EDFA with laser AGC in time domain must be studied. The EDFA model for transient gain dynamics without AGC can be found out in [2-5], and while the modeling of dynamic characteristics of pure fiber laser can be referred to [6-11]. To the best of our knowledge, so far, there have not been any published results in modeling of a combined (hybrid) system with a (many) single-pass traveling signal(s) field and as well a lasing field. In this chapter, we will numerically model such a system.

5.2 The Dynamic Amplifier Model

For a time-dependent numerical model, like the previous chapter, we will restrict ourselves to a simplified analysis of the EDFA by reducing the problem to that of a

two-level gain medium and use simplifying assumptions to reduce the order of the differential equations. The modeling is based on such an assumption--the transit time of the pump and signal through the EDF medium is faster than the time dependent changes of the atomic population [p.441, 2], i.e., the fluorescence lifetime [p.417, 2] or the modulation period [12]. As a result, the time variation term in coupled propagation-rate equations may be neglected, and while the spatial variation term is sustained. The original equations to describe the whole system is the following coupled propagation-rate equations (Giles' model with time-dependent) with appropriate boundary and input conditions [13; p.411, 2]

$$\frac{dN_2}{dt} = \sum_k I_k \sigma_{ak} \frac{N_1(r,\phi,z)}{h\upsilon_k} - \sum_k I_k \sigma_{ek} \frac{N_2(r,\phi,z)}{h\upsilon_k} - \frac{N_2(r,\phi,z)}{\tau}$$

$$\frac{\partial P_k(z,t)}{\partial z} - \frac{1}{v_g}\frac{\partial P_k(z,t)}{\partial t} = u_k(\alpha_k + g_k^*)\frac{N_2}{N_t}P_k(z,t) \qquad (5.1)$$

$$+ u_k 2g_k^* \frac{N_2}{N_t} h\upsilon_k \Delta\upsilon_k - u_k \alpha_k P_k(z,t)$$

where the optical spectrum is sliced into k intervals of width $\Delta\nu_k$, and intensity $I_k(r, \phi, z)$; the term of " $\frac{1}{v_g}\frac{\partial P_k(z,t)}{\partial t}$ " could be omitted if one of the above conditions is met. Actually, the small transit time of the pump and signal through the EDF medium means that the v_g is large enough such that the term consisting of v_g can be neglected. Note that the model in [4,5] was something like the "lumped element" model, but the longitudinal coordinate was already integrated.

Cares among the relative magnitudes of pulses width, fluorescence lifetime and transit time must be exercised as one handles such specific problems.

The EDFA model assumes a commercially available alumino-germano silicate fiber (Lucent fiber E006), and thus all of the numerical conclusions reported here apply to this specific fiber. However, the modeling algorithm can be applied more generally to any other EDFA configurations taking into account their specific characteristics. The fiber is completely characterized knowing only four parameters; the Er^{3+} absorption coefficient $\alpha(\lambda)$, the gain coefficient $g(\lambda)$, the fiber excess loss l (0.0033 dB/m), and fiber saturation parameter $\zeta = A\, n_t/\tau = 5.58 \times 10^{14}\ m^{-1}\ s^{-1}$. Here A is the erbium core area, n_t is the ion density, τ is the metastable lifetime (10 ms).

The dynamic model used here is based on the spectrally resolved numerical model of Giles, i.e., Eq.5.1, which assumes a homogeneous broadened gain medium. The forward and backward ASE spectra are well resolved in 651 wavelength bands ($\Delta\lambda = 0.2$ nm intervals) over the 1470 nm to 1600 nm range.

The space and time are decomposed into a grid of M x N discrete bins Δz and Δt, respectively. The space equations are integrated iteratively for each time $t = k\,\Delta t$ ($k = 1, 2, \ldots, N$). The initial conditions of the system for the metastable state population [i. e., $n_2\ (z, t = 0)$], is given by solving the steady state inversion

equation of Eq.5.1. The algorithm uses the initial conditions to evaluate the inversion for the first time step Δt. The calculated value of the inversion is then used to calculate the signal, ASE noise spectra, and pump powers. These powers are then used to evaluate the inversion at the next time step 2Δt. By this computationally intense iterative process, we were able to capture and accurately characterize the dynamic behavior of the EDFA.

5.3 Simulation Results and Comparisons with Experiments

The EDFA model assumes a completely homogeneous medium and a commercially available alumino-germano silicate fiber (Lucent fiber E006) with slightly different specifications than those used in the measurements described above. Consequently, the simulation results presented here are not intended for a quantative comparisons with those of the measured data but rather to show the same qualitative trends exihibited by the experimental measurments. The model assumes the same dual-stage EDFA configuration and input parameters (input signal levels, pump power and wavelength, wavelength assignment and number of channels, surviving channel gain, and lasing wavelength) used in the experimental measurements. In some cases, when it was necessary to strictly simulated the eight channels, these channels were spaced 1.6-nm apart in the 1549.4 to 1560.6 nm amplifier band. Since the dynamic model used here assumes a completely homogenous gain, all simulation results presented in this section takes into

account only the dynamic power excursion component arising from relaxation oscillations in the laser.

Fig. 5.1 shows the simulation results corresponding to the experimental results shown in Fig. 3.4c. These results are obtained using the same eperimental parameters used in Fig. 3.4c. As can be seen from the figure, both the frequency and amplitude of the transient power excursions of the surviving channel are lower in the case of adding channels versus that of dropping channels. These simulation results are in excellent qualitative agreement with the experimental results shown in Fig.3.4c. Both simulation and experiment indicate that dropping of channels results in much more severe effects on the surviving channels.

The simulated gain recovery time, t_{rec}, and the relaxation oscillation frequency of the feedback loop along with experimntal results are also shown in Figs.3.5 and 3.6 of chapter 3, respectively. As can be seen from the Figs.5.2 and 5.3, the simulation results are in good qualitative agreement with the experimental measurements, confirming the fact that wavelengths that result in higher dynamic power excursions exhibit longer gain recovery times and lower oscillation frequencies. This is further illustrated by the simulation results shown in Figs.5.2 and 5.3, where the set of curves included in the Figs.5.2 and 5.3 represent a sequence of decreasing denominators in Eq.3.1, starting from maximum value at

the 1530-nm curve at the bottom (minimum power excursions) to the minimum value at the 1563-nm curve at the top (maximum power excursions).

Fig.5.4 shows the simulation results corresponding to the experimental results shown in Fig.3.7. As can be seen from the Fig.5.4, the simulation results are in good qualitative agreement with the experimental measurements shown in Fig.3.7, confirming the fact that as the number of switched channels increases, both the frequency and amplitude of the power excursions experienced by the surviving channels increase.

References:

[1] J.L. Zyskind, Y. Sun, A.K. Srivastava, J.W. Sulhoff, A.J. Lucero, C. Wolf and R.W. Tkach, "Fast power transients in optically amplified multiwavelength optical networks", Proc. OFC'96, San Jose, CA, Postdeadline Paper, PD31 (1996).

[2] E. Desurvire, "Erbium-Doped fiber amplifiers--principles and applications", (John Wiley & Sons, 1994), Chapt.5.

[3] J. Freeman and J. Conradi, "gain modulation response of erbium-doped fiber amplifiers", 5, 224 (1993).

[4] Y. Sun, G. Luo, J.L. Zyskind, A.A.M. Saleh, A.K. Srivastava and J.W. Sulhoff, "Modeling of gain dynamics in erbium-doped fiber amplifiers", LEOS'96, Boston, MA, ThM3, P.365.

[5] Y. Sun, G. Luo, J.L. Zyskind, A.A.M. Saleh, A.K. Srivastava and J.W. Sulhoff, "Model for gain dynamics in erbium-doped fiber amplifiers", Electron. Lett., 32, 1490 (1996).

[6] M. Ding and P.E. Cheo, "Analysis of Er-doped fiber laser stability by suppressing relaxation-oscillation", IEEE photon. Technol. Lett., 8, 1151 (1996).

[7] T. Tellert, F. Di. Pasquale, and M. Federighi, "Theoretical analysis of the dynamic behavior of highly-efficient erbium/ytterbium codoped fiber lasers", IEEE photon. Technol. Lett., 8, 1462 (1996).

[8] Y.T. Chieng, G.J. Cowle, and R.A. Minasian, "Optimization of wavelength tuning of erbium-doped fiber ring lasers", J. Lightwave Technol., 14, 1730 (1996).

[9] Y.T. Chieng, "Derivation of the mode build-up time of tunable fiber lasers", IEEE photon. Technol. Lett., 8, 211 (1996).

[10] Y.T. Chieng and G.J. Cowle, "Relaxation oscillation suppression in tunable fibre lasers", Electron. Lett., 30, 1419 (1994).

[11] M.Y. Frankel, R.D. Esman, and J.F. Weller, "Rapid continuous tuning of a single-polarization fiber ring laser", IEEE photon. Technol. Lett., 6, 591 (1994).

[12] C.R. Giles, E. Desurvire, and J.R. Simpson, "Transient gain and cross talk in erbium-doped fiber amplifier", Optics Letts., 14, 880 (1989).

[13] C.R. Giles and E. Desurvire, "Modeling erbium-doped fiber amplifiers", IEEE J. Lightwave Technol., 9, 271 (1991).

Chapter 6
Modeling of EDFA Chains with Dynamic Laser AGC

6.1 Introduction

We have seen in chapter 3 that both the static power excursions due to SHB and dynamic power excursions arising from inherent laser relaxation-oscillations are small for a single amplifier. If we consider an amplified lightwave system where each amplifier is clamped by laser AGC, what would be the whole effect on the system arising from both of them? This chapter presents a logical model and numerical simulation results for EDFA chains. We show that any degradation at the first EDFA has a cumulative effect at the output of all subsequent EDFA's in the chain. This has the important implication that the length of the chain is a function of the design parameters of the first EDFA in the chain.

6.2 Simulation of transients in EDFA chains stabilization

To be able to see what is the system impact arising from lasing relaxation-oscillations, this section presents numerical results for EDFA chain stabilization, restricted to homogeneous broadening cases. Note that such a simulation model omits such a physical mechanism: the interplay of relaxation-oscillations and SHB. Stabilization is achieved in the following two steps:

1. The gain experienced by individual channels at each EDFA is clamped via all-optical feedback in a ring laser configuration at each amplifier.

2. We filter the compensating signal generated in each stage by using a wavelength selective coupler at both the outputs and inputs.

One concern in using this approach is the possibility of distortion in the initial transients. Fig.6.1 shows the output after the 1st, 3rd, and 6th amplifiers for a lasing wavelength of 1545-nm at each amplifier. The following can be observed from Fig.6.1: 1) There is a significant difference between the initial over and undershoots; 2) The output power is clamped more rapidly; 3) The oscillations of the surviving channel are noticably distorted after the 6th amplifier. All three effects are somewhat related.

When channels are dropped, for all but the 1st EDFA in the chain, the input is an oscillatory signal from the previous stage. The initial spike of the surviving signal, which is determined by the recovery characteristic time of the EDFA, the initial gain of the EDFA, and the initial input waveform of the surviving signal, occurs on a much faster time scale than the lagging lasing signal which can build up to compensate for the dropped channel. The faster power overshoots of the surviving channels limit the power available to the compensating signals to lower values for longer chains. For long enough chains the fast power transients can actually cause the first peak of the compensating signal to be below its steady state power level. The undershoot of the surviving signal is proportional to the overshoot of the lasing signal. Therefore, since the fast power transient in the surviving channel has suppressed the overshoot of the

compensating signal, very little of the undershoot of the surviving signal is associated with the compensating signal for longer chains.

When the oscillating input signal goes below its steady state value this is sensed by the now built up lasing signal which acts to counter this in much the same way it would compensate for a dropped channel. In this way, the undershoots of the surviving signal are clamped. The built up lasing signal at each amplifier is now able to clamp the 2^{nd} overshoot peaks to much smaller power excursions than the first occurrence. Rather than causing the oscillation, the lasing signal is now helping to damp it. The clamping of the output power of the surviving channels is thus accelerated.

The phase difference between the oscillating input signal going into the EDFA's beyond the first, and the lasing signal stabilizing the particular EDFA can lead to distortion in the oscillations of the output surviving signals. Each subsequent amplifier can add its own distortion to an already distorted signal. The effects of this distortion on data format needs to be further investigated.

6.3 Empirical model

1) Analyzing the SHB's effect:

Since the dynamic model used here can not take into account SHB effects, we will outline an approximate linear relationship between static power excursion due to SHB and the number of amplifiers in a cascade. We assume that a cascaded amplifier

system with each gain clamped by laser AGC; and all channels (including laser control channel) locate in a flat spectral gain regime; the static power excursions maitain the same provided the good gain controllabity is satisfied; and 4 of 8 channels dropped. Suppose that there is 30 dB difference (in terms of my experimental observations from OSA) between signal peak and ASE peak level and almost equal peak power level among lasing channel and signal channels for 15 dB gain compressions. After 4 channels have drooped, the lasing channel power will add 3 dB more compared to initial power level to clamp the signal gain if without the existence of SHB, and while now 2.7 dB higher (here the worst case was considered as the lasing wavelength is around 1534 nm) due to the effect of SHB. With the increase of the amount of amplifiers passed by the surviving channel, the surviving channel power increases by 0.3 dB (My experimental measurement was 0.31 dB. For easy estimation, 0.3 dB was counted) every time it passes a succeeding amplifier and while the lasing channel power level decreases by 0.3 dB. Such an analysis will remain the same until a short chains of such a system (~5 EDFAs), where the surviving channel will have the same power level as the lasing channel. In this way, the static power excursion (ΔP_{SHB}) will linearly accumulate. After the number of the amplifier that the surviving channel passes through is more than the 5th, the lasing channel power reduces again and begins to be less than the surviving channel power, this case will continue until the lasing peak power remains 15 dB more than the ASE peak level (based on my experimental observations, it was confirmed that the peak power of lasing channel must be at least 15 dB higher than the ASE peak to observe the good gain controllability). At this

point, the surviving channel peak power level becomes (30+1.5+15)=46.5 dB over the ASE peak level, i.e., the static power variation due to SHB is 16.5 dB. It indicates that the static power variations will linearly accumulate as the sizes of cascaded amplifiers are less than 55. After the 55th amplifier, as the numbers of amplifiers increase, the degree of gain controllability becomes worse and worse, i.e., the power added to the surviving channel becomes larger and larger (the amount added to surviving channel is >0.3 dB), and while the power level of lasing channel becomes lower and lower. The amount of amplifier would be less than 50 (it is hard to estimate how many amplifiers) to see the lasing power level to be close to ASE peak level. As the input power of surviving channel surpasses the maximum critical signal power level (see chapter 4) of such a gain-clamped amplifier, the amplifier will loss the characteristics with a gain-clamped, and the self-regulation behavior [1] of EDFA chains will appear. The analyses here showed the worse case where the lasing wavelength locates around 1534 nm, the amount of amplifiers would be larger than 55 to achieve the same static power excursions as the other lasing wavelengths are selected. Note that both the static power excursion of 0.3 dB and the difference of 30 dB of the signal power level and ASE peak level were based on my experimental measurement of a MONET 2-stage amplifier, and thus it is approximate to our evaluations since we here assumed all channels lay within a flat spectrum regime and while our DUT was not; for a specific application, these values may change but the method stated here does provide a guide for how to analyze the system effect.

For cases of 7 out of 8 channels dropped, the static power excursion could be up to 0.62 dB for 15 dB gain compressions as the lasing wavelength is selected as 1534 nm. Assuming that to achieve good gain controllability the lasing peak power should be at least larger than total signal powers. The other assumptions remain the same as previous ones. Additional assumptions are: surviving channel input power= -8.45 dBm, the modulation channel= 0 dBm, and the lasing channel = the sum of both surviving channel and modulation channel power =0.58 dBm. After the modulation channel dropped, the surviving channel would take ~14 amplifiers to achieve the same power level as the lasing channel; and then it would take approximately additional 24 amplifiers to see the lasing power level at least over 15 dB of the ASE peak. Therefore, after the surviving channel passed through a chain of 38 (14+24) amplifiers, the good gain controllability of the amplifier would be lost, and while it would take 55 amplifiers for the case of half channels dropped. It indicates that the case of 7 out of 8 channels dropped has more severe effect on an amplified system than the case of 4 out of 8 channels dropped.

2) Analyzing lasing relaxation-oscillations' effect:

The analyses for dynamic power excursions are more uncertain, as stated in last section, compared to those in 1) provided just based on such a similar logical calculations. One can state qualitatively--If the input modulated surviving signal(s) is (are) with in-phase the inherent lasing relaxation-oscillations of the immediately following amplifier, the resonant phenomena would be seen, i.e., dynamic power

excursions would be enhanced. However, if the lasing wavelength selected is different for individual amplifier, then it is possible to reduce the dynamic power excursions of the surviving channel as a result of different oscillation frequency of each amplifier.

In summary, although both of these effects on an individual amplifier are small, and while the impairments on chains of such an EDFA system might be serious.

References:

[1] N. Edagawa, S. Yamamoto, H. taga, M. Suzuki, and H. Wakabayshi, "Long-haul optical transmission system using optical amplifiers and their future trends", in Proc. SubOptic93, Syst. Opt. Amplifier, 1993, p.55.

Chapter 7
Analytical Modeling of Amplifiers with Laser AGC and Flat Spectral Gain

7.1 Introduction

Despite the large research effort on gain-flattened EDFAs for WDM, the stabilization of the flattened gain has received relatively little attention [1,2]. When the power load of an EDFA increase, the gain will be compressed, and as well such changes at different channels (at different wavelengths) will normally be different--even if the gain spectrum was initially flat [2]. This is an inherent property of most types of EDFs. Thus, the dynamic range of gain-flattened EDFAs for WDM is limited, unless one implements some active control of the spectrum (there is another issue--a gain-level-independent shape of the gain spectrum, so-called dynamic gain flatness, where the shape of the gain spectrum does not depend on the operating gain level, or, the population inversion [3]). What is needed is a multi-channel equalized/flattened and stabilized gain amplifier. This chapter will give a method in designing an equalized/flattened and stabilized gain EDFA based on optimizing the EDFA itself by controlling the lasing wavelength, loop cavity loss, and doped fiber length for a given gain of each channel.

There are different ways to describe (quantify) the gain flatness, for example, $\frac{\Delta G}{G}$ was used in [4]; $\frac{\mu_G}{\sigma_G}$ in [5] where μ and σ are standard deviation and mean of gain (G) values, respectively. Here we use the gain title to quantify the gain flatness. This may be helpful to identify the issue related to analog CATC WDM transmission systems [6].

AC gain tilt and DC gain tilt are defined as the variable gain of an erbium-doped fiber amplifier (EDFA) with input laser wavelength chirp due to modulation, and with different static laser unmodulated wavelengths of no modulation, respectively [7]. For amplitude modulated (AM) subcarrier multiplexed (SCM) TV signals, ac gain tilt in EDFA's is known to lead to composite second-order (CSO) signal degradation in optically amplified links and CATV distribution networks [8], and as well the gain variations will result in the gain tilt variations. Therefore, the some signal gain associated with small ac gain tilt must be controlled or the gain tilt will change as the gain of an EDFA changes. With the use of EDFA's with laser automatic gain control (AGC), the signal(s) gain can be controlled to some extent (not completely, due to the inhomogeneity of erbium laser medium [9], or the total cavity loop loss variations [10]) and such EDFAs behave some new features, and thus the dependence of gain tilt variations on gain variations [8] should be examined again. Presently we can not model effectively the inhomogeneity of erbium laser medium, and thus here we just analyzed the AC gain tilt behavior of homogeneously broadened EDFA's with laser

AGC. In the following, a very simple formula of (normalized) ac gain tilt for a homogeneously broadened EDFA with laser automatic gain control was derived, and then we followed the steps in [8] to discuss the problems. Finally, we gave a compromised design consideration for such an EDFA.

7.2 Analytic studies

Under the assumption of a homogeneously broadened gain medium, the gain of an EDFA with laser AGC is given as [11],

$$G_k = \exp\left\{-\alpha_k L + \frac{P_l^{IS}}{P_k^{IS}}\left[\ln(G_l) + \alpha_l L\right]\right\} \tag{7.1}$$

or

$$G_k = \exp\left\{-\alpha_k L + \frac{(g^*(\lambda_k) + \alpha(\lambda_k))}{(g^*(\lambda_l) + \alpha(\lambda_l))}\left[\ln\beta + \alpha_l L\right]\right\}$$

(7.2)

where the subscripts "k" and "l" represent the signal and laser channel, respectively; G the gain; $P_{l,k}^{IS} \equiv \frac{A}{\Gamma_{l,k}(\sigma_a(\lambda_{l,k}) + \sigma_e(\lambda_{l,k}))\tau}$ the intrinsic saturation power of laser (l) and signal (k) channel; $g^*(\lambda_{k,l})$ and $\alpha(\lambda_{k,l})$ are gain and absorption coefficients; L the EDF length; $\beta \equiv G_l$, i.e., the total cavity loss exactly equal to the gain at lasing wavelength. Having introduced the dB gain, $G_k(dB)=10\log_{10}(G_k)$, to (7.1),

$$G_k^{dB} = A\left\{-\alpha_k L + \frac{P_l^{IS}}{P_k^{IS}}\left[\frac{\beta}{A} + \alpha_l L\right]\right\} \quad \text{(in dB)} \tag{7.3}$$

Here $A \equiv (10\log_{10} e) = 4.343$, β's dimensionless unit (exponential value) has also been converted to dB, G_l^{dB}. α_{kl}'s are not exponential values, but dB/m values.

First of all, we evaluate the derivative of β with respect to G_k.

$$\frac{d\beta}{dG_k^{dB}} = \frac{P_k^{IS}}{P_l^{IS}} \tag{7.4.1}$$

or,

$$\frac{d\beta}{dG_k^{dB}} = \frac{Co(\lambda_l)}{Co(\lambda_k)} \tag{7.5}$$

where $Co(\lambda_{kl}) \equiv g^*(\lambda_{kl}) + \alpha(\lambda_{kl})$, the sum of the gain and absorption coefficients. In (7.4.1) or (7.5), λ_k must be constant as dG_k^{dB} is evaluated. Note that if the derivative of β with respect to G_k is taken in terms of (7.1), the result would be as follows (a little different from (7.4.1)),

$$\frac{d\beta}{dG_k} = \frac{\beta}{G_k}\frac{P_k^{IS}}{P_l^{IS}} \tag{7.4.2}$$

It can be easily changed to (7.4.1) in terms of $\frac{d\beta}{dG_k}\frac{G_k}{\beta} = \frac{d\beta/\beta}{dG_k/G_k} = \frac{d(\ln\beta)}{d(\ln G_k)} = \frac{d\beta^{dB}}{dG_k^{dB}}$.

Next, find out the ac gain tilt, denoted T_{ac},

$$T_{ac}(\beta,\lambda_k) \equiv \frac{\partial G_k^{dB}(\beta,\lambda_k)}{\partial \lambda_k}$$

$$= A \cdot \left[-L\frac{d\alpha_k}{d\lambda_k} + \frac{(\frac{\beta}{A}+\alpha_l L)}{Co(\lambda_l)}\frac{dCo(\lambda_k)}{d\lambda_k} \right] \qquad \text{(in dB / nm)} \tag{7.6}$$

where we chose to use a derivative with respect to wavelength instead of optical frequency. Note that β must be constant when T_{ac} is evaluated [8]. From (7.6) we see that there exists an explicit relationship between the ac gain tilt and the cavity loss β and the amplifier length L. However, low cavity losses can not definitely lead to small ac gain tilt values (the smaller gain tilt values at some wavelengths are , the smaller effects on the CSO, CTB, and XM for AM-FDM optical analog video transmission systems at these wavelengths[12]) since the sign of two derivatives in the bracket of RHS of (7.6) will also affect the entire values, for example, such as the case of Fig.7.1. The relationship between the gain tilt and EDF length was plotted in Fig.7.2. It was shown that for the EDF parameters we selected here there exists a minimum gain tilt (zero point) at an optimum length and small gain tilt values around this zero point. To be able to obtain a perfect gain-flattened spectrum over some wavelengths range just based on the optimision of the EDFA itself, we must let the expression (7.6) be equal to zero over such a wavelength range. Through some basic calculations, the following relationship was obtained,

$$\frac{\beta}{L} = A \cdot \left(\frac{Co(\lambda_l)}{1 + \frac{dg^*(\lambda_k)}{d\alpha_k}} - \alpha_l \right) \tag{7.7}$$

or

$$\frac{\beta}{L} = A \cdot \left(\frac{Co(\lambda_l)}{1 + \exp\left(\frac{\frac{hc}{\lambda_c} - \frac{hc}{\lambda_k}}{KT} \right)} - \alpha_l \right) \tag{7.8}$$

where the relationship between $g^*(\lambda)$ and $\alpha(\lambda)$ has been accounted for [8]. It was seen that to be able to achieve the flattened gain around wavelength λ_s, the (7.8) must be met, i.e., there exists some relationship between the total laser cavity loss (β) and the length (L) of EDF, or the cavity loss scaled to unit length of EDF, $\frac{\beta}{L}$, must meet (7.8), which must be taken into account when we design such a gain-flattened EDFA with a limited dynamic range. Fig.7.3 plots the $\frac{\beta}{L}$ against the signal wavelength in terms of (7.7). It was

seen that 1) not all signal wavelengths meet the (7.7) since the values of the LHS of (7.7) associated with these wavelengths are less than zero; 2) there does not exist a continue wavelength range where the ($\frac{\beta}{L}$)'s have the same values, which indicates that spectrum range in the point of view of 100% gain flatness does not exist. As a result,

we have to plot the (7.6) against the signal wavelength for different lasing wavelengths to find out which wavelength ranges are best relatively flatten. Here we use the gain tilt concept instead of $\frac{\Delta G}{G}$ (relative errors) or another new figures of merit (standard deviation) defined by P. Wysocki [5] to describe the gain spectrum flatness. *We claim that the smaller the absolute gain tilt values and the sum of all gain tilt values around some signal wavelengths range, the more flatter the signal spectrum around such wavelengths range.* Fig.7.4 plotted the cases of lasing wavelengths 1450, 1512, 1530, 1552, 1610 nm. It was shown that there exists widest spectrum range of the flatness as the lasing wavelength is selected as 1530, 1552 nm and the signal spectrum ranges locates around 1580~1600 nm.

Finally, we can write the following expression of ac gain tilt changes with gain variations,

$$\begin{aligned}\gamma(\lambda_k) &\equiv \frac{dT_{ac}(\beta,\lambda_k)}{dG_k} \\ &= \frac{\partial T_{ac}(\beta,\lambda_k)}{\partial \beta}\frac{d\beta}{dG_k} \\ &= \frac{1}{Co(\lambda_k)}\frac{dCo(\lambda_k)}{d\lambda_k}\end{aligned} \tag{7.9}$$

Again, λ_k must be constant as dG_k is evaluated. Equation (7.9) shows exactly the same result as equation (4) in [8], where without laser AGC scheme is added and has nothing to do with the parameters associated with lasing features such as loop loss and

lasing wavelength. In terms of (7.9) if the gain at a wavelength λ_k increases by 1 dB, the ac gain tilt at this wavelength will change by γ . We will call γ the normalized ac gain tilt change. It was found out from (7.9) that γ 1) does not vary with the input pump and signal powers--this is not an obvious reflection of characteristic of an EDFA with laser AGC since [4] showed the identical result; 2) has nothing to do with the cavity loss, the length (L) of EDF, and the selection of lasing wavelength, which indicates that the amount of variation of ac gain tilt is equal to that of signal gain as the parameters stated here changed since both the ac gain tilt and signal gain will change with them (see (7.3) and (7.6)). In other words, the AC gain tilt would be clamped if the gain was clamped by laser AGC; and 3) depends on the values and signs of $\frac{d\alpha_s}{d\lambda_s}$, and $\frac{dg_s^*}{d\lambda_s}$ ($\frac{dg_s^*}{d\lambda_s}$ has the same sign as $\frac{d\alpha_s}{d\lambda_s}$). Fig.7.5 plotted the γ as a function of signal wavelength for EOO6 EDF.

7.3 Design considerations

In this section we will discuss optimum design issues in terms of the previous results. Here we classify the following two types of issues: 1) flattened gain spectrum ranges; and 2) and zero gain-tilt at discrete wavelengths.

1) To achieve as wide as possible flat spectrum range (~20 nm, from 1580 to 1600 nm) the optimum lasing wavelength is ~1530, 1552 nm for the cavity loss and EDF length

examined here. In other words, the optimum design depends on the specific design requirement.

2) The cavity losses per unit length associated with the zero gain-tilts vary with the lasing and signal wavelengths. Fig.7.2 may be acted as a guide to select the lasing and signal wavelengths when one deals with an analog CATV WDM transmission systems.

In summary, the optimum design for an EDFA with equalized/flattened and stabilized characteristics is system dependent. Additionally, such a design must be combined with the other considerations of EDFA properties, such as low noise figure, gain controllability, maximum critical input signal power, small inhomogeneity of erbium ions (small spectral hole burning favoring the lasing wavelength close to the signal band), etc. As a result, the design of such an EDFA must be compromised, referring to Chapter 8.

References:

[1] R. Lebref, E. Delevaque, B. Landousies, H. Poignant, M. Guibert, T. Georges, "An advanced amplifier structure for WDM transmissions: The multichannel equalized and stabilized gain amplifier", Optical Amplifiers and their Applications Conf., Monterey, CA, Vol. 11, pp.81-84, 1996 OSA Tech. Dig. Series.

[2] J. Nilsson, W.H. Loh, S.T. Hwang, J.P. de Sandro, and S.J. Kim, "Simple gain-flattened erbium-doped fiber amplifier with a wide dynamic range", OFC'97, Dallas, Texas, OSA Technical Digest, WF3, p.129; and references therein.

[3] J. Nilsson, Y.W. Lee, and W.H. Choe, "Erbium doped fibre amplifier with dynamic gain flaness for WDM", Electron. Lett., Vol. 31, pp.1578-1579, 1995.

[4] M. Nishimura, "gain-flattened erbium-doped fiber amplifiers for WDM transmission", OFC'97, Dallas, Texas, OSA Technical Digest Series, 6 (1997) 127, WF1.

[5] P.F. Wysocki, R.E. Tench, M. Andrejco, D. DiGiovanni, and I. Jayawardene, "Options for gain-flattened erbium-doped fiber amplifiers", OFC'97, Dallas, Texas, OSA Technical Digest Series, 6(1997) 127, WF2.

[6] T.H. Wood, A.K. Srivastava, J.L. Zyskind, J.W. Sulhoff and C. W OFC'97, Dallas, Texas, OSA Technical Digest Series, 6 (1997) 320, ThP2.

[7] K. Kikushima, "AC and DC gain tilt of erbium-doped fiber amplifiers", J. Lightwave Technol., Vol. 12, pp.463-470, 1994.

[8] J. Nilsson, Y.W. Lee, S.J. Kim, S.H. Lee, and W.H. Choe, "Analysis of AC gain tilt in erbium-doped fiber amplifiers", IEEE Photon. Technol., Lett., Vol. 8, 515-517, and references therein.

[9] G. Luo, J.L. Zyskind, Y. Sun, A.K. Srivastava, J.W. Sulhoff, and M.A. Ali, "Relaxation-oscillations and spectral hole burning in laser automatic gain control of EDFA's", OFC'97, Dallas, Texas, OSA Technical Digest Series, 6 (1997) 130, WF4.

[10] J.F. Massicott, S.D. Willson, R. Wyatt, J.R. Armitage, R. Kashyap, D. Williams and R.A. Lobbett, "1480nm pumped doped fibre amplifier with all optical automatic gain control", Electron. Lett., Vol.30, pp.962-964, 1994.

[11]A.A.M. Saleh, R.M. Jopson, J.D. Evankow, and J. Aspell, "Modeling of gain in erbium-doped fiber amplifiers", IEEE Photon. Technol., Lett., Vol. 2, pp.714-717, 1990.

[12] C.Y. Kuo and E.E. Bergmann, "Erbium-doped fiber amplifier second-order distortion in analog links and electronic compensation", IEEE Photon. Technol., Lett., Vol. 3, 829-831.

Chapter 8
Optimum Designs of EDFAs with Laser AGC

8.1 Introduction

This chapter will present all possible considerations (on the basis of all previous related chapters) affecting the design of an EDFA with laser AGC and such an amplified cascade system. It is our purpose that designs a gain-clamped amplifier to meet a specific application. The design consideration of a single amplifier will be described first, and then such a cascaded amplified system. Finally, some design approaches not based on the optimization of the amplifier itself are proposed.

8.2 Optimizing a single amplifier design itself

Table 8.1 presented all possible design considerations for a single amplifier with laser AGC. Note that there still exists a few "unclear" items which remain to be investigated in the future work. In terms of this table, like the design of a "common" amplifier without AGC [1], one can not design an amplifier with all preferred benefits. A particular optical optical amplifier is designed for a specific application, and the requirements of the application in turn determine the design. Even if the design is restricted to a particular application there still often exists some design trade-offs. For example, there are some different requirements between the static and dynamic gain-clamped amplifier design. Note that the item (in the table) of "high oscillation frequency" is based on the consideration: the higher damping rates are, the higher

oscillation frequencies are; one prefers higher damping rates. For fiber length column, one should be reminded that at short fiber length, lasing occurs close to the gain peak; as length increases, there is a regime of low population inversion at the output end of the fiber that reabsorbs signal light, preferentially at shorter wavelengths, EDFL's tend to lase at longer wavelengths where absorption is low.

8.3 Optimizing an Amplified Lightwave System

Assuming the issue we are considering is: there is a amplified lightwave cascade system where each amplifier's gain is clamped by laser AGC mechanism. How can we optimize the design of such a system just based on the selections of the system parameters themselves? Our starting point is not to try to optimize individual amplifier performance parameters [2] to achieve the optimization of the whole system because the interactions between individual amplifier must be accounted for. Here we just gave a proposal applying to a specific application requirement--in terms of optimizing both static and dynamic parameters since there still definitely exists a lot of design trade-offs for such an amplified system, like the design of a single amplifier shown in previous section. We wish that our design could satisfy the following requirements: low accumulated noise figure, small accumulated static and dynamic power excursions, low initial spike rates, and high damping rates based on these parameters which might accumulate with the increase of the number of amplifiers in the network: noise figure, static and dynamic power excursions, and power transient speeds. *The central design idea is that we try to let the final dynamic power excursions of the*

whole system cancel out (the idea of "cancel out each other" has been used a lot in fiber optics fields) and then consider other requirements. The selection of lasing wavelength for first amplifier is our first concern--a long lasing wavelength (>ASE peak) which is close to the signal band is preferred for the first amplifier to achieve low noise figure, small static power excursions, low initial spike rate. For the following amplifiers designs, the selections of system parameters depend on the specific application requirement (but the final dynamic power excursion must be canceled out to the minimum degree in terms of different parameters choices of the system, such as selecting different lasing wavelengths for individual amplifier). For example, if the small static power excursion is our main concern the lasing wavelength should not be located around the ASE peak. Note that there are a variety of approaches to achieve the same purpose since one system parameter is affected by more than one elements and thus there exists various choices to implement a specific design.

8.4 Additional optimized approaches

The previous two sections have addressed issues related to the optimization of a single amplifier with laser AGC and such a cascaded system in terms of the optimization of the amplifier's parameters themselves. This section will propose some additional schemes to achieve our optimized designs since there exists a lot of trade-offs just based on the design of the amplifier itself's optimization--external controls are needed. The issue of reducing static power excursions arising from SHB will be described first, and then dynamic power excursions arising from inherent laser relaxation-oscillations.

8.4.1 Reducing SHB's effects

1) using two lasing control channels, locating on either side of signal band separately, to reduce the effect of SHB since the closer the lasing channel to the signal channels, the smaller the SHB effect. However, because of the mainly homogeneous gain broadening of EDF, simultaneous multiwavelength lasing in EDFL is very sensitive to variations in the cavity losses. This implies that the gain provided by EDF at one wavelength uniquely determines the gain at all other wavelengths. Any change of the wavelength dependence of the cavity losses will, at some of the lasing wavelength, typically break the requirement that the gain equals the cavity losses. Then lasing stops at those wavelengths. Moreover, because the gain spectrum depends on the operating level of the gain, also wavelength-independent loss variations normally break the required gain-loss balance [3]. Fortunately, the above difficulties have been overcome. A wealth of reports on simultaneous multi-wavelength oscillation have been published. These schemes include[4]: using a fiber laser that includes two birefringent fibers, a fiber laser with a grating wavelength division multiplexer, and a fiber ring laser using in-fiber comb filters. Additionally, dual wavelength operation has been achieved using a fiber ring laser with two cavities that share one EDFA, a coupled dual-cavity fiber laser incorporating four fiber gratings, a mode-locked fiber ring laser that includes a birefringent component in its cavity, and so on. We might select one economic and robust scheme to achieve our purpose.

2) Same as 1) but using linear (F-P) laser scheme to implement simultaneously two lasing channel. The schematic setup is given in Fig.8.1, where the cavity loss

associated with lasing wavelength 1 and 2 is adjusted by variable attenuator 1 and 2, respectively; two polarization controllers (PC's) are used to control the polarization of each lasing channel. Note that whatever scheme 1) or 2) is adopted, one does not desire to use more than 2 lasing channels to control the gain or it would reduce the pump efficiency.

8.4.2 Reducing lasing relaxation-oscillations' effects

1) using the same schemes as those mentioned in section 8.3.1. But here we must implement two relaxation-oscillations with out-of-phase caused by two lasing wavelengths, and thus these two dynamic oscillations can cancel each other to a minimum level. A careful adjustment of cavity elements, such as the variable attenuator, PC, etc. must be exercised.

2) using an external feedback control mechanism, similar to the report in [5], which adopted a nonlinear absorber implemented by a nonlinear amplified loop mirror.

References:

[1] J.-M. P. Delavaux and J.A. Nagel, "Multi-stage erbium-doped fiber amplifier designs", J. Lightwave Technol. 13, 703 (1995).

[2] M.A. Ali, A.F. Elrefaie, R.E. Wagner, and S.A. Ahmed, "Performance of Erbium-doped fiber amplifier cascades in WDM multiple access light networks", IEEE, PTL, 6, 1142 (1994).

[3] J. Nilsson, Y.W. Lee, and S.J. Kim, "Robust dual-wavelength ring-laser based on two spectrally different erbium-doped fiber amplifiers", IEEE, PTL, 8, 1630 (1996); and references therein.

[4] S. Li, H. Ding, and K.T. Chan, "Erbium-doped fibre lasers for dual wavelength operation", Electron. Lett., 33, 52 (1997).

[5] Y.T. Chieng and G.J. Cowle, "Suppression of relaxation-oscillations in tunable fiber lasers with a nonlinear amplified loop mirror", IEEE, PTL, 7, 485 (1995).

Chapter 9
Future Research Prospects

9.1 Introduction

In this chapter, some of my future research plans, related to the amplifier gain control and how to effectively model spectral hole burning (SHB) of the EDFA, will be described here. Note that they are only the author's point of view, which remains to be further studied and confirmed.

9.2 Comparisons of different control schemes

Recently, different AGC schemes for fast power transients have been reported, including pump control [1], link control [2], lasing control [3], hybrid (lasing + link) control [4]. First of all, we analyzed advantages and disadvantages of each control scheme in terms of response speed, control efficiency, performance degradation(such as the noise figure), requirement for the EDFA, thermal stability, robust, complexity/flexibility, cost and point of view of system or network, and then a new control scheme applying to a large amplified network system was proposed.

1) *response speeds*: pump control ~8 μs; link control~4 μs, both of them will be improved by faster control electronic circuit elements; laser AGC slowest, around hundreds of μs, determined by the slow gain dynamics of the EDFA and the transit

time through the feedback loop--linear laser cavity design is preferred to reduce the transit time of the lasing wave. Note that one should not be confused with such a statement--"An all optical scheme always offers faster acting speed than an optoelectronically mixed scheme" (due to the existence of one active component--EDFA inside the loop, an all optical scheme does not show its advantage). Principally, the feedforward loop mechanism is faster than feedback loop one since the former can save the time of the generation of an error signal.

2) *control efficiency*: the power excursion degree of surviving channels for different control scheme didn't show obvious differences if the optimum approach for each scheme is adopted.

3) *performance degradation:* The laser AGC scheme will degrade the noise figure of the amplifier due to the introduction of additional channel (lasing), the pump efficiency will decrease because the lasing channel has to consume pump power. For the pump and link control, we did not see any performance degradation of the amplifier due to the addition of these control mechanisms.

4) *requirement for the EDFA:* The laser AGC and pump control scheme do not require the signal bands and lasing channel to lie within the flat spectrum gain region of the amplifier, and while the link and hybrid control scheme do.

5) *thermal stability:* If the laser AGC scheme was implemented by a linear cavity, where two ends of cavity are constructed by two Bragg gratings, there might exist the thermal stability.

6) *robust:* Each scheme itself (in its entirety) does not have special requirement, just depending on the robustness of individual fiber component and optoelectronical device.

7) *complexities/flexibilities*: The laser AGC--all optical passive gain control, requiring no external monitoring or feedback electronics, and the laser feedback loop can be easily added to an commercially available EDFA; both link and pump controls-- an active control scheme

8) *cost*: Both pump and link control methods need fast control circuit, the more fast, the more expensive; and while the laser AGC requires inexpensive devices.

9) *point of view of system or network*: link control and hybrid (lasing + link) control are an optimum selection.

A new control scheme applying to a large amplified network system, where individual amplifier does not have flat-gain spectrum range, was proposed--we adopt hybrid (lasing + pump) control scheme for the first moderate sized amplified chains, and then the pump control scheme is employed to suppress fast power transients as the size of network becomes larger and larger.

Although there have existed a few approaches to implement gain control mechanism, we have not yet addressed such a problem: how can we deal with the issue related to the random transient errors (such as random link failures)? It might be related to

protocol issues [5] and would become a challenge research topic. Additionally, what are solutions to bi-directional transmissions system?

9.3 How to effectively model SHB

Here I will describe some thoughts on how to characterize and effectively model the SHB in an EDFA since at present we have only the formal theory of SHB [6], which is not practical, can not effectively model actual problems.

1) Assuming that the general inhomogeneous gain coefficient and the hole width expression for a no Stark split two-level atomic system still applies to the case of a Stark split three-level atomic system. Actually, Ref.[6] used the same ideal. However, here we are not interested in generalizing the treatment process, but directly assume that a modified formula will apply to our case, where the unsaturated gain coefficient should be redetermined experimentally (might be an empirical formula) by the gain medium (erbium ions).

2) Essentially, the inhomogeneity property of the amplifier reflects the degree of how a saturating signal affects the other signals within the spectrum band. Specifically, the stronger the homogeneity effect is, the severer a saturating signal affects the other signals, and vise verse. Therefore, a correlation function about gain-slope, ASE-slope, or second-order distortion of the EDFA may be introduced to describe such a "coupling" degree among different spectrum components. We use different ways to

quantify the inhomogeneous characteristics of the EDFA instead of the width and depth of the hole. Our purpose is to define some macroscopically (easily measured) physical parameters to describe the SHB.

3) For numerical modeling, the experimental data for static power excursion could be embedded into the rate-propagation equations based on homogeneous broadening assumption to express the contribution arising from the SHB.

References

[1] A. K. Srivastava, Y. Sun, J.L. Zyskind, J.W. Sulhoff, C. Wolf, and R.W. Tkach, "Fast gain control in an Erbium-doped fiber amplifier", Optical amplifiers and their application, Monterey, CA, PDP4, 1996.

[2] J.L. Zkskind, A.K. Srivastava, Y. Sun, et al., "Fast link control protection for surviving channels in multiwavelength optical networks", ECOC'96, Oslo, Postdeadline paper.

[3] G. Luo, J.L. Zyskind, Y. Sun, A.K. Srivastava, J.W. Sulhoff, and M.A. Ali, "Relaxation-oscillations and spectral hole burning in laser automatic gain control of EDFA's", in OFC'97, 130, WF4, Dallas, Texas.

[4] J.L. Jackel and D. Richards, "All-optical stabilization of cascaded multichannel erbium-doped fiber amplifiers with changing numbers of channels", in OFC'97, 84, TuP4, Dallas, Texas.

[5] B. Awerbuch, B. Patt-Shamir, and G. Varghese, "Self-stabilizing end-to-end communication", J. of Hight Speed Networks, 5, 365 (1996).

[6] E. Desurvire, Erbium-Doped Fiber Amplifiers: Principles and Applications, John Wiley & Sons, Inc., New York (1994), p.59.

Chapter 10

Conclusion

This thesis presented a detailed experimental and theoretical analysis of gain dynamics of an all-optically stabilized multi-channel EDFA and the impact on WDM networks performances. Specifically, this thesis analyzed and examined the critical factors such as, lasing wavelength, amplifier operating point, gain recovery time, relaxation oscillation frequency of the feedback loop, cavity structure, cavity losses, signal(s) and laser powers, lasing direction, switching speeds, and the number of channels dropped/added, that affect the transient power excursions in the surviving channel. We showed that any degradation at the first EDFA has a cumulative effect at the output of all subsequent EDFA's in the chain. This has the important implication that the length of the chain is a function of the design parameters of the first EDFA in the chain.

The main objective of this work was to protect surviving channels against such impairments, by minimizing the impact of variations in the number of wavelength channels in operation, and of rapid changes in their signal power levels. The basic requirement is that the quality of service for any given channel passing through an optical amplifier shall not be adversely impacted by anything that happens to any of other channels passing through the same amplifier. This requirement applies both to amplifiers in WDM repeaters network elements, and to amplifiers included in other network elements. We considered means of adjusting the flattened-gain amplifier's

total output power to maintain constant per-channel output power with a minimally degraded SNR, regardless of the number of channels present.

This thesis was divided into two overlapping phases, experimental and theoretical. First, we considered the applicability of laser automatic gain control (AGC) to control fast power transients in WDM optical networks and reported the first high resolution measurements of transients in such gain controlled EDFA's. Second, we implemented a dynamic simulation tool for modeling the behavior of a single amplifier and amplifier chains, with and without stabilization. We developed an approximate rate equation model for a homogeneously broadened 3-level multi-excited-mode laser system, where relaxation-oscillations characteristic parameters, i.e., threshold pumping rate, pumping factor, damping rate, and oscillation frequency were derived based on a 4-level laser system model. The experimental results are then compared with those predicted using the dynamic simulation tool and approximately theoretical results.

We showed the degradations imposed by each of these factors on the transient power excursions of the surviving channel and explored the limitations that any of these degradations can impose on the stabilization techniques. We devised, compared, and demonstrated several active techniques, such as, link control, pump control, and a passive all-optical gain control techniques, for stabilizing the per-channel output power both for single amplifier and cascades of amplifiers.

Our primary concern and focus were on the passive technique, since, as this thesis has showed, this technique was simple, inexpensive, and robust, requiring neither monitoring of the amplifier output nor any active feedback.

The overall objective was to investigate numerically and experimentally the optimum configuration of an EDFA with laser AGC for WDM applications as a function of all the relevant performance parameters such as, lasing wavelength, amplifier operating point, cavity structure, cavity length and losses, signal(s) and laser power, and laser propagation directions. We devised and examined several different approaches to reduce and/or eliminate the spiking amplitudes associated with relaxation-oscillations.

Another critical performance criterion is to ensure sufficient gain flatness to permit amplifiers to be cascaded while maintaining acceptable inter channel power variations and signal-to-noise ratios at all wavelengths. Since gain flatness depends on the signal input power levels, stabilizing the amplifier gain is a must. Therefore, the issue of a multi-channel equalized/flattened and stabilized gain amplifier was also addressed.

	Lasing wavelength	*Lasing direction*	*Operating gain*	Pump wavelength	*P(p,in)*	Photon lifetime	*Symmetric cavity or not*	Doped density	Pump direction	EDF length
Low noise figure	away ASE peak	forwrad	high	980 nm	high	N/A	small(high) in(out)put loss	unclear	forward	short
Good G controllability	ASE peak	N/A	low	N/A	N/A	N/A	N/A	unclear	N/A	long
High pump effeiciency	ASE peak	backward	low	1480 nm	unclear	N/A	small(high) in(out)put loss	unclear	unclear	relative position of sig. laser
Low lasing threshold	ASE peak	N/A	low	980 nm	N/A	large	N/A	high	N/A	short
Small SHB	away ASE peak	unclear	high	unclear	high	N/A	unclear	unclear	N/A	dependent
High damping rate	ASE peak	unclear	varying	980 nm	high	large	unclear	high	unclear	short
Low initial spike rate	longer	unclear	almost no effect	980 nm	high	small	unclear	high	unclear	short
Small overshoot	away ASE peak	unclear	high	980 nm	large	small	unclear	high	unclear	short
small undershoot	away ASE peak	unclear	high	980 nm	large	small	unclear	high	unclear	short
High osciation fre. (recovery)	ASE peak	unclear	low	980 nm	high	small	unclear	high	unclear	short
High osciation fre. (saturation)	ASE peak	unclear	high	980 nm	high	small	unclear	high	unclear	short
large P(critical,in,sig.)	dependent	N/A	low	N/A	high	N/A	N/A	dependent	N/A	short
large QCE	short (<ASE peak) dependent (>ASE peak)	N/A	high	N/A	low	N/A	N/A	dependent	N/A	dependent

Table 8.1

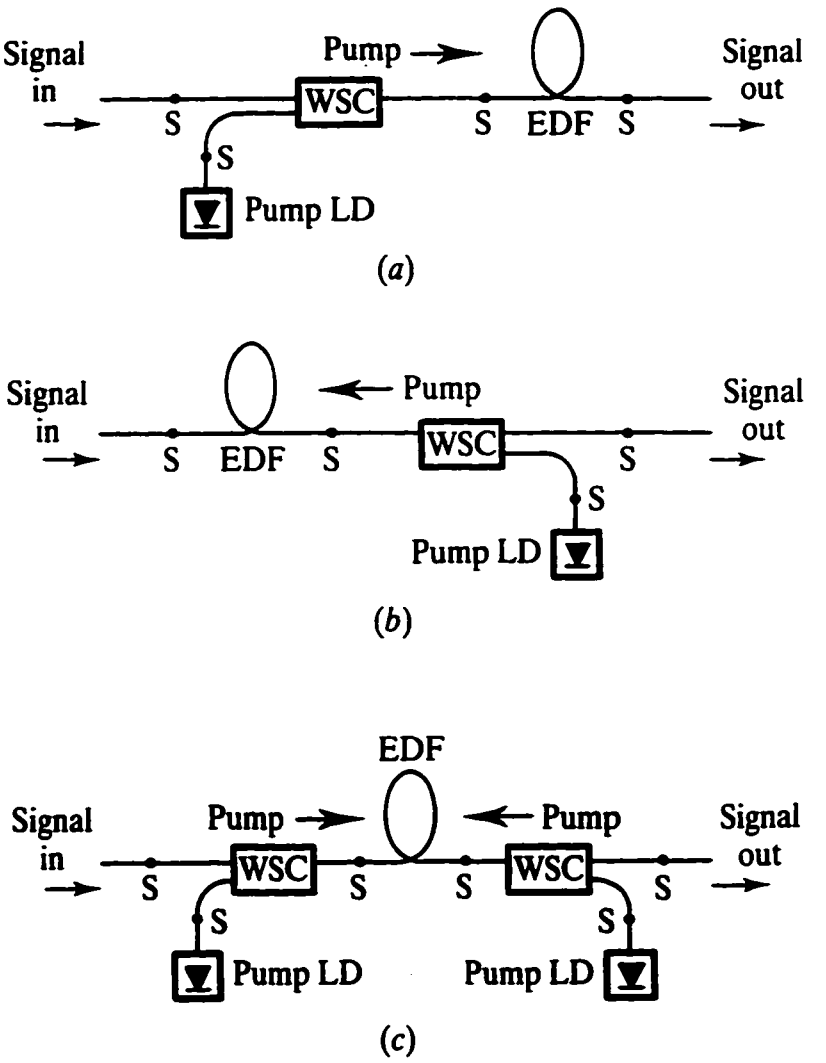

Fig. 2.1

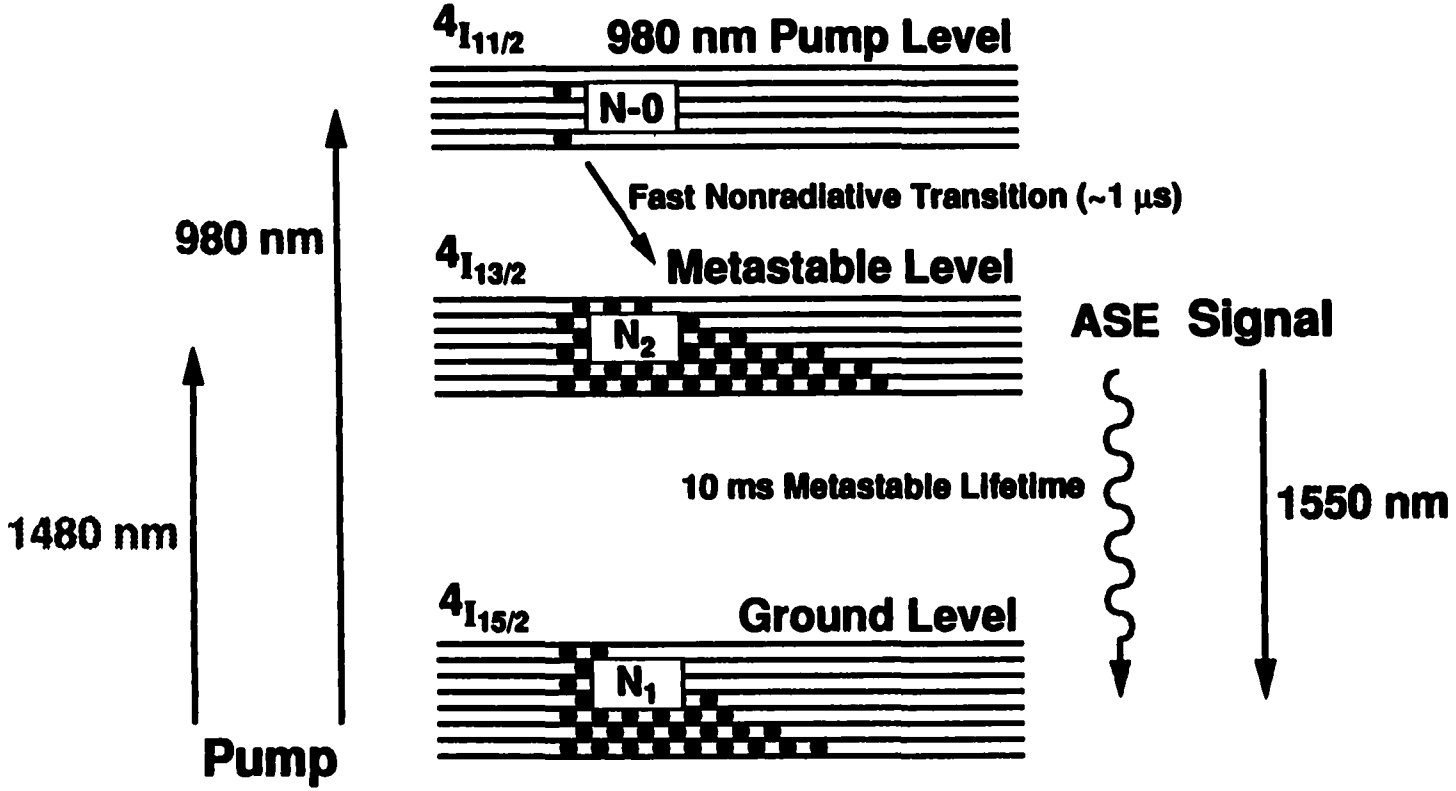

Fig. 2.2

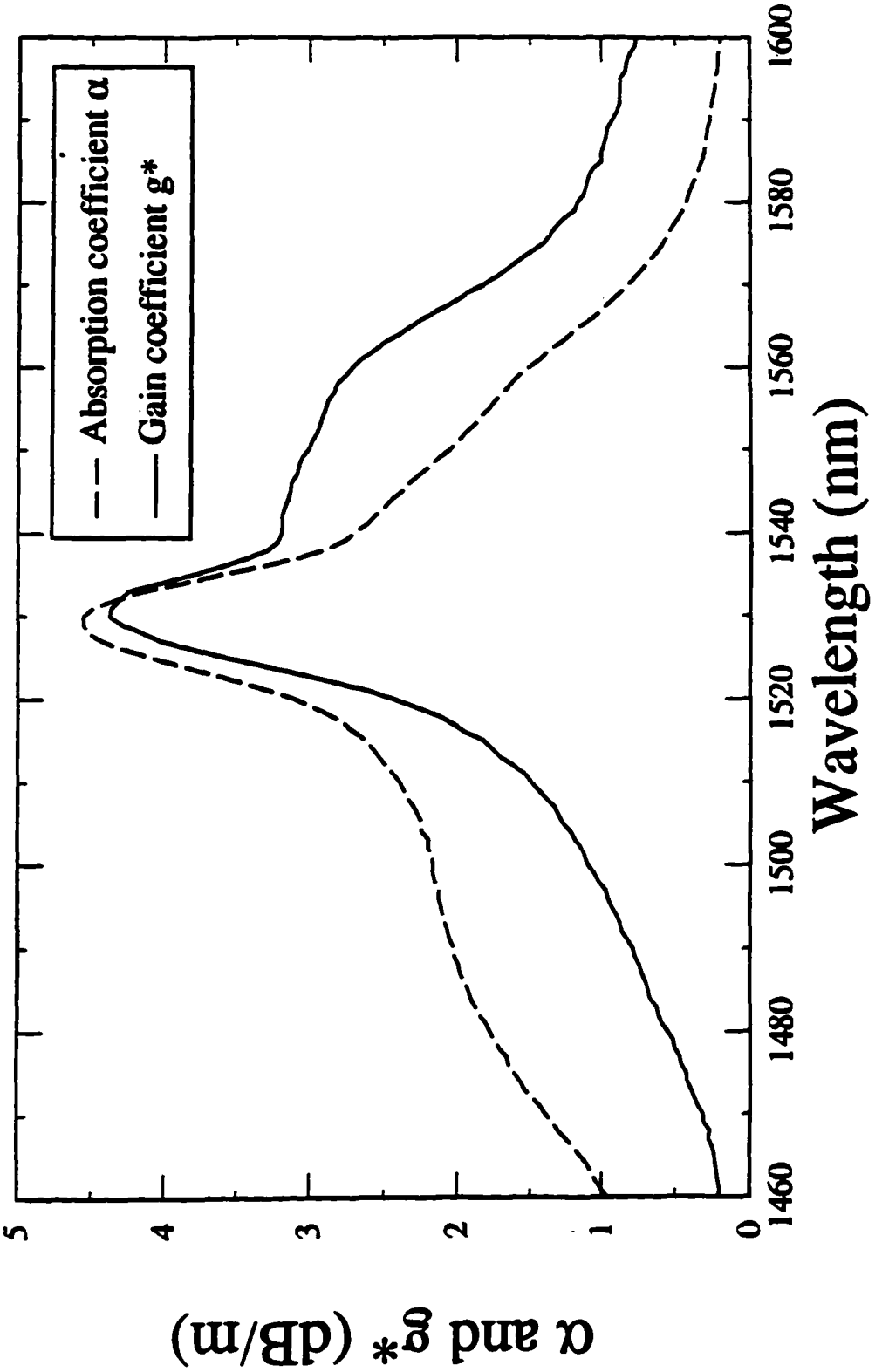

FIG. 2.3

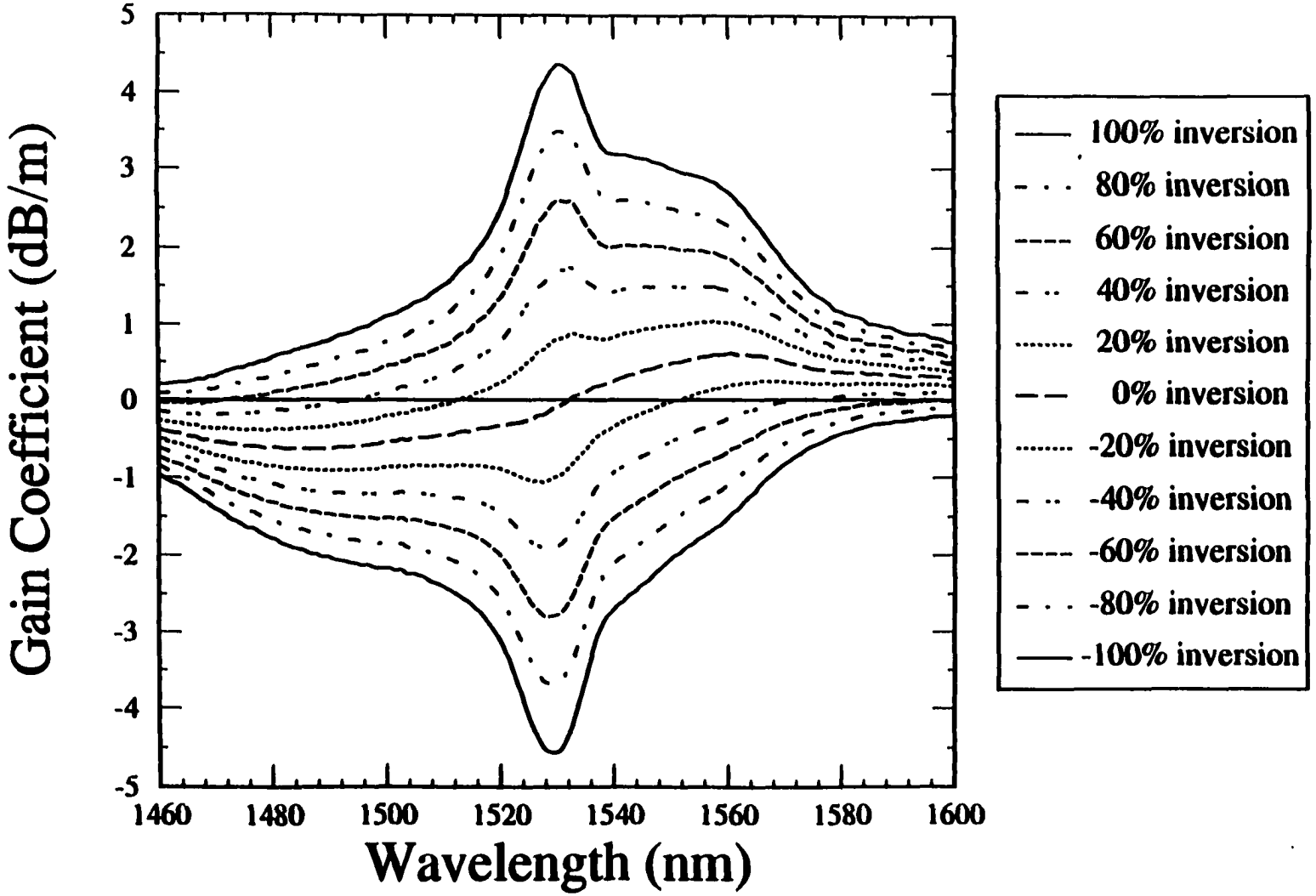

Fig. 2.4

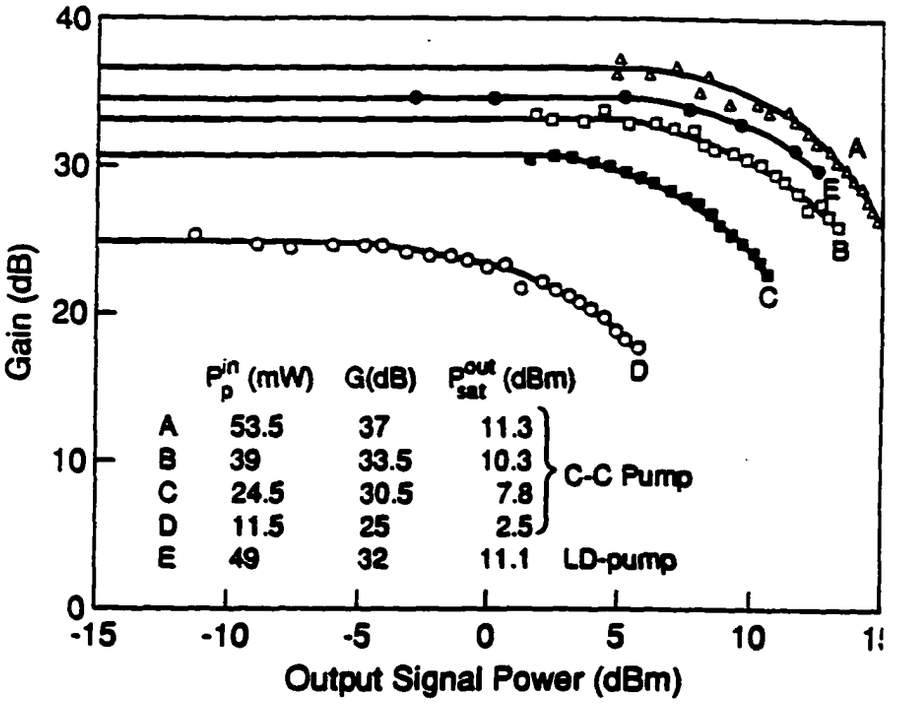

Fig. 2.5

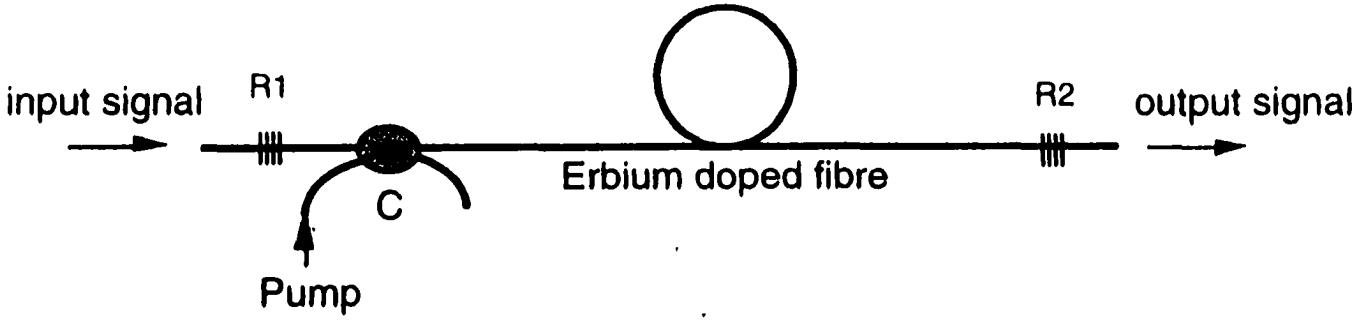

configuration (a)

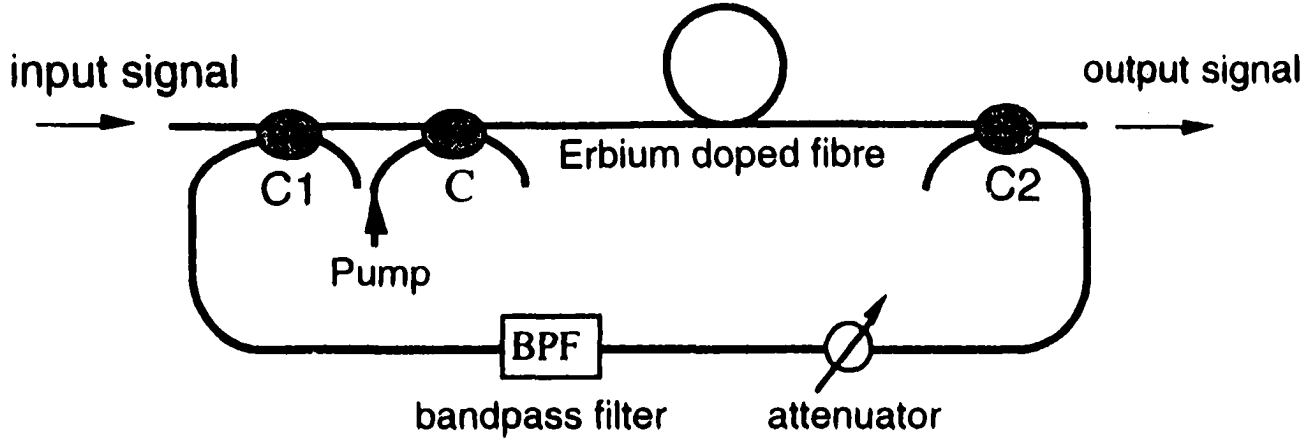

configuration (b)

Fig. 3.1

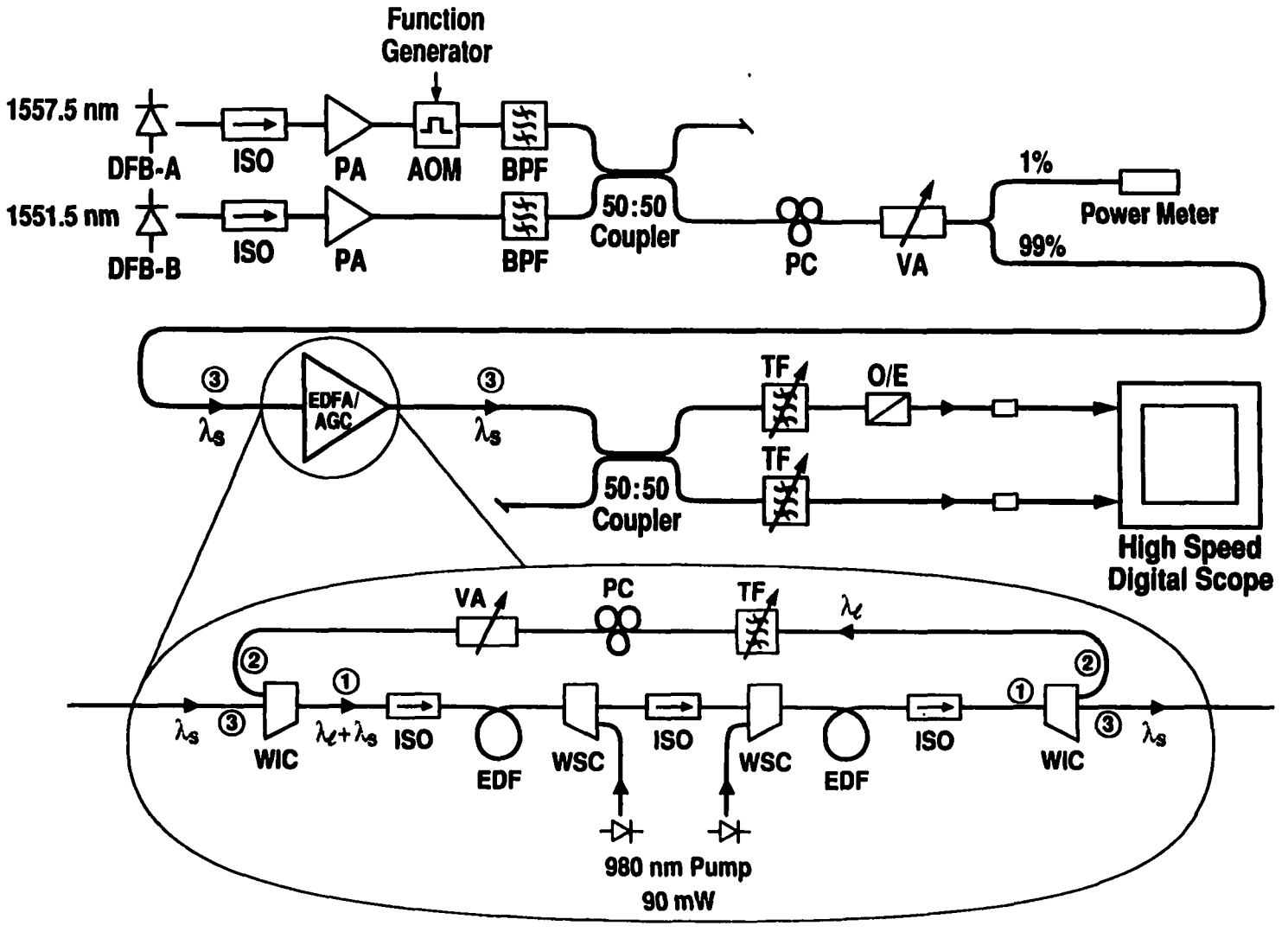

Fig. 3.2

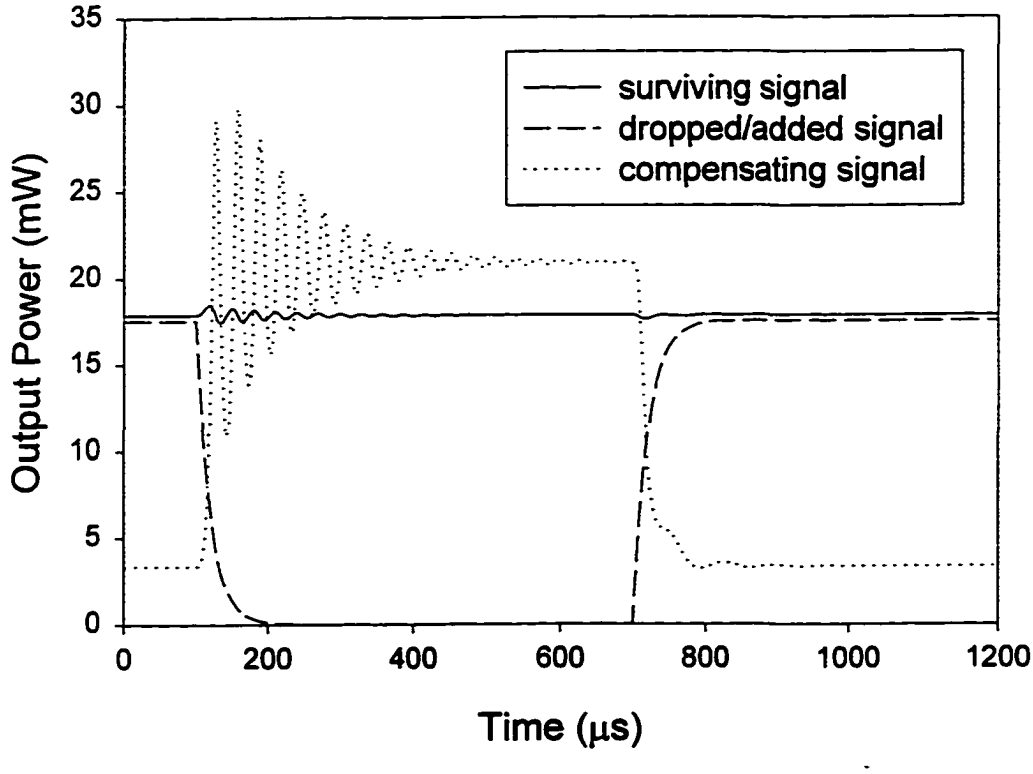

Fig. 3.3

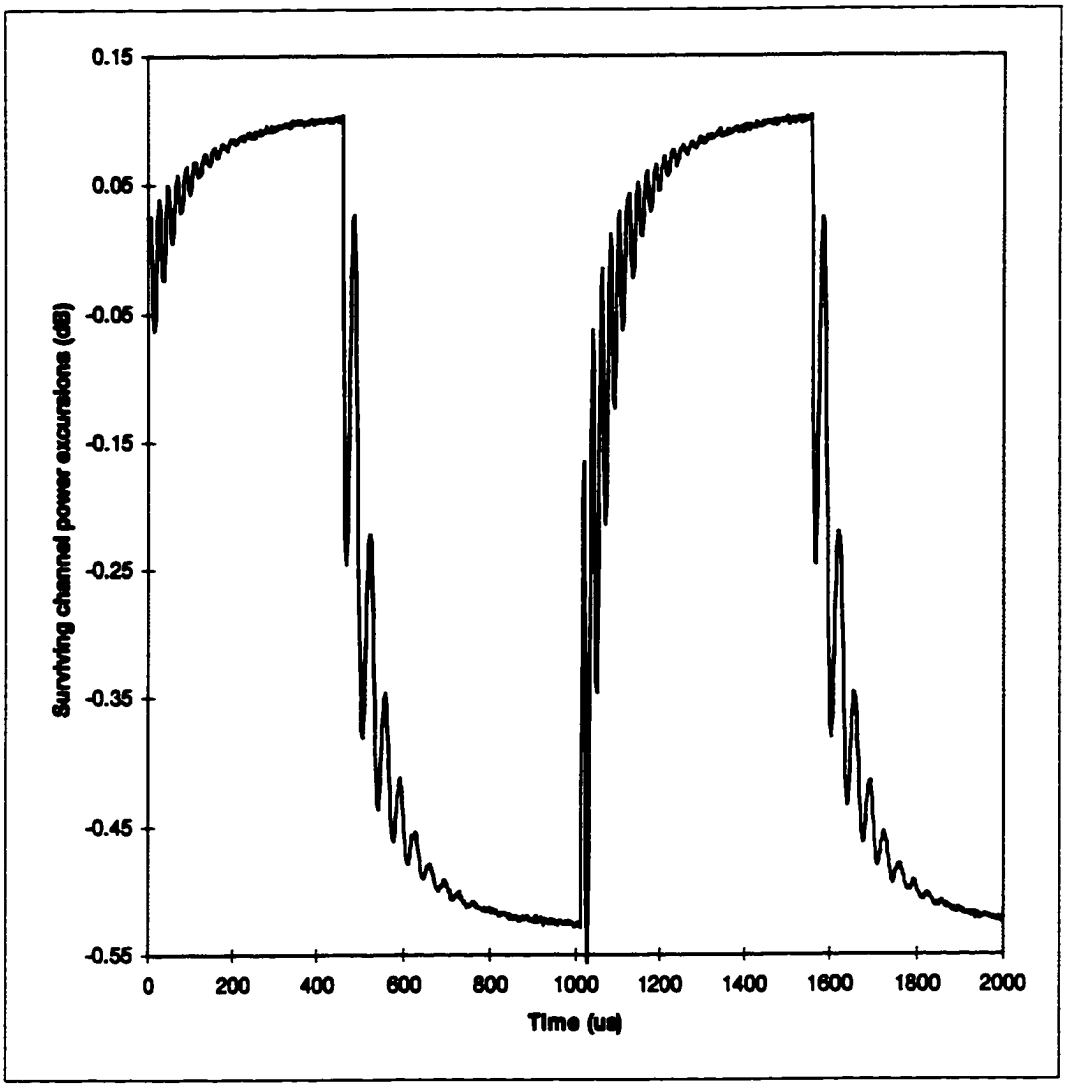

Fig.3.4(a)

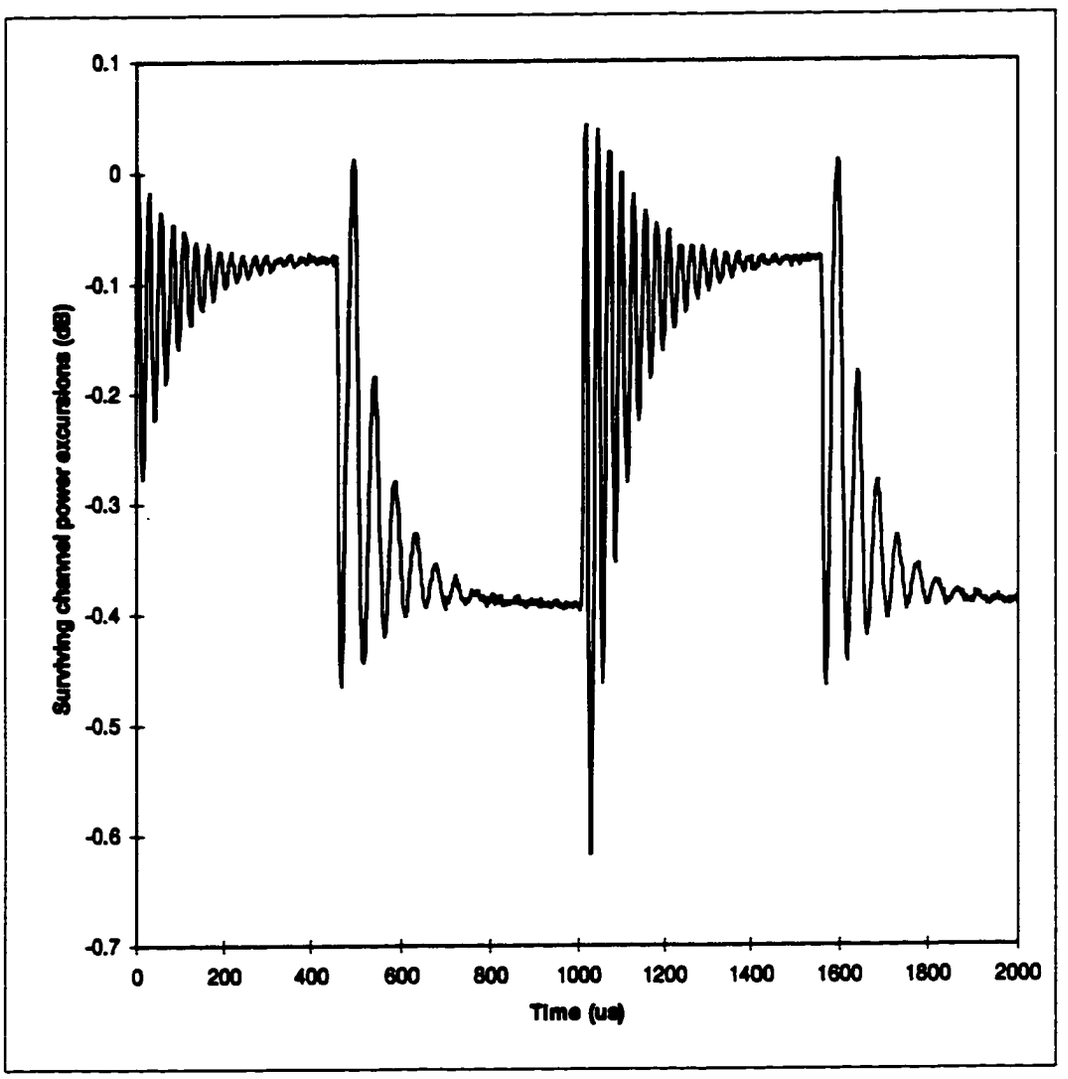

Fig.3.4(b)

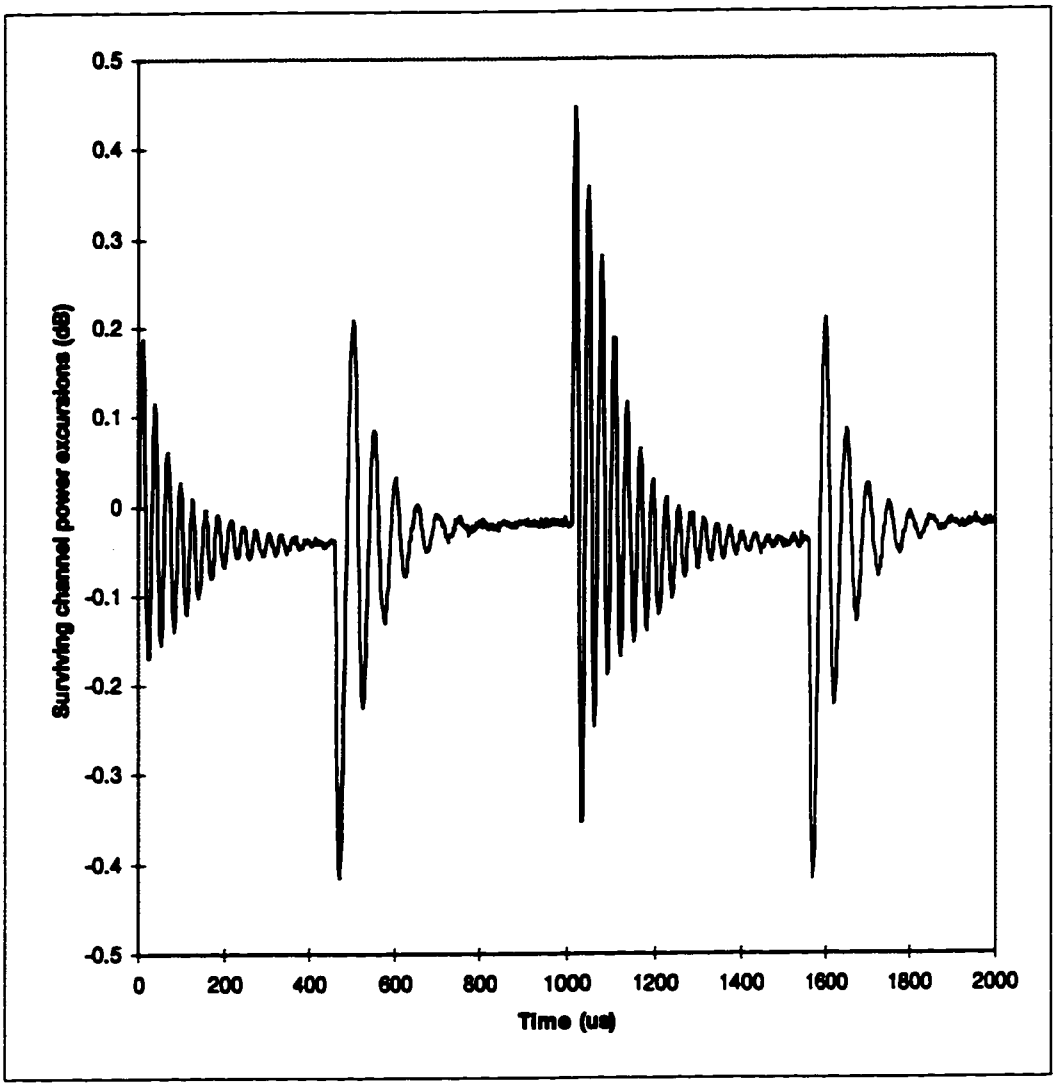

Fig.3.4(c)

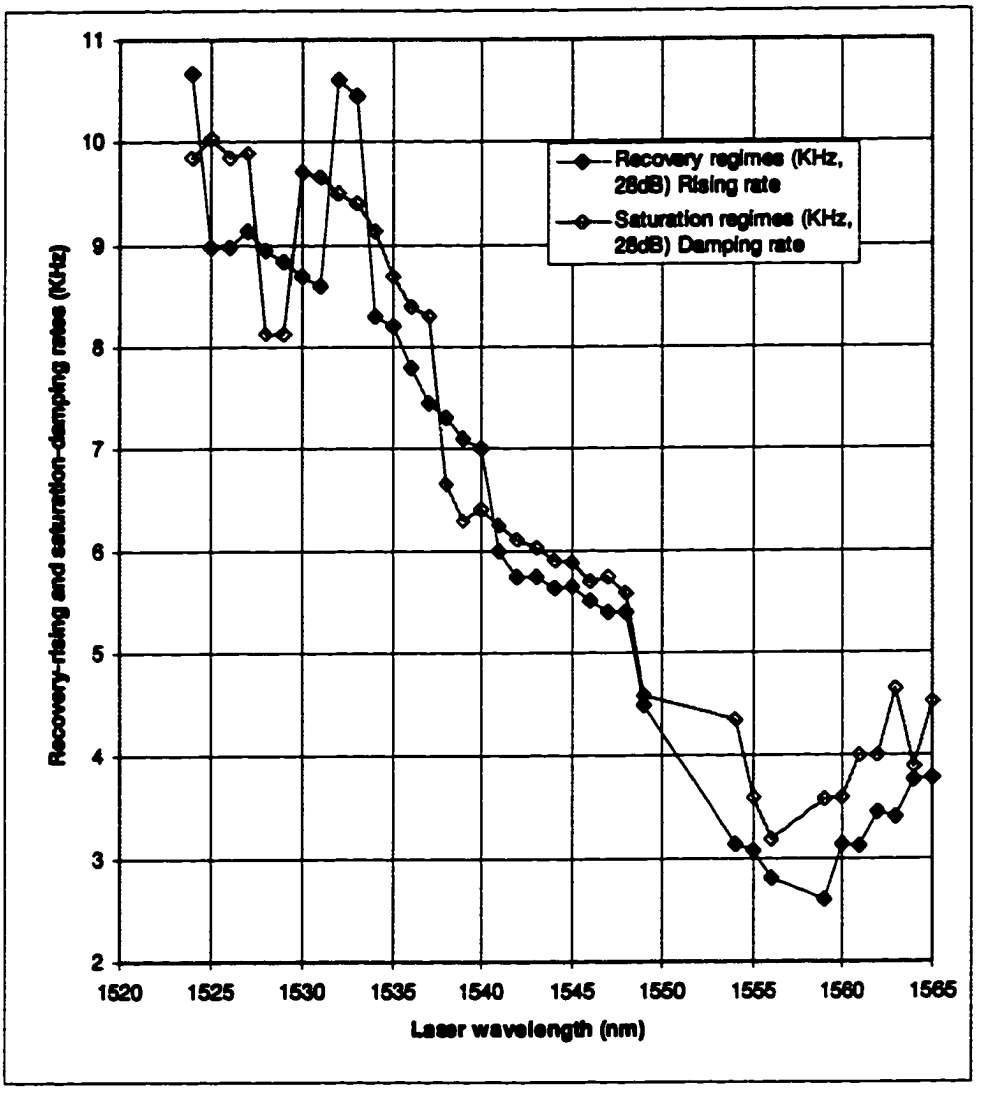

Fig.3.5

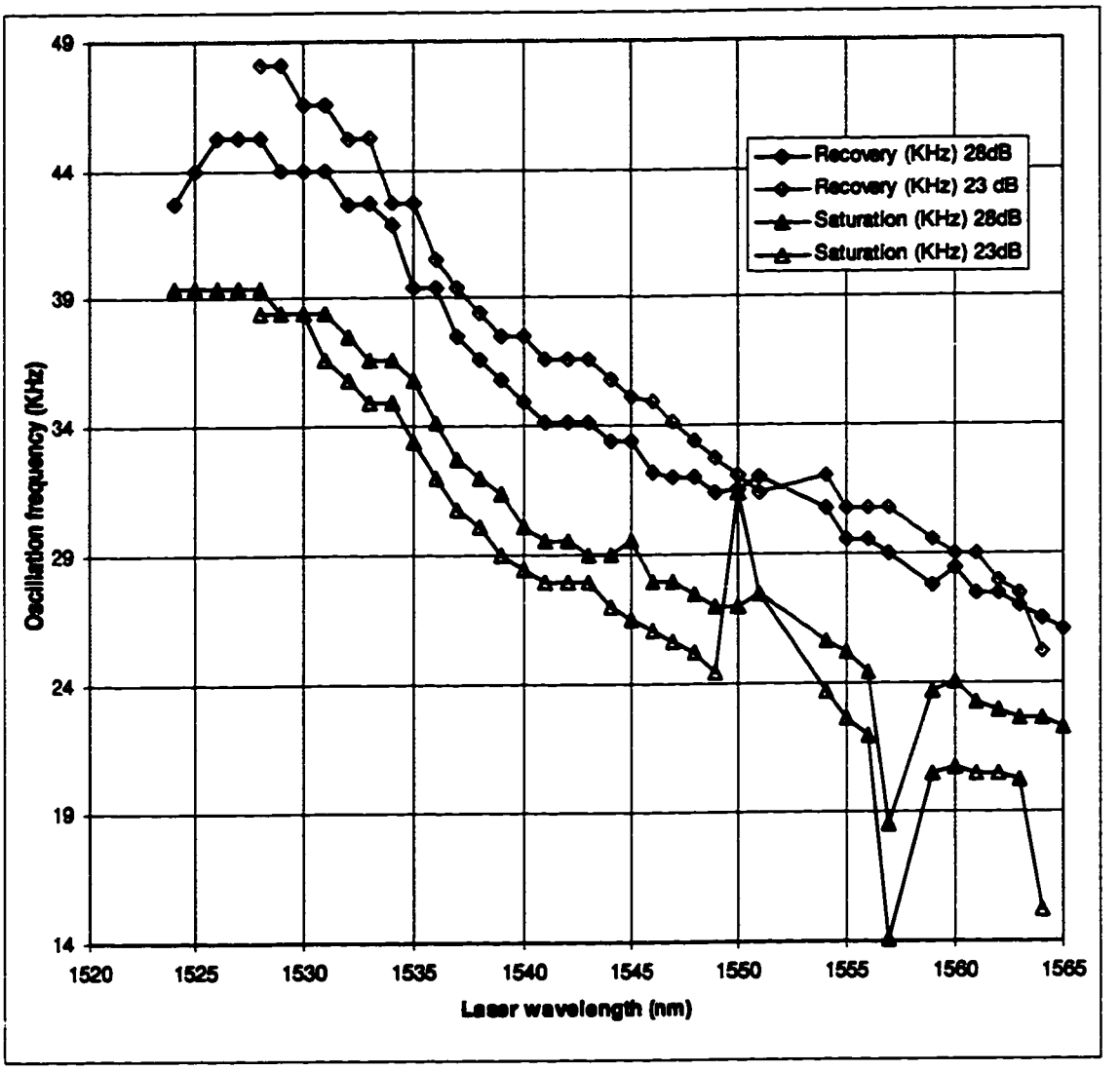

Fig.3.6

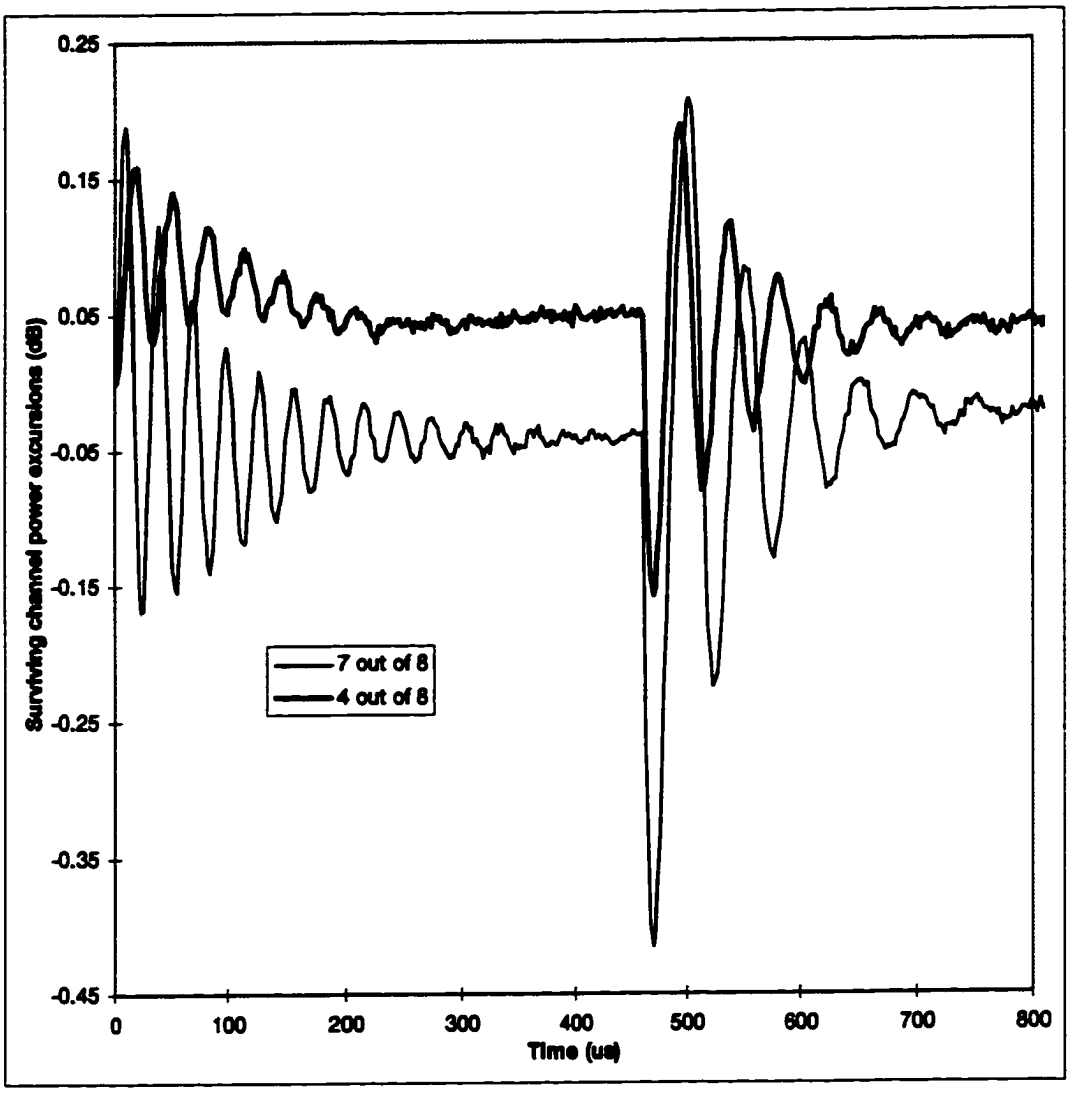

Fig.3.7

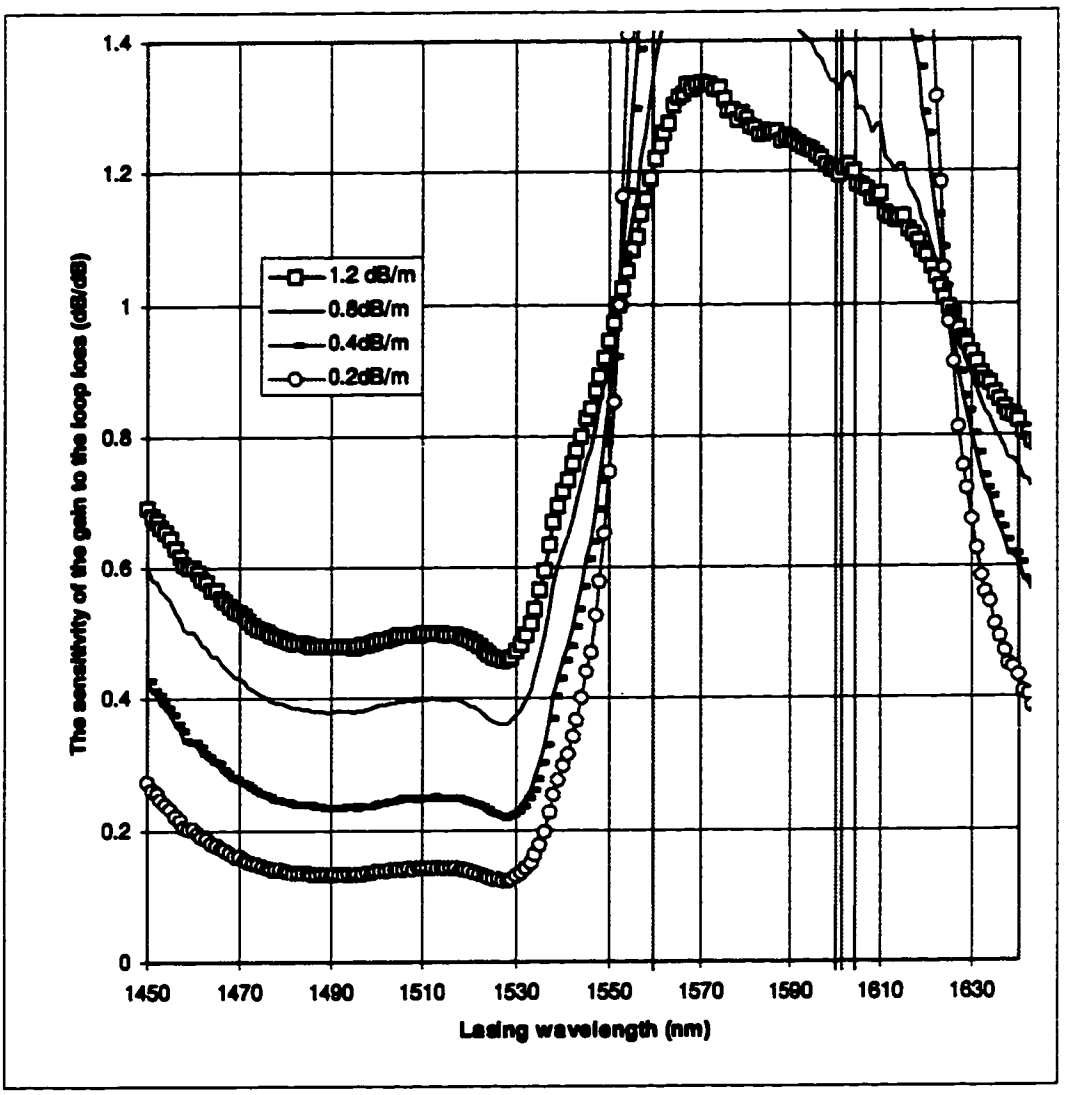

Fig.4.2

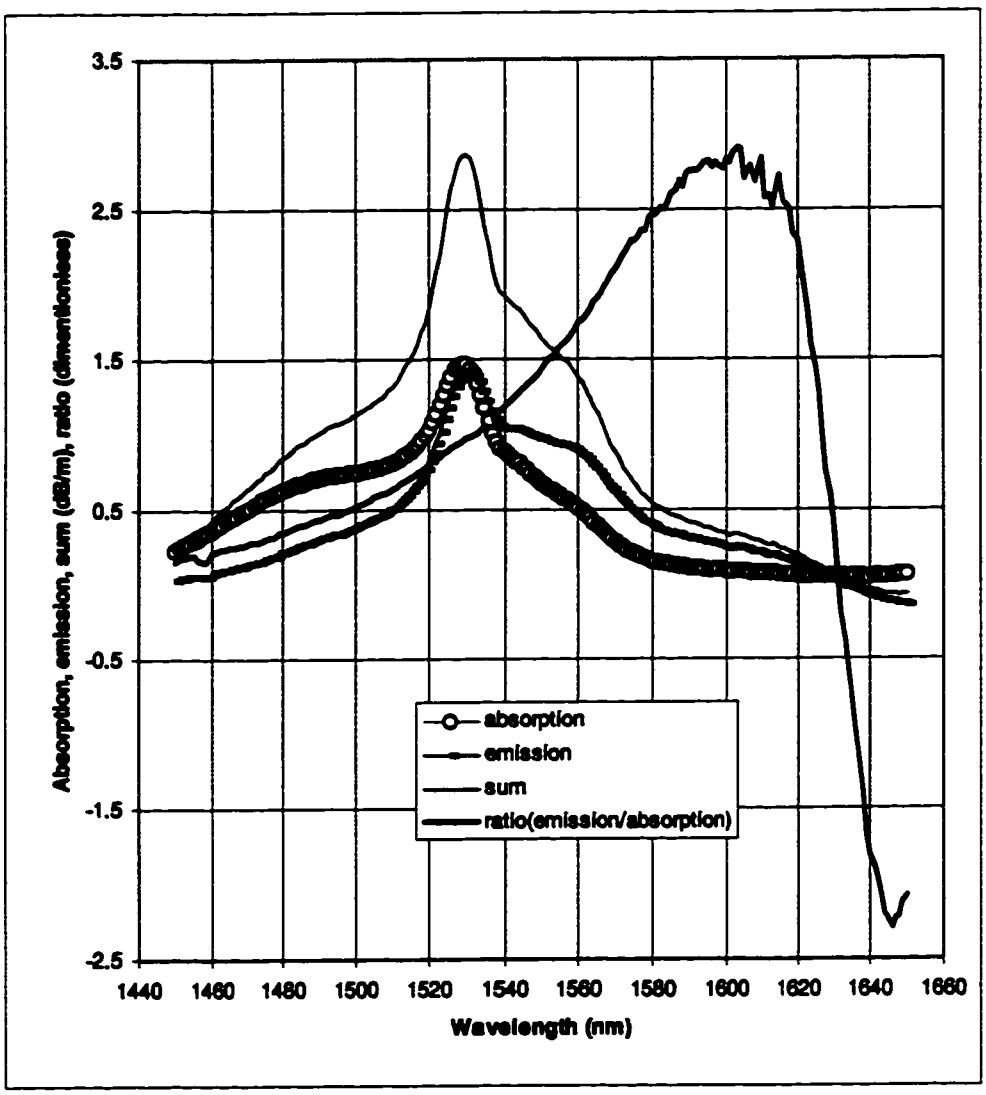

Fig.4.3

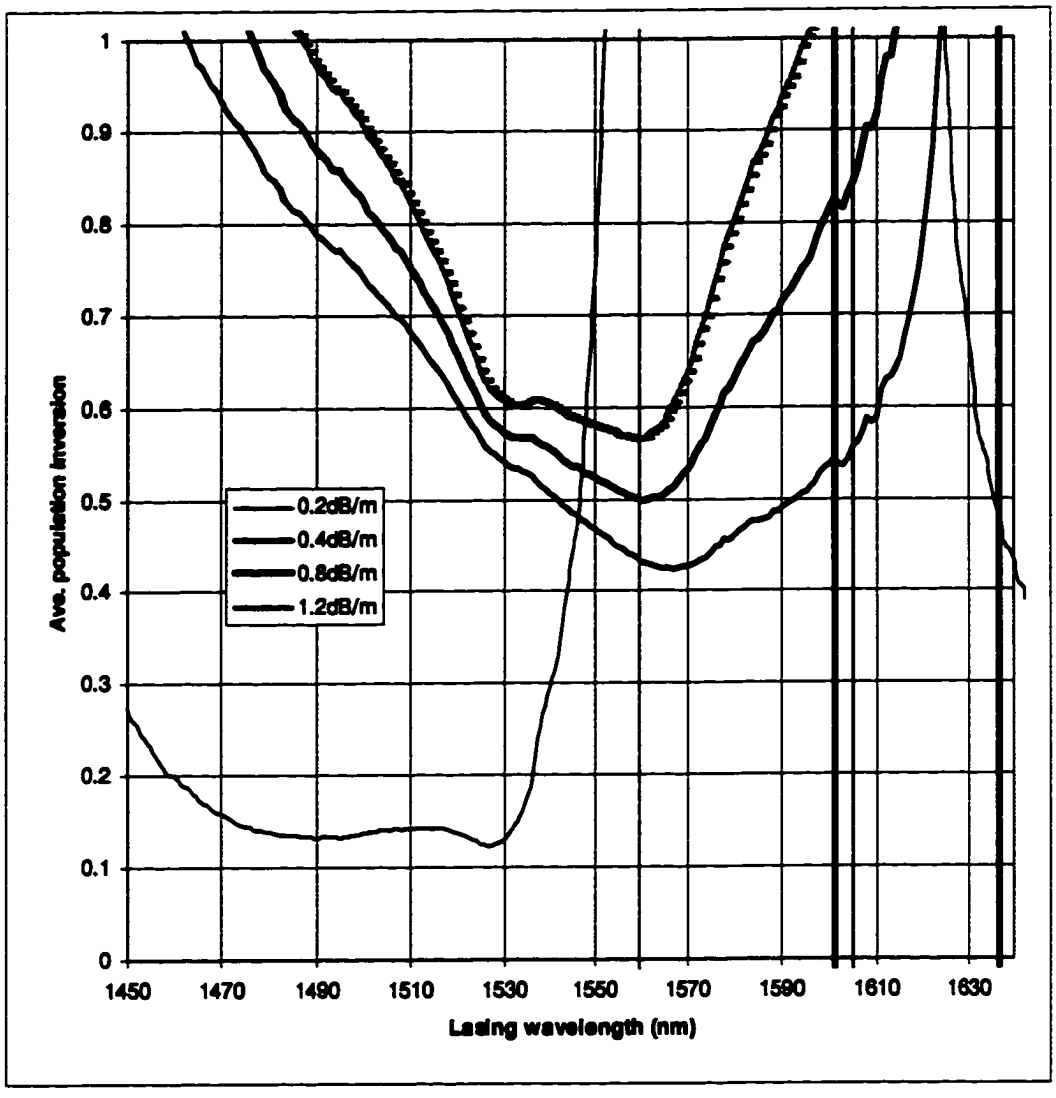

Fig.4.4

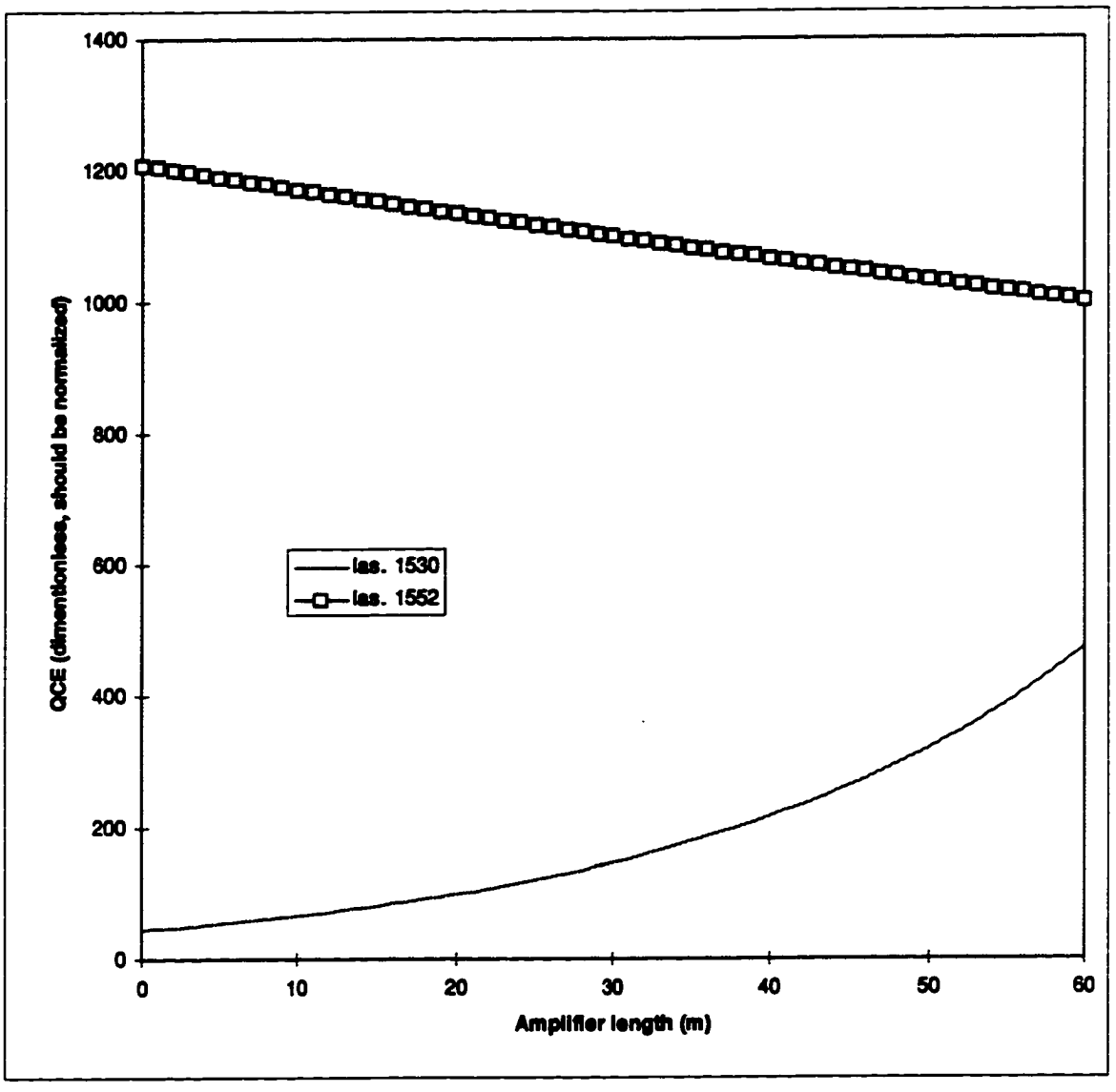

Fig.4.5

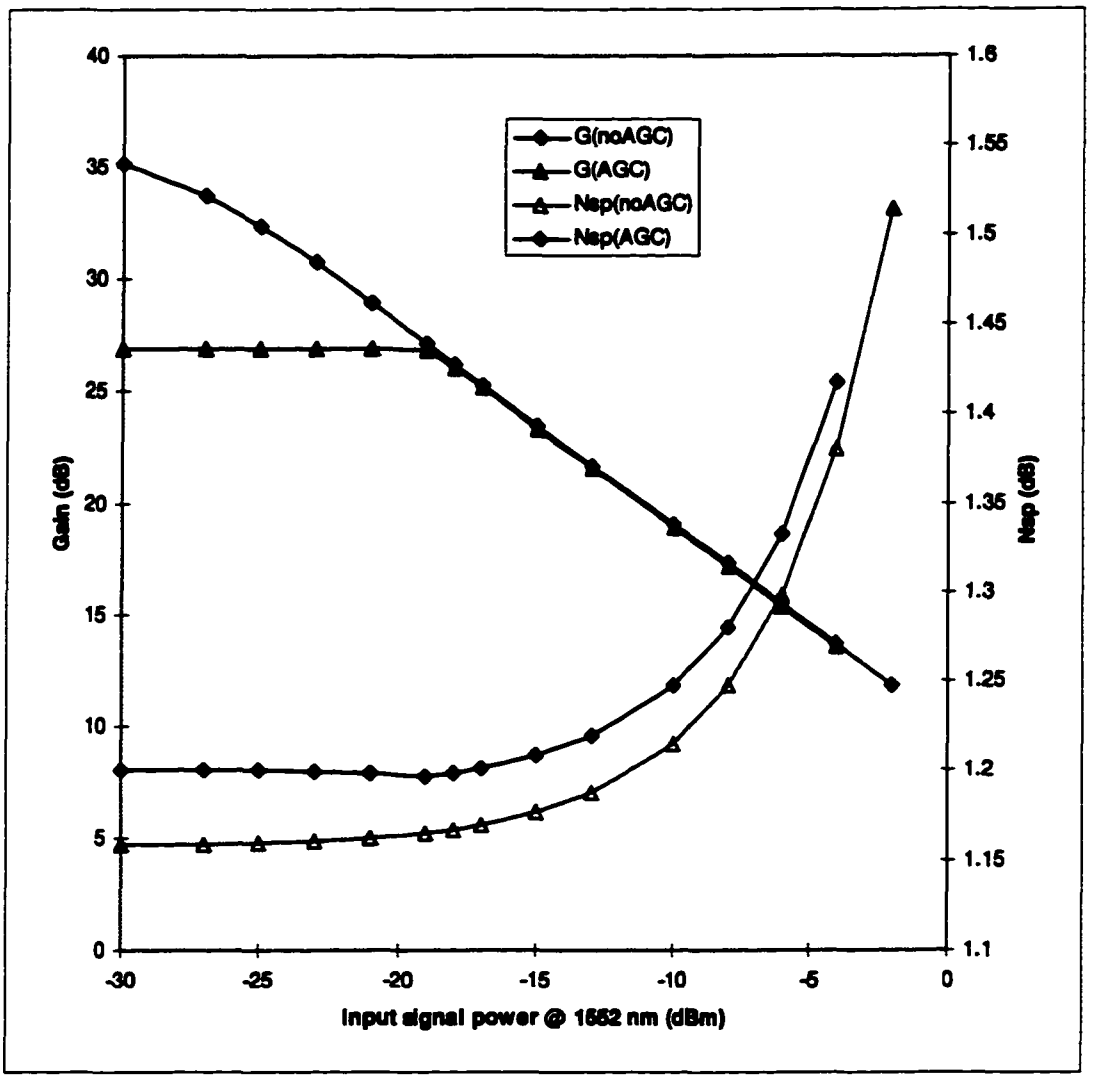

Fig. 4.6

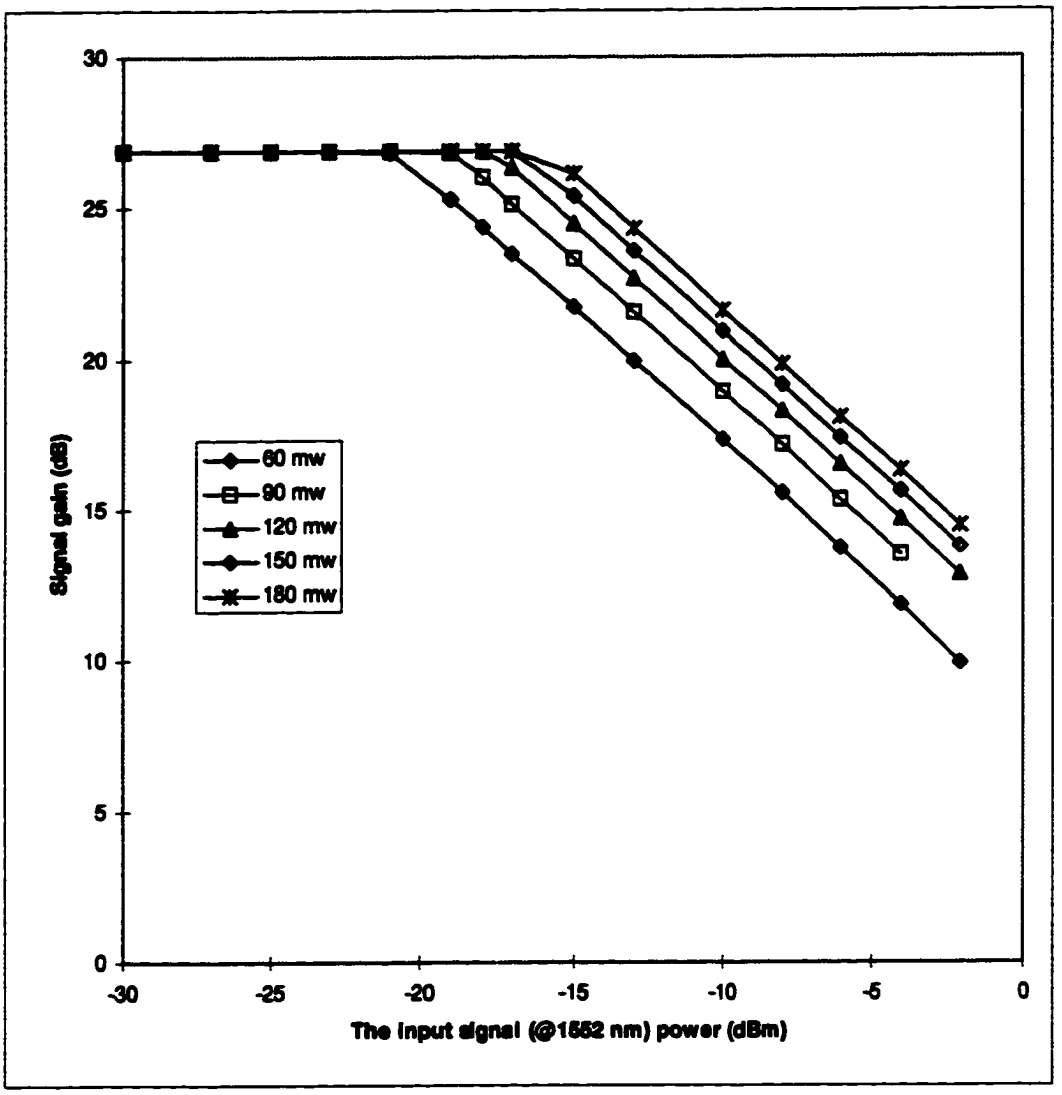

Fig.4.7

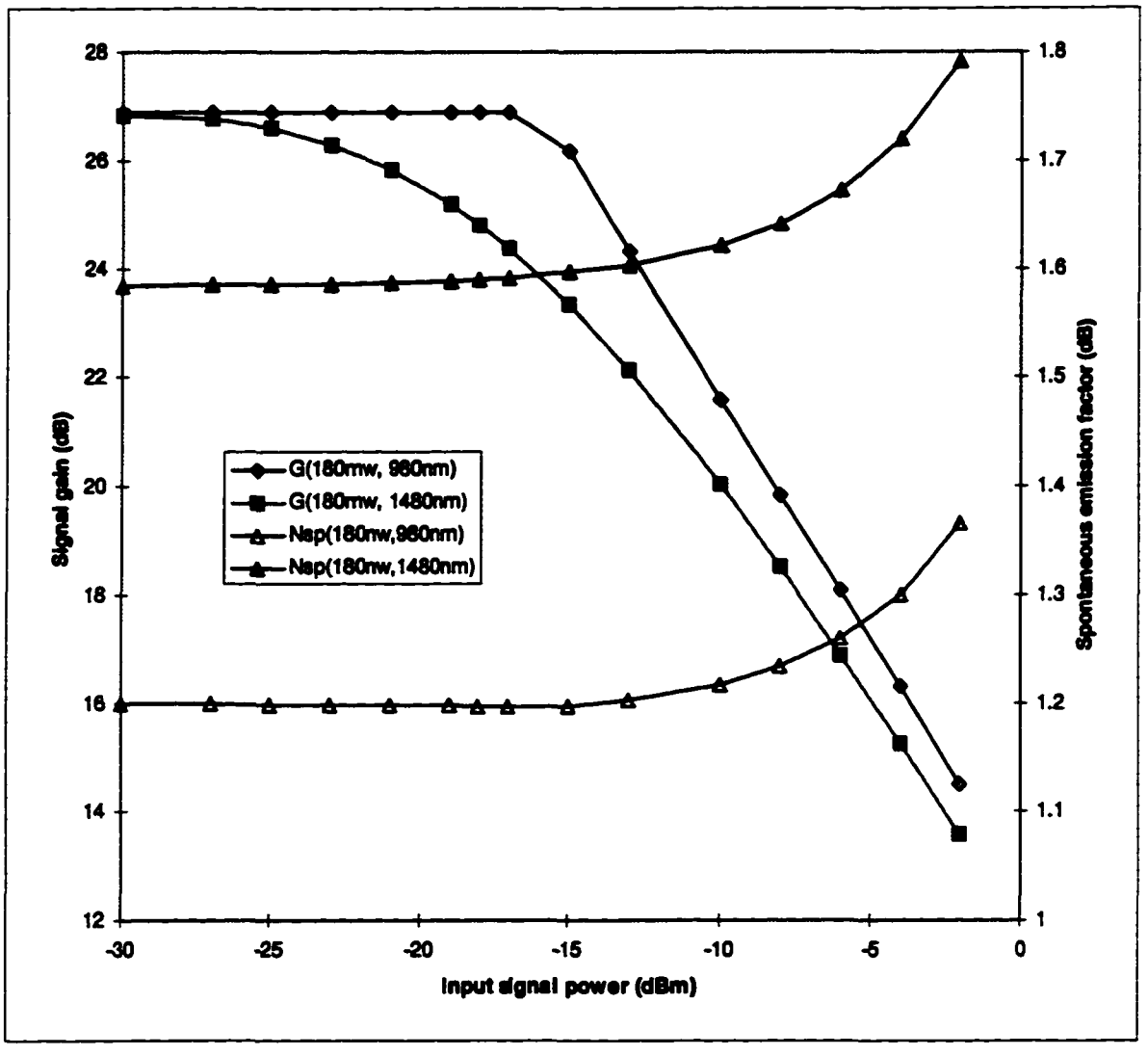

Fig. 4.8

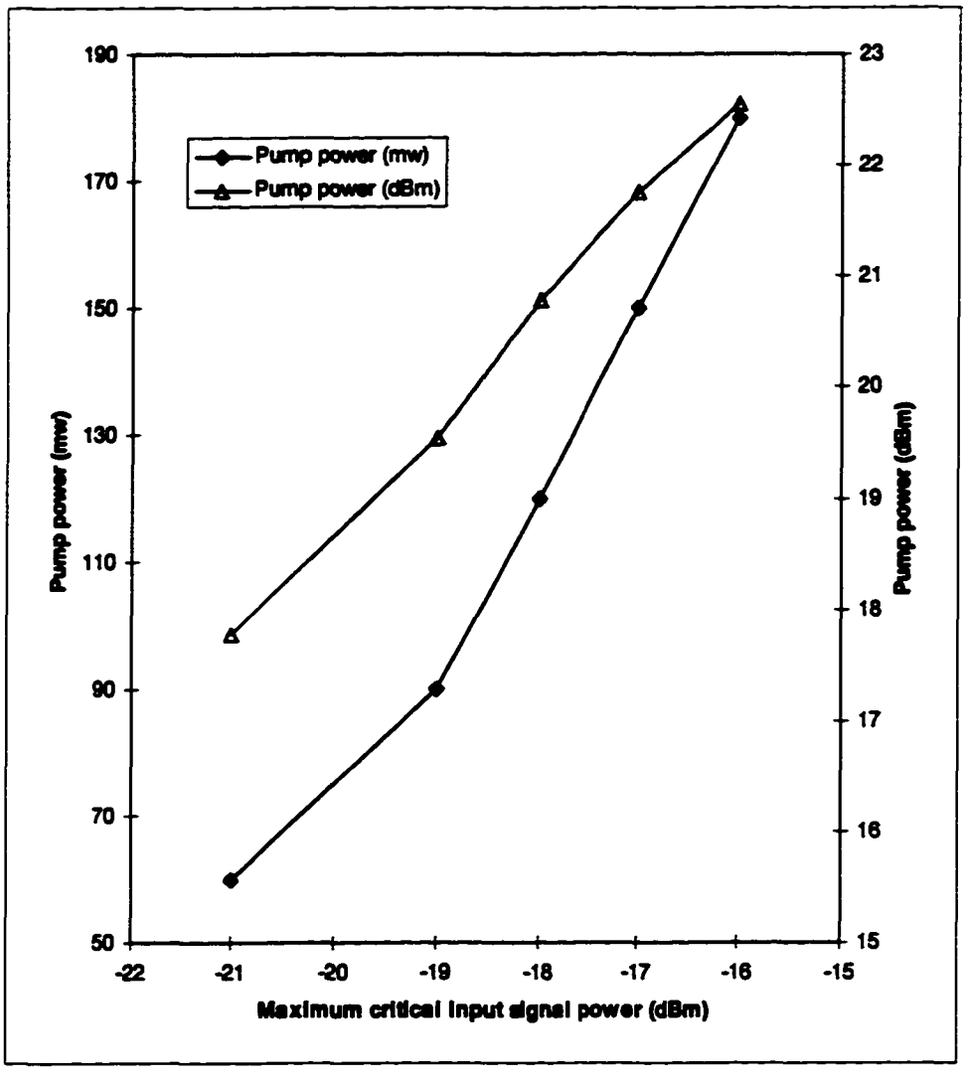

Fig.4.9

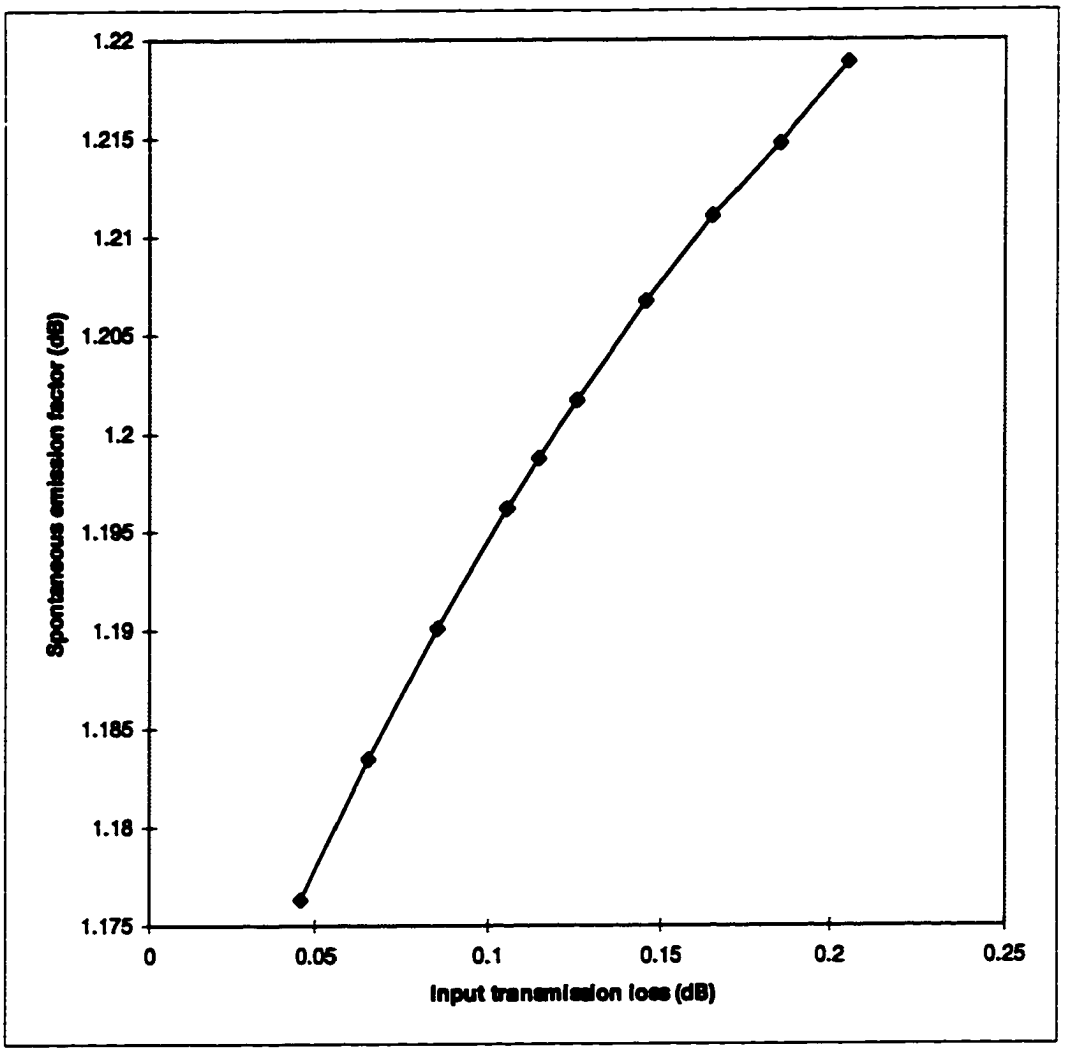

Fig.4.10

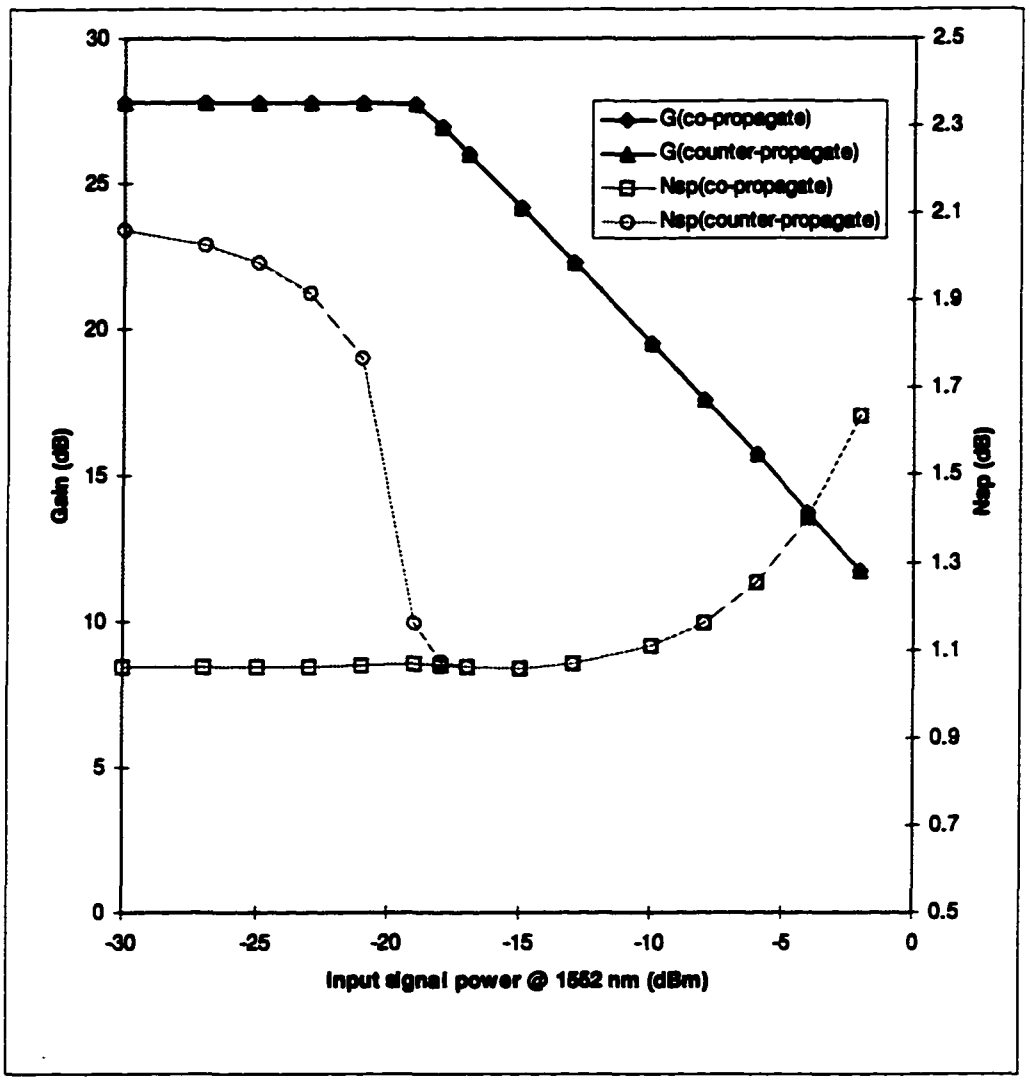

Fig.4.11

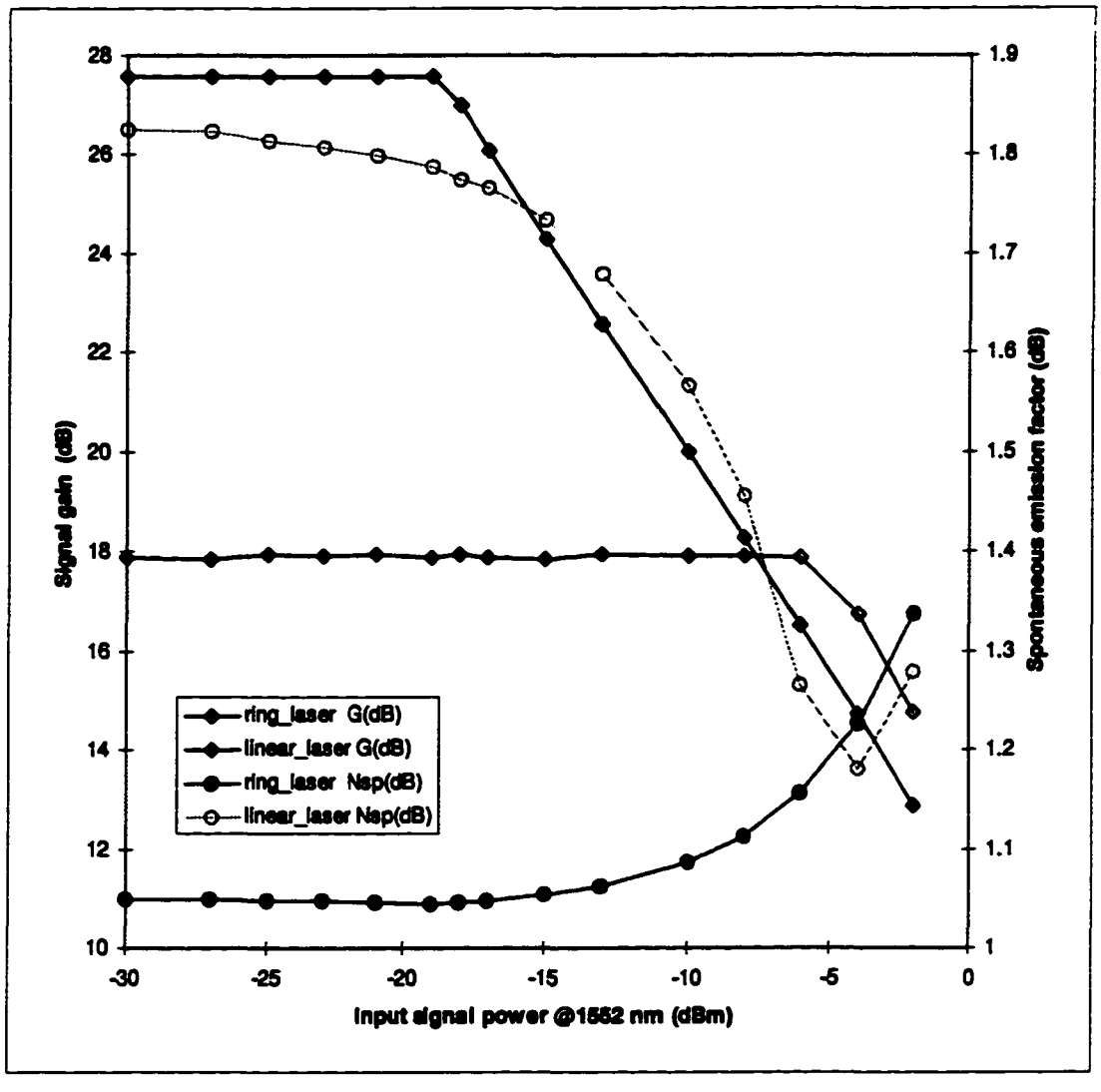

Fig.4.12

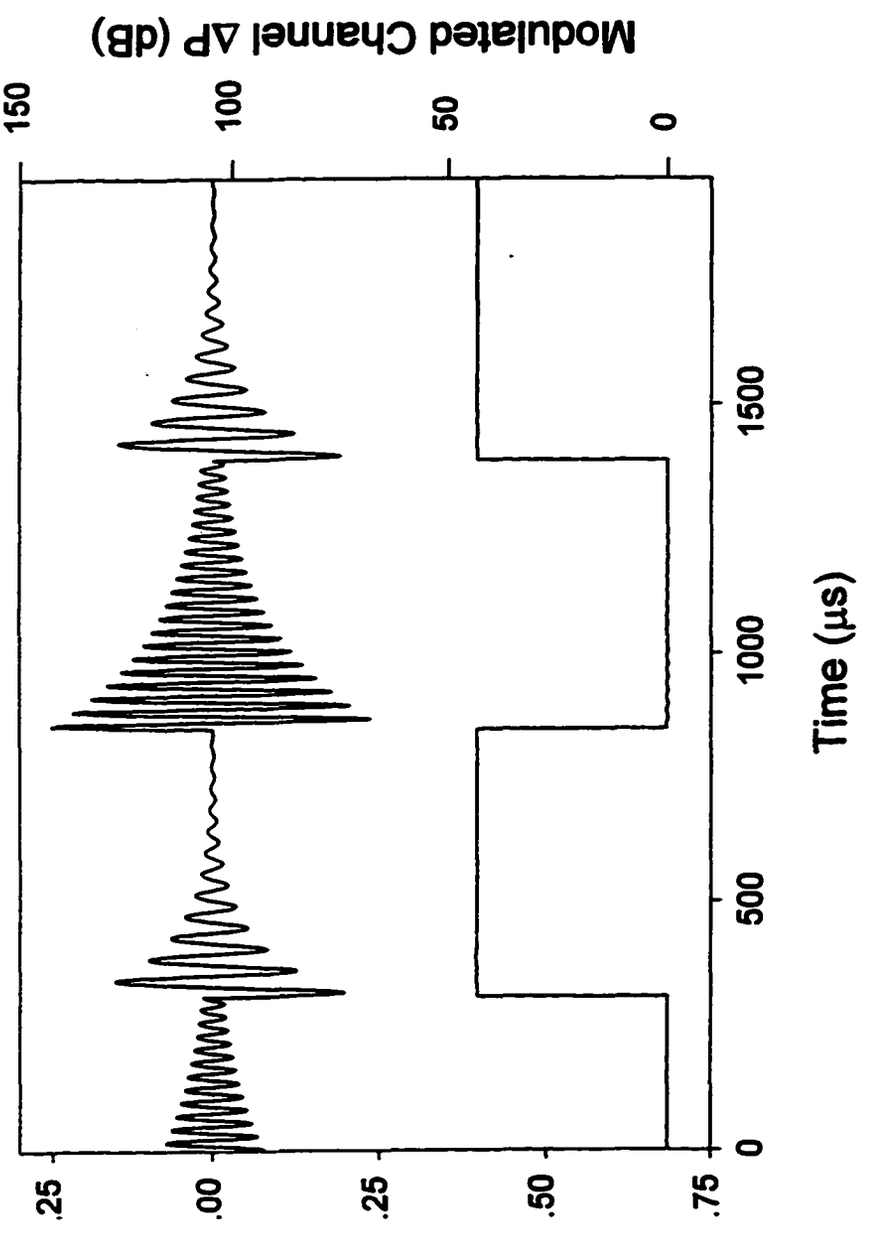

Fig. 5.1

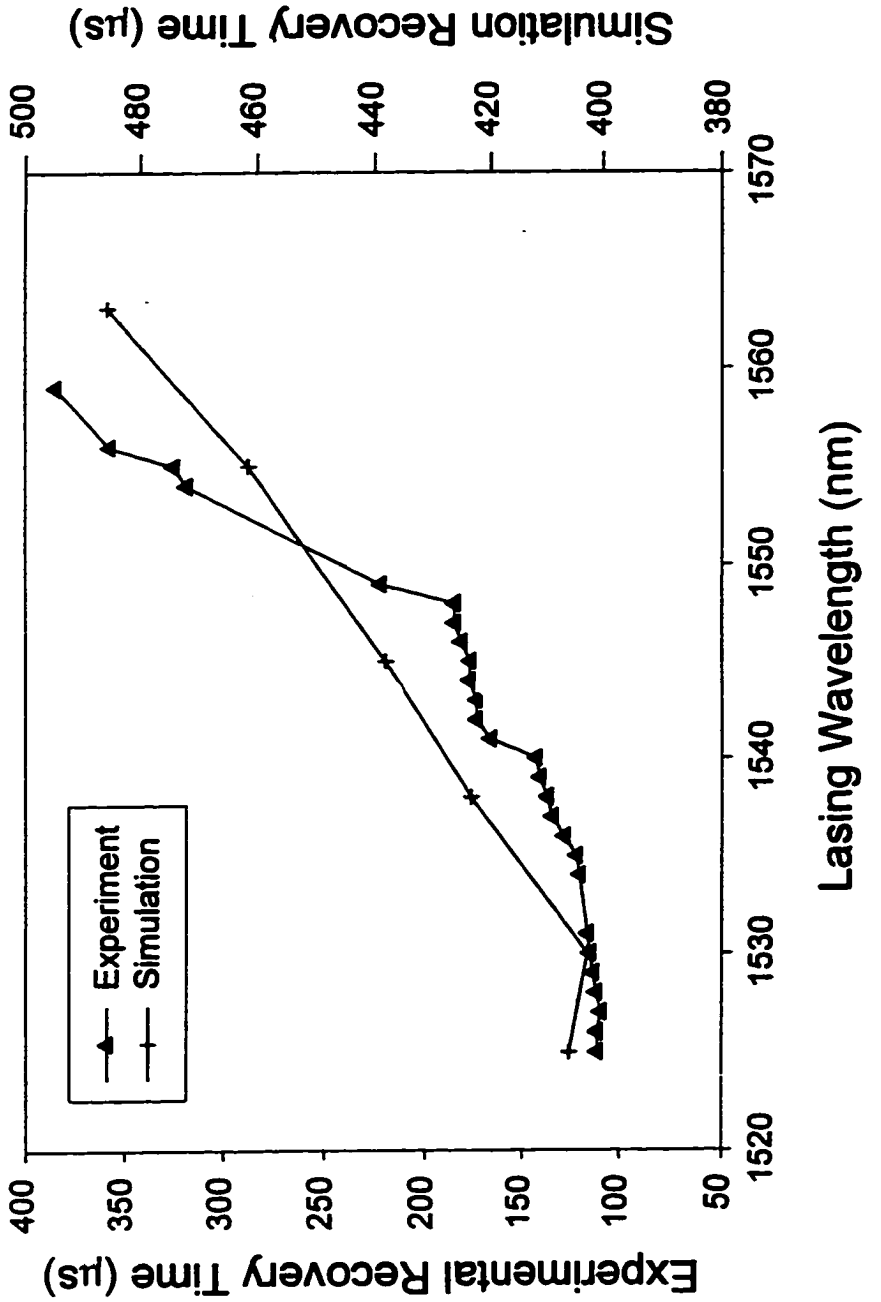

Fig. 5.2

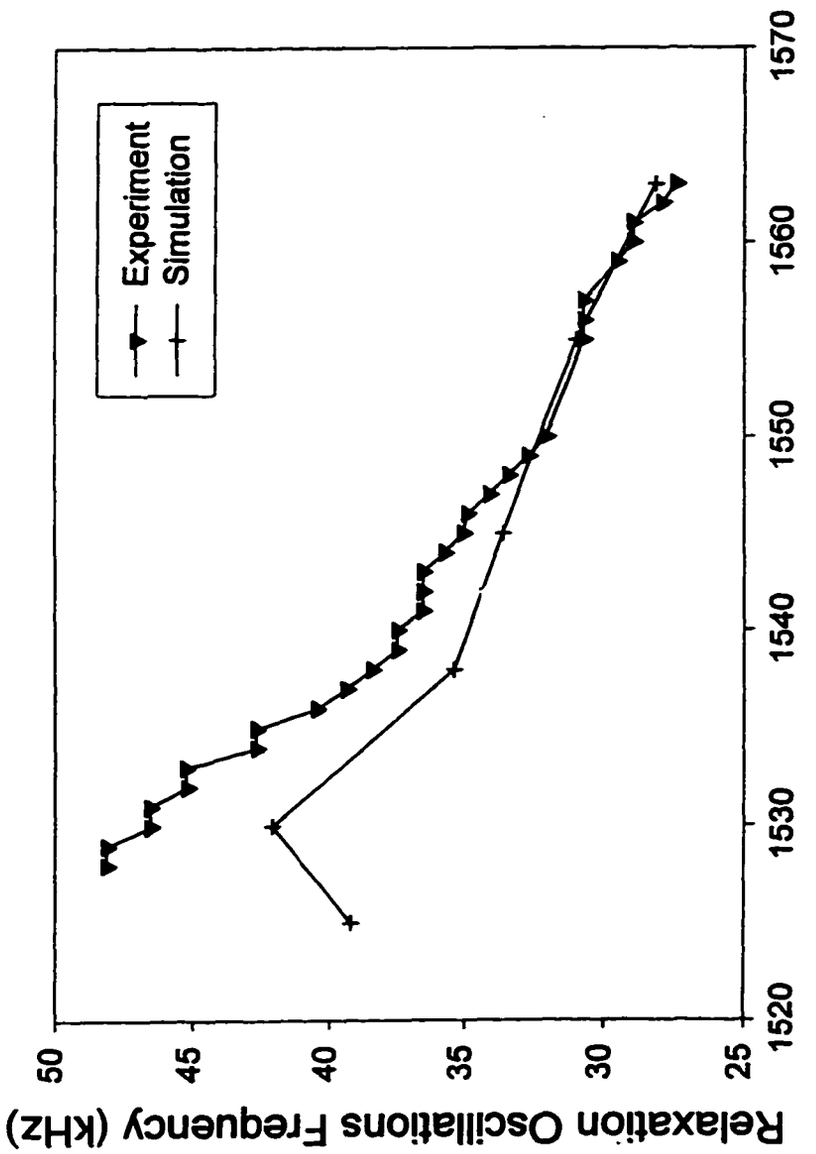

Fig. 5.3

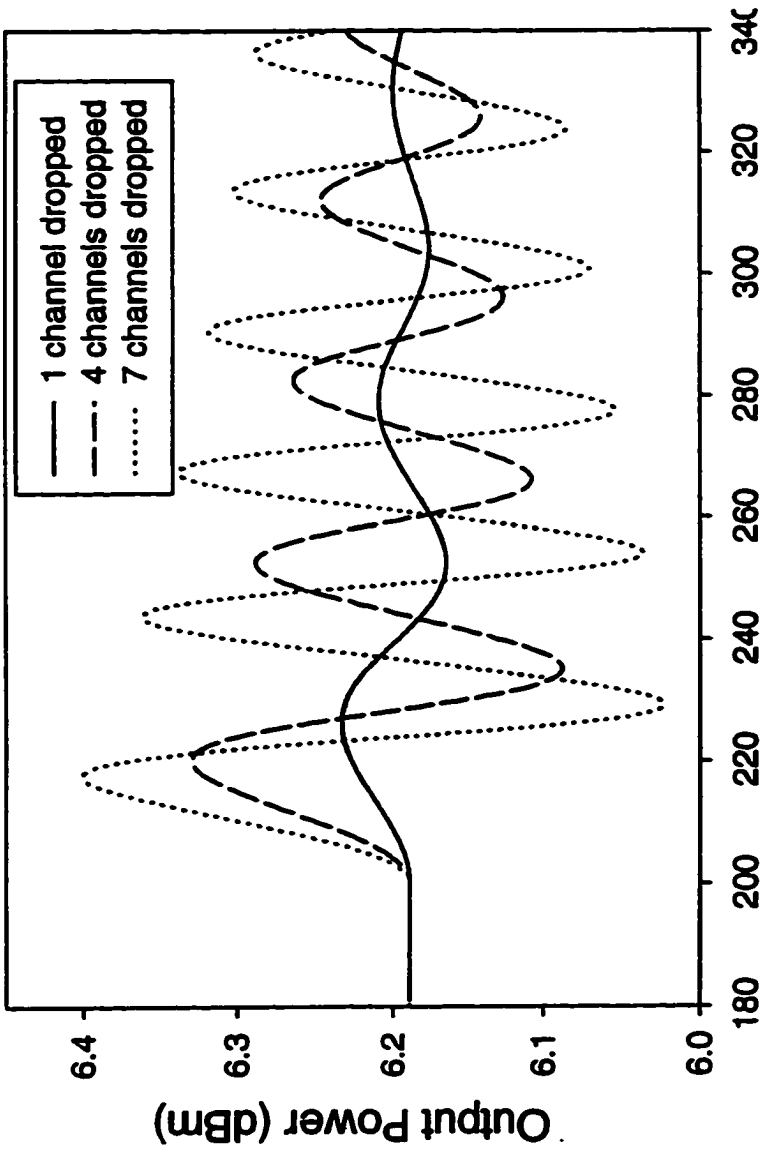

Fig. 5.4

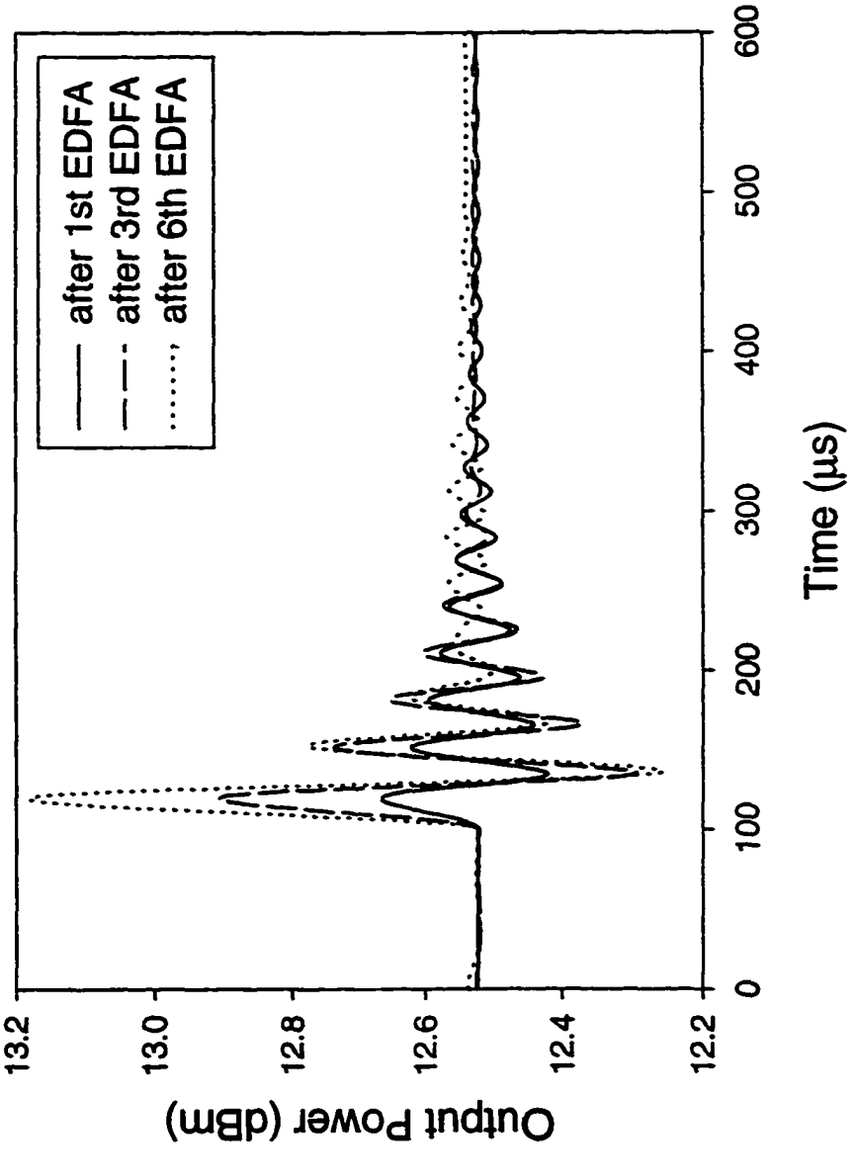

Fig. 6.1

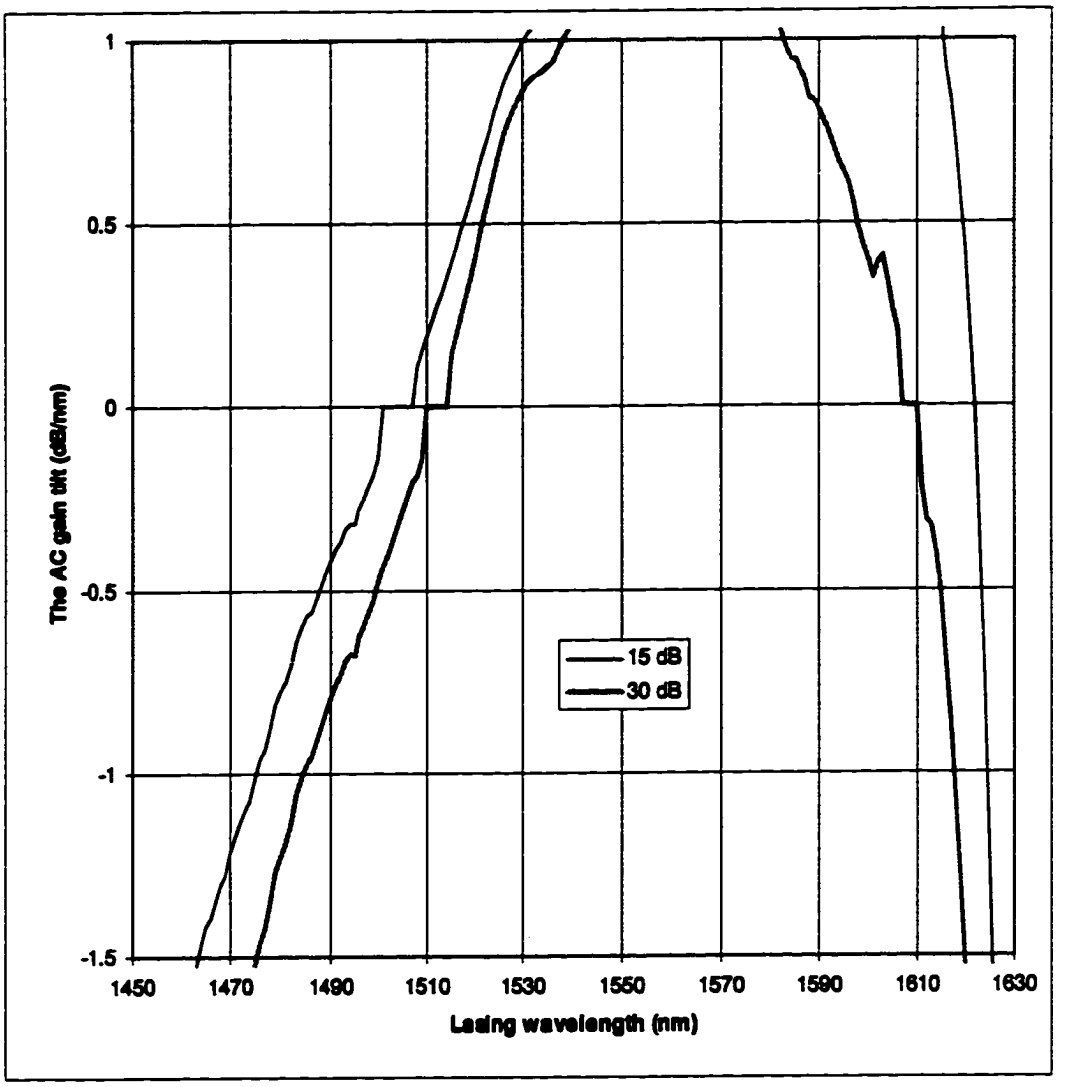

Fig. 7.1

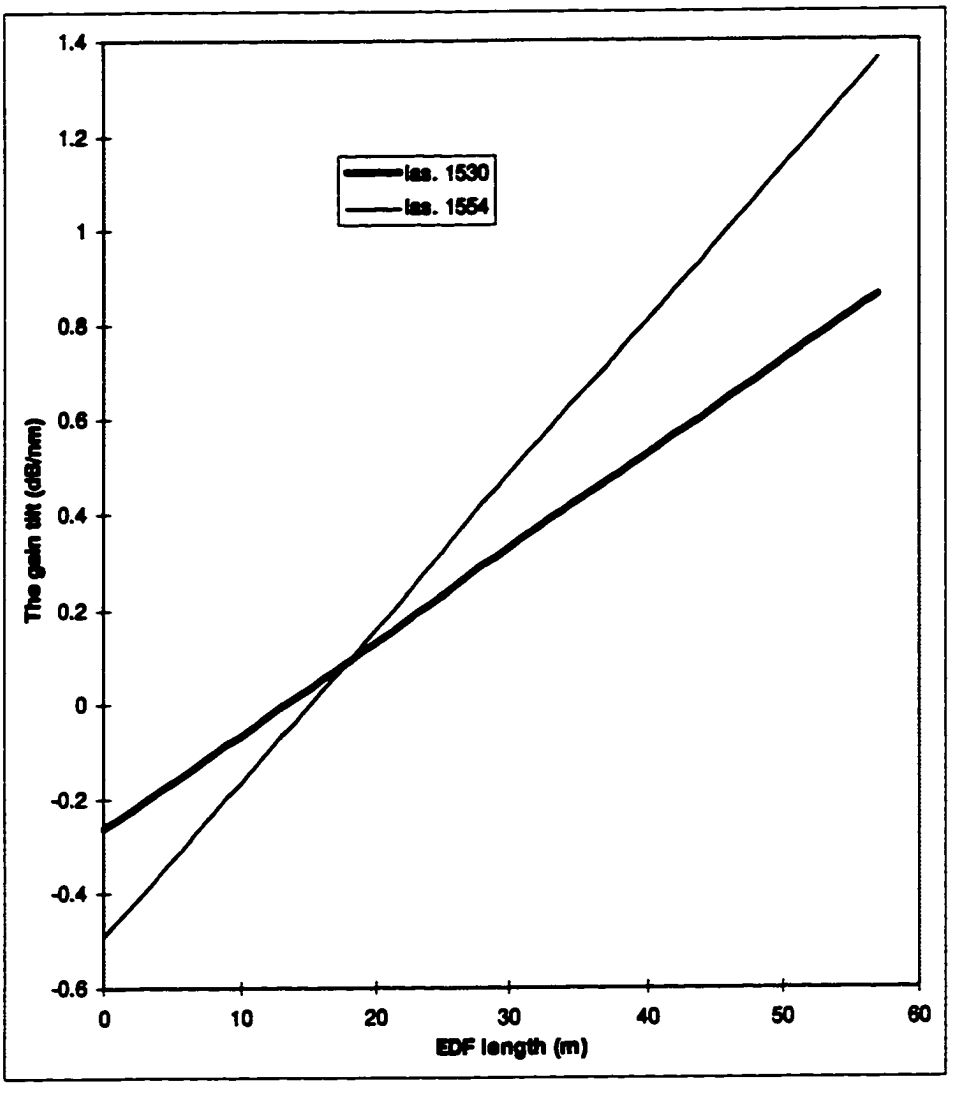

Fig. 7.2

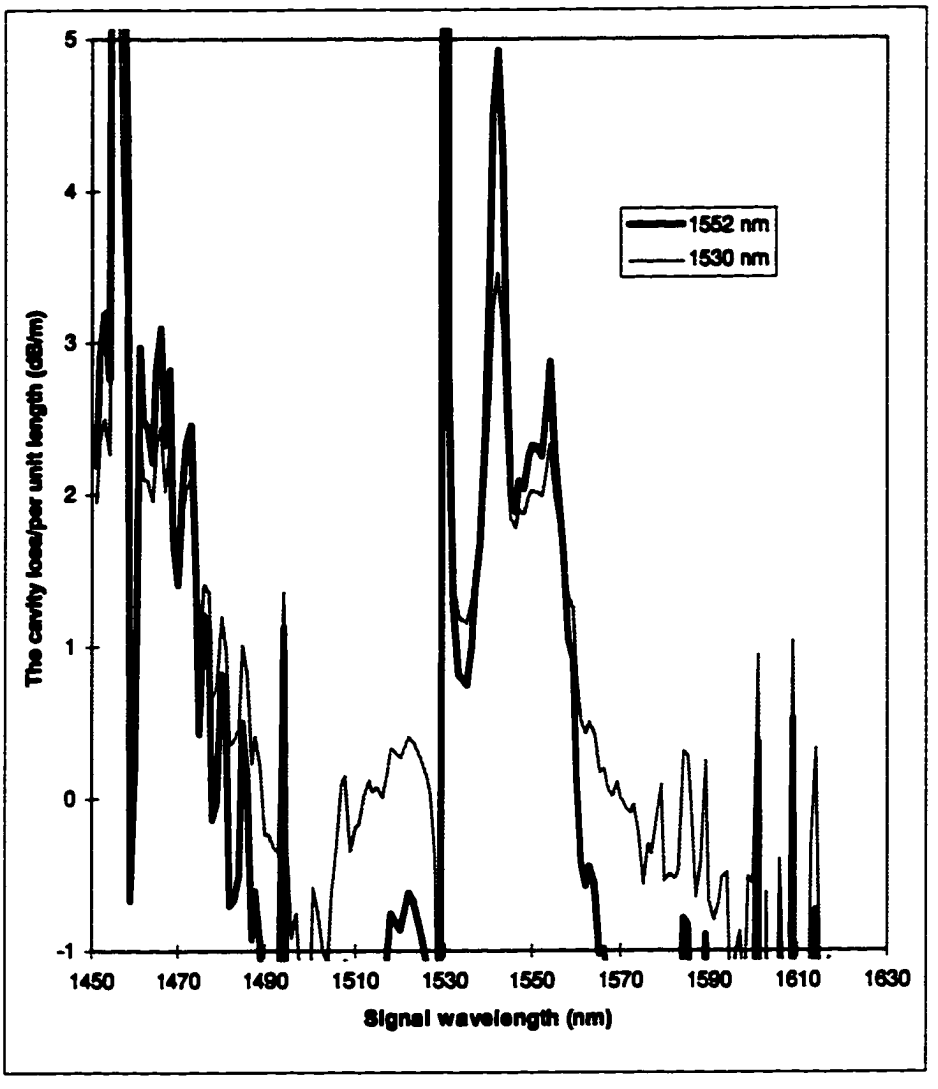

Fig. 7.3

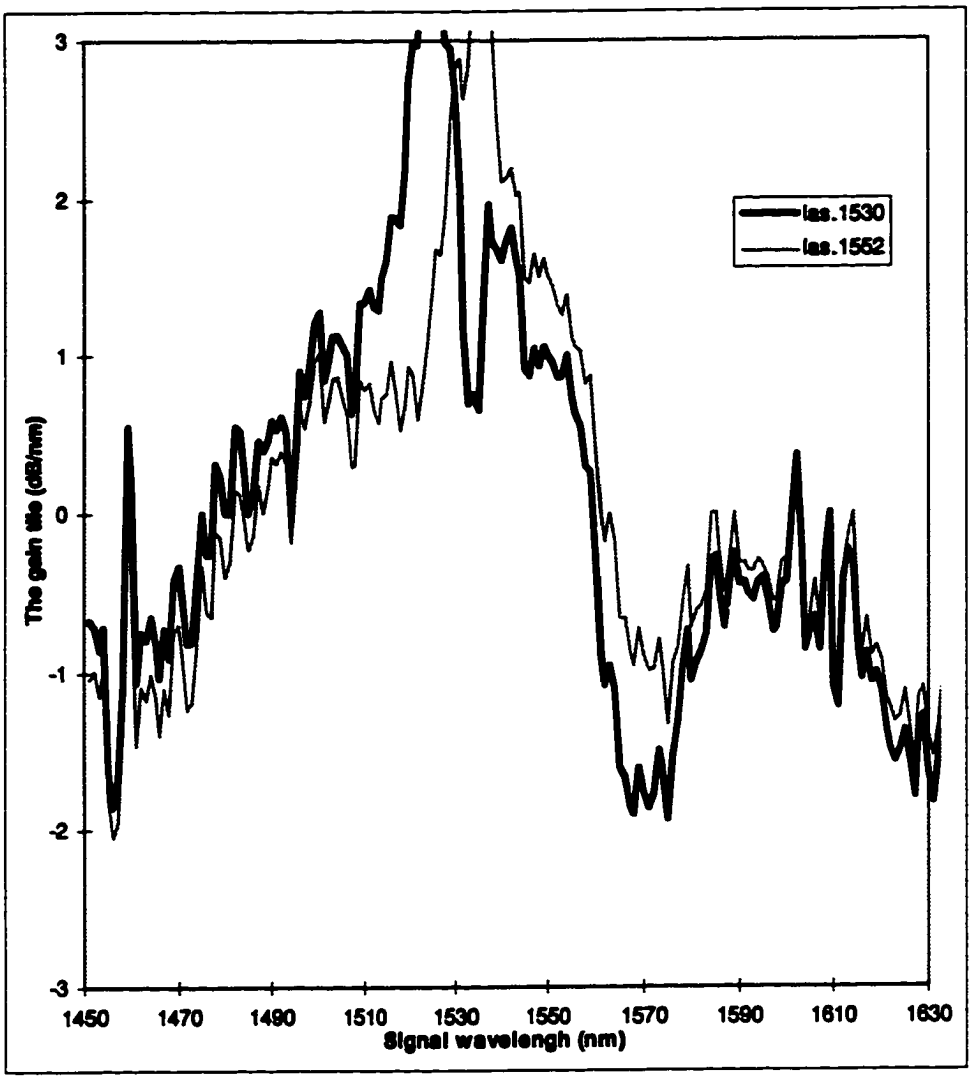

Fig. 7.4

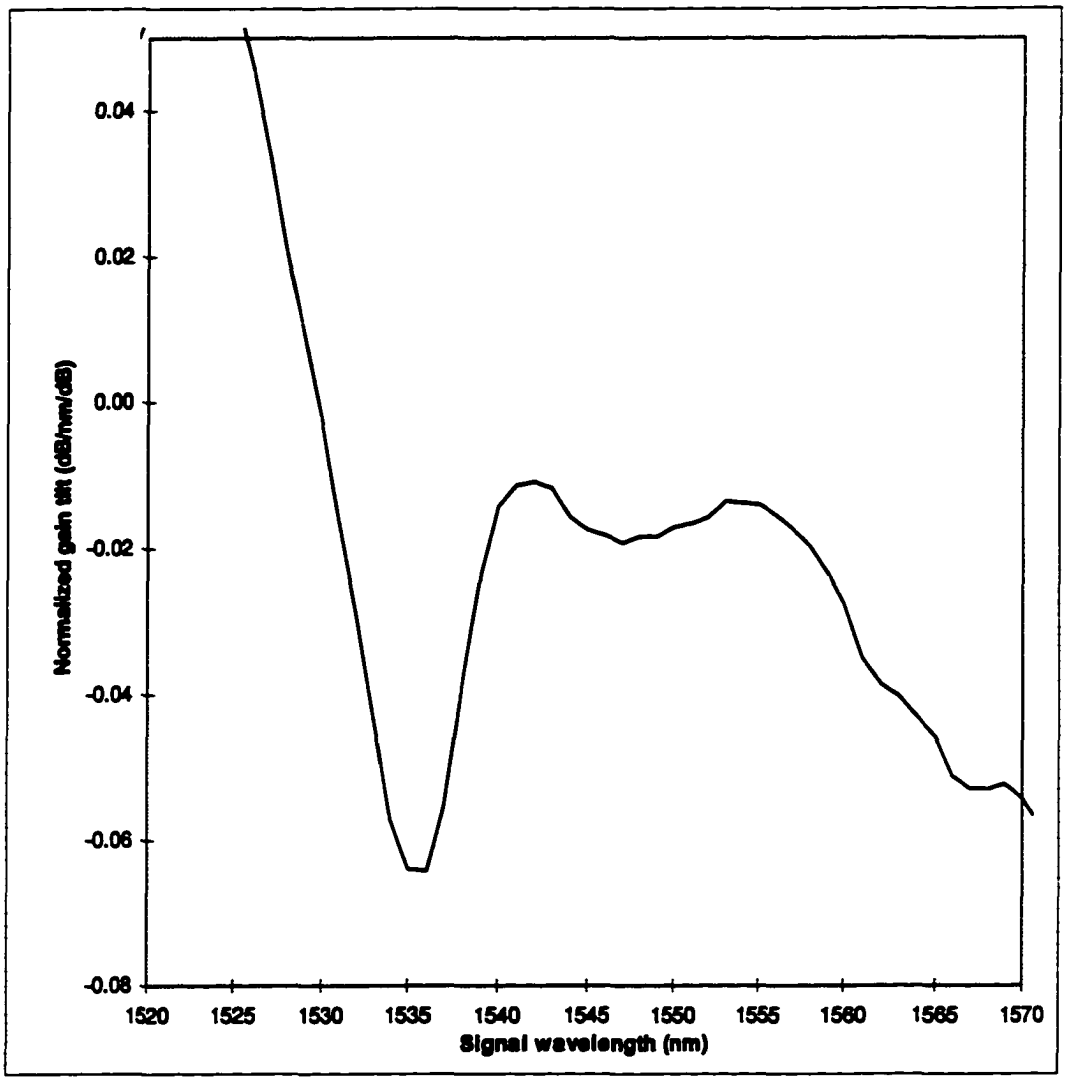

Fig. 7.5

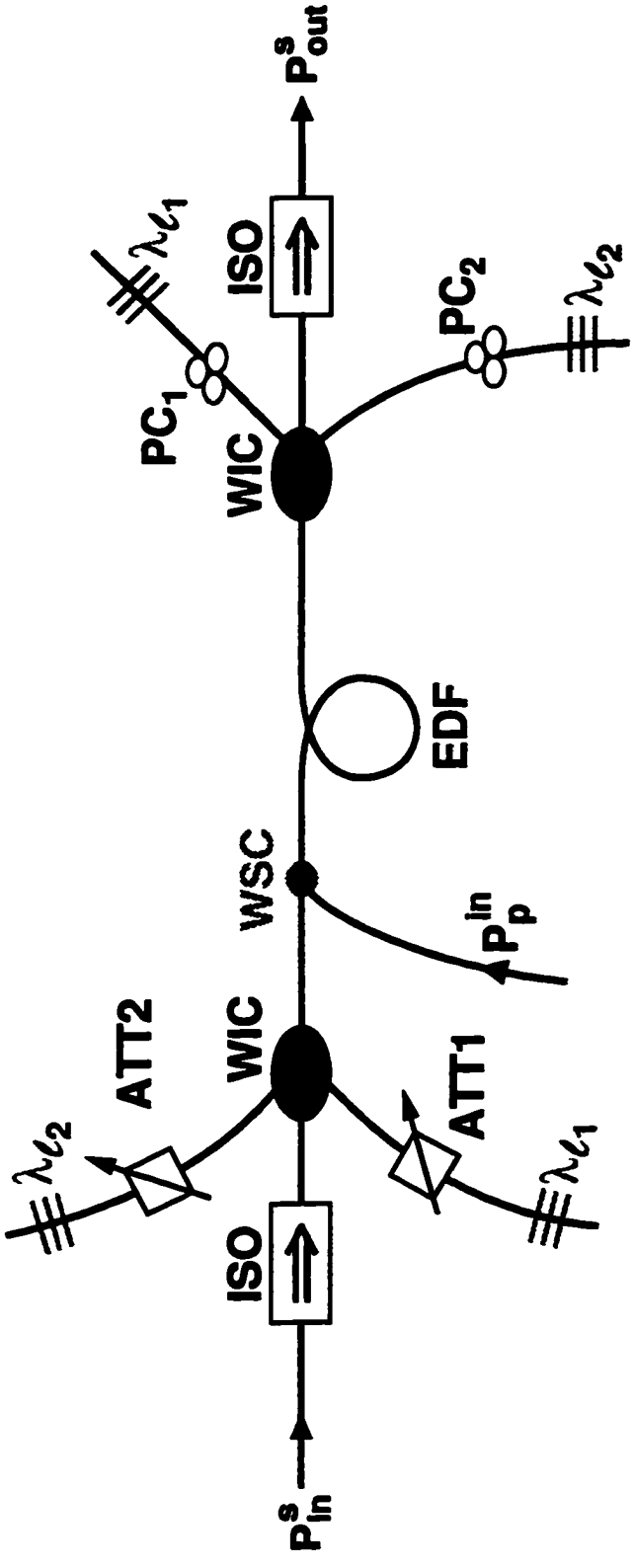

Fig. 8.1

Bibliography:

Ali, M.A., A.F. Elrefaie, A.F. Wagner, and S.A. Ahmed, "Performance of Erbium-doped fiber amplifier cascades in WDM multiple access light networks", PTL, 6, 1142 (1994).

Awerbuch, B., B. Patt-Shamir, and G. Varghese, "Self-stabilizing end-to-end communication", J. of Hight Speed Networks, 5, 365 (1996).

Baney, D.M., "Gain and noise characterization of EDFAs for WDM applications", OFC'97, Dallas, Texas, OSA Technical Digest Series, 6 (1997) 103, WA1.

Barros, M.R.X. de, G. Nykolak, D.J. DiGiovanni, A.Bruce, W.H.Grodkiewicz, and P.C. Becker, "Performance of a high concentration Er -doped alumino silicate fiber amplifier", IEEE Photon. Technol. Lett., Vol.8, pp.761-763, 1996.

Bertilsson, K. and P.A. Andrekson, "Modeling of noise in erbium-doped fiber amplifiers in the saturated regime", J. Lightwave Technol. 12 (1994) 1198.

Boyd, R.W. and S. Mukamel, "Origin of spectral holes in pump-probe studies of homogeneously broadened lines", Phys. Rev. A29, 1973(1984).

Chieng, Y.T., "Derivation of the mode build-up time of tunable fiber lasers", IEEE photon. Technol. Lett., 8, 211 (1996).

Chieng, Y.T. and G.J. Cowle, "Suppression of relaxation-oscillations in tunable fiber lasers with a nonlinear amplified loop mirror", IEEE, PTL, 7, 485 (1995).

Chieng, Y.T. and G.J. Cowle, "Relaxation oscillation suppression in tunable fibre lasers", Electron. Lett., 30, 1419 (1994).

Chieng, Y.T., G.J. Cowle, and R.A. Minasian, "Optimization of wavelength tuning of erbium-doped fiber ring lasers", J. Lightwave Technol., 14, 1730 (1996).

Chow, J., G. Town, B. Eggleton, M. Ibsen, K. Sugden, and I. Bennion, "Multiwavelength generation in an Erbium-Doped fiber laser using in-fiber comb filters", IEEE, Photon. Technol. Lett., 1996, 8, p.60 .

Chung, Joon, Sang Yong Kim and Chang Joon Chae, "All-optical gain-clamped EDFAs with different feedback wavelengths for use in multiwavelength optical networks", Electron. Lett., 1996, 32, p.2159.

Cognolato, L., A. Gnazzo, B. Sordoo, and C. Bruschi, "Tunable Erbium-doped silica fiber ring laser source: design and realization", J. Opt. Commun., 1995, 16, P.122.

Delevaque, E., T. Georges, J.F. Bayon, M.Monerie, P. Niay and P. Bernage, "Gain control in Erbium-doped fibre amplifiers by lasing at 1480nm with written on fibre ends", Electron. Lett., 1993, 29, p.1112 .

Desurvire, E., "Erbium-doped fiber amplifiers: basic physics and characteristics", ed. M.J.F. DiGonnet, in *Rare-earth-doped fibers and devices* (Marcel Dekker, New York, 1992)

Desurvire, E., M. Zirngibl, H.M. Presbym, and D. DiGiovanni, "Dynamic gain compensation in saturated Erbium-doped Fiber Amplifiers", IEEE photonics Technol. Lett., 1991, 3, p.453.

Desurvire, E., J.L. Zyskind and J.R. Simpson, "Spectral gain hole-burning at 1.53 um in erbium-doped fiber amplifiers", IEEE Photonics Technol. Lett., 2(1990) 246.

Desurvire, E., Erbium-Doped Fiber Amplifiers: Principles and Applications, John Wiley & Sons, Inc., New York (1994).

Desurvire, E., C.R. Giles, J.R. Simpson and J.L. Zyskind, "Efficient erbium-doped fiber amplifier at a 1.53 um wavelength with a high output saturation power", Optics Lett., 14(1989) 1266.

Desurvire, E., C.R. Giles, and J.R. Simpson "Gain saturation effects in high-speed, multichannel erbium-doped fiber amplifiers at λ=1.53 nm", IEEE J. Lightwave Technol. 7(1989) 2095.

Desurvire, E., "An explicit analytical solution for the transcendental equation describing saturated erbium-doped fiber amplifiers", Optical Fiber Technology, 2 (1996) 367

Dai, H., J. Pan, C. Lin, "All-optical gain control of in-line EDFA for hybrid AM/digital WDM systems", in OFC'97, OSA Technical Digest, WF6, pp. 133-134,Dallas, Texas

Delavaux, J. -M. P and J.A. Nagel, "Multi-stage erbium-doped fiber amplifier designs", J. Lightwave Technol. 13 (1995) 703.

Ding, M. and P.E. Cheo, "Analysis of Er-doped fiber laser stability by suppressing relaxation-oscillation", IEEE photon. Technol. Lett., 8, 1151 (1996).

Edagawa, N., S. Yamamoto, H. taga, M. Suzuki, and H. Wakabayshi, "Long-haul optical transmission system using optical amplifiers and their future trends", in Proc. SubOptic93, Syst. Opt. Amplifier, 1993, p.55.

Fake, M., T.J. simmons, J. Massicott, R. Wyatt, "Optically stabilized EDFA for in-band WDM systems", OFC'95, Tech. dig., TuP3, p.79.

Frankel, M.Y., R.D. Esman, and J.F. Weller, "Rapid continuous tuning of a single-polarization fiber ring laser", IEEE photon. Technol. Lett., 6, 591 (1994).

Freeman, J. and J. Conradi, "gain modulation response of erbium-doped fiber amplifiers", 5, 224 (1993).

Georges, T. and E. Delevaque, "Analytic modeling of high-gain erbium-doped fiber amplifiers", Optics Lett., 17 (1992) 1113.

Giles, C.R. and E. Desurvire, "Modeling erbium-doped fiber amplifiers", IEEE J. Lightwave Technol., 9(1991) 271.

Giles, R. and T. Li, "Optical amplifiers transform long-distance lightwave telecommunications", Proc. of The IEEE, 84, 870 (1996).

Henry, P.S., R.A. Linke, and A.H. Gnauck, "Introduction to Lightwave Systems", in *Optical Communications Systems*, ed. S.E. Miller and I.P. Kaminow, Academic Press (1988) 781.

Ibrahim, H., D. Ronarc'h, L. Pophillat, A. Moalic, M. Guibert, J.Le Roch, and P. Jaffre, "Comparison between erbium-doped fluoride and silica fiber amplifiers in an AM-CATV transmission system", IEEE PTL, 5, 540 (1993).

Jackel, Janet Lehr and Dwight Richards, "All-optical stabilization of multi-wavelength EDFA chains: a network-level approach", LEOS'96, PostDeadline papers, Boston, MA.

Jackel, J.L. and D. Richards, "All-optical stabilization of cascaded multichannel erbium-doped fiber amplifiers with changing numbers of channels", in OFC'97, 84, TuP4, Dallas, Texas.

Jopson, R.M. and A.A.M. Saleh, "Modelingof gain noise in erbium doped fiber amplifiers", SPIE Fiber Laser Sources and Amplifiers III, 1581 (1991), 114.

Kikushima, K., "AC and DC gain tilt of erbium-doped fiber amplifiers", J. Lightwave Technol., Vol. 12, pp.463-470, 1994.

Kuo, C.Y. and E.E. Bergmann, "Erbium-doped fiber amplifier second-order distortion in analog links and electronic compensation", IEEE Photon. Technol., Lett., Vol. 3, 829-831.

Laming, R.I., L. Reekie, P.R. Morkel, and D.N. Payne, "Multichannel crosstalk and pump noise characterisation of Er^{3+}-doped fiber amplifier pumped at 980 nm", Electron. Lett., 25 (1988) 455.

Landousies, B., T. Georges, E. Delevaque, R. Lebref, and M. Monerie, "Low power transient in multichannel equalized and stabilized gain amplifier using passive gain control", Electron. Lett., 1996, 32, p.1912.

Laude, J.P., "Wavelength Division Multiplexing", Prentice Hall, 1993.

Lebref, R., E. Delevaque, B. Landousies, H. Poignant, M. Guibert, T. Georges, "An advanced amplifier structure for WDM transmissions: The multichannel equalized and stabilized gain amplifier", Optical Amplifiers and their Applications Conf., Monterey, CA, Vol. 11, pp.81-84, 1996 OSA Tech. Dig. Series.

Li, S., H. Ding, and K.T. Chan, "Erbium-doped fibre lasers for dual wavelength operation", Electron. Lett., 33, p.52 (1997).

Luo, G., J.L. Zyskind, Y. Sun, A.K. Srivastava, J.W. Sulhoff, and M.A. Ali, "Relaxation-oscillations and spectral hole burning in laser automatic gain control of EDFA's", in OFC'97, WF4, Dallas, Texas.

Luo, G., J.L. Zyskind, Y. Sun, A.K. Srivastava, J.W. Sulhoff, C. Wolf, and M.A. Ali, "Performance degradation of all-optical gain-clamped EDFAs due to relaxation-oscillations and spectral hole burning in amplified WDM networks", submitted to IEEE Photon. Technol. Lett.

Luo, G., J.L. Zyskind, J. Nagle, and M.A. Ali, "Experimental and theoretical performance degradation analysis of all-optical gain-clamped EDFAs due to relaxation-oscillations and spectral hole burning in amplified WDM networks", submitted to J. Lightwave Technol.

Luo, G., et al., "An approximate solution of multimode relaxation-oscillations in a three-level laser system", to be submitted to IEEE PTL.

Luo, G., et al., "What is real gain stabilization condition in a laser AGC scheme", to be submitted to Electron. Lett.

Luo, G., J. Nagle, J.L. Zyskind, D. Richards, J.W. Sulhoff, and M.A. Ali, "How can we reduce the noise figure penalty in laser automatic gain control?", to be submitted to Electron. Lett..

Marcuse, D., "Pulsing behavior of a three-level laser with saturable absorber", IEEE J. Quantum Electron., Vol. QE.-29, pp.2390-2396, 1993.

Martin, J.C., J.M. Alvarez, and M.A. Rebolledo, "Erbium-doped fiber characterization by fluorescence dynamics measurement", IEEE. Quantum Electro., 32, 1727 (1996).

Massicott, J.F., S.D. Willson, R.Wyatt, J.R. Armitage, R. Kashyap, D. Williams, and R.A. Lobbett, "1480nm pumped erbium doped fibre amplifier with all optical automatic gain control", Electron. Lett., 1994, 30, p.962.

Massicott, J., C. Lebre, R. Wyatt, R. Kashyap, D. Williams, and A. Yu, "Low noise, all-optical gain controlled Er^{3+} doped fibre amplifier using asymmetric control laser cavity design", Electron. Lett., 1996, 32, p.816.

Mazurczyk, V.J. and J.L. Zyskind, "Polarization dependent gain in erbium-doped-fiber amplifiers", IEEE Photon. Technol. Letts. 6 (1994) 616.

McCumber, D.E., "Theory of phononterminated optical masers", Phys. Rev., 134A (1964) 299; see also: J. Nilsson et al., "Analysis of AC Gain Tilt in Erbium-doped Fiber Amplifiers", 8 (1996) 515.

Mears, R.J., L. Reekie, I.M. Jauncey, and D.N. Payne, Electron. Lett., 23 (1987) 1026.

Motoshima, K., K. shimizu, K.Takano, T. Mizuochi, and T. KiTayama, "EDFA with dynamic gain compression for multiwavelength transmission systems", OFC'94, Tech. Dig., p.191.

Nilsson, J., W.H. Loh, S.T. Hwang, J.P. de Sandro, and S.J. Kim, "Simple gain-flattened erbium-doped fiber amplifier with a wide dynamic range", OFC'97, Dallas, Texas, OSA Technical Digest, WF3, p.129; and references therein.

Nilsson, J., Y.W. Lee, and W.H. Choe, "Erbium doped fibre amplifier with dynamic gain flaness for WDM", Electron. Lett., Vol. 31, pp.1578-1579, 1995.

Nishimura, M., "gain-flattened erbium-doped fiber amplifiers for WDM transmission", OFC'97, Dallas, Texas, OSA Technical Digest Series, 6 (1997) 127, WF1.

Okamura, H., "Automatic optical-loss compensation with Er-doped fibre amplifier", Electron. Lett., 1991, 27, p.2155.

Okamura, H., "Automatic optical loss compensation with Erbium-Doped fiber amplifier", J. Lightwave Technol., 1992, 10, p.1110.

Onaka, H., et al., "1.1 Tb/s WDM transmission over a 150 Km 1.3 um zero-dispersion single-mode fiber", OFC'96, San Jose, CA, OSA Technical Digest Series, Postdeadline paper PD19.

Park, N. and P.F. Wysock, "24-line multimave length operation of Erbium-doped fiber-ring laser", IEEE photon. Technol. Lett., Vol.8, pp. 1459-1461, 1996.

Pasquael, Fabrizio Di, "Modeling of highly-efficient grating-feedback and Fabry-Perot Er-Yb co-doped fiber lasers", IEEE J. Quantum Electron., Vol. QE.-32, pp.326-332, 1996.

Peroni, M. and M. Tamburrini, "Gain in erbium-doped fiber amplifiers: A simple solution for the rate equation", Optics Lett., 15 (1990) 842; see also ref. [1] pp. 40-43.

Pfeiffer, Th. and H. Bulow, "Analytical gain equation for erbium-doped fiber amplifiers including mode field profiles and dopant distribution", IEEE Photon. Technol. Lett., 4 (1992) 449.

Ronarch, D., et al., "30 dB optical net gain at 1.543 um in Er^{3+} doped fluoride fibre pumped around 1.48 um", Electron. Lett., 27 (1991) 908.

Saleh, A.A.M., R.M. Jopson, J.D. Evankow and J. Aspell, "Modeling of gain in erbium-doped fiber amplifiers", IEEE Photonics Technol. Lett., 2(1990) 714.

Saruwatari, M., "Optical Amplifiers and their Applications", Chapt.2, John Wiley & Sons, ed. S. Shimada and H. Ishio, 1994.

Seikai, S., K. Kusunoki, and S. Shimokado, "Experimental studies on wavelength division bidirectional optical amplifiers using an Er^{3+}-doped fiber", J. Lightwave Technol. 12 (1994) 849.

Smart, R.G., J.L. Zyakind, J.W. Sulhoff, and D.J. DiGiovanni, "Dependence of performance of saturation in-line erbium-doped fiber amplifiers on pump wavelength around 1480 nm", OFC'93, San Jose, CA, OSA Technical Digest Series, ThF5.

Snitzer, E., Phys. Rev. Lett., 7 (1961) 444.

Srivastava, A.K., J.L. Zkskind, J.W. Sulhoff, J.D. Evankow, Jr., M.A. Mills, "Room temperature spectral hole-burning in erbium-doped fiber amplifiers", OFC'96, San Jose, California, TuG7, p.33, OSA Technical Digest Series.

Srivastava, A.K., Y. Sun, J.L. Zyskind, J.W. Sulhoff, C. Wolf, and R.W. Tkach, "Fast gain control in an Erbium-doped fiber amplifier", Optical amplifiers and their application, Monterey, CA, PDP4, 1996.

Sun, Y., G. Luo, J.L. Zyskind, A.A.M. Saleh, A.K. Srivastava and J.W. Sulhoff, "Model for gain dynamics in erbium-doped fiber amplifiers", Electron. Lett., 32, 1490 (1996).

Sun, Y., G. Luo, J.L. Zyskind, A.A.M. Saleh, A.K. Srivastava and J.W. Sulhoff, "Modeling of gain dynamics in erbium-doped fiber amplifiers", LEOS'96, Boston, MA, ThM3, P.365.

Tellert, T., F. Di. Pasquale, and M. Federighi, "Theoretical analysis of the dynamic behavior of highly-efficient erbium/ytterbium codoped fiber lasers", IEEE photon. Technol. Lett., 8, 1462 (1996).

Waldhauer, F.D., "Feedback", John Wiley & Sons, 1982.

Wood, T.H., A.K. Srivastava, J.L. Zyskind, J.W. Sulhoff and C. W OFC'97, Dallas, Texas, OSA Technical Digest Series, 6 (1997) 320, ThP2.

Wysocki, P.F., R.E. Tench, M. Andrejco, D. DiGiovanni, and I. Jayawardene, "Options for gain-flattened erbium-doped fiber amplifiers", OFC'97, Dallas, Texas, OSA Technical Digest Series, 6(1997) 127, WF2.

Yariv, A., "Quantum Electronics", 3rd Edition, Wiley, 1988, P.181.

Yamada, M., M. Shimizu, T. Kanamori, Y. Ohishi, Y. Terunuma, et. al., "Low-noise and high-power Pr^{3+}-doped fluoride fiber amplifier", IEEE PTL, 7, 869 (1995).

Yamada, M., H. Ono, T. Kanamori, T. Sakamoto, Y. Ohishi, and S. Sudo, "A low-noise and gain-flattened amplifier composed of a silica-based and a fluoride-based Er^{3+}-doped fiber amplifier in a cascade configuration", IEEE PTL, 8, 620 (1996).

Yamada, M., T. Kanamori, Y. Terunuma, K. Oikawa, M. Shimizu, S. Sudo, and K. Sagawa, "Fluoride-based erbium-doped fiber amplifier with inherently flat gain spectrum", IEEE PTL, 8, 882 (1996).

Yu, A. and M.J. O'Mahony, "Properties of gain controlled erbium doped fibre amplifiers by lasing", Electron. Lett., 1995, 31, p.1348; "Modelling of laser-controlled

erbium-doped fiber amplifiers", OFC'96, San Jose, OSA Technical Digest, WK14, p.163.

Zervas, M.N. and R. Laming, "Performance limits of erbium-doped fibre amplifiers due to internal rayleigh back-scattering", OFC'93, San Jose, CA, OSA Technical Digest Series, ThF1.

Zirngibl, M., "Gain control in Erbium-Doped Fibre Amplifiers by an all-optical feedback loop", Electron. Lett., 1991, 27, p.560.

Zyskind, John, "Performance issues in optically amplified systems and networks", OFC'97, Dallas, Texas, 1997 OSA Technical Digest Series,TuP1.

Zkskind, J.L., A.K. Srivastava, Y. Sun, et al., "Fast link control protection for surviving channels in multiwavelength optical networks", ECOC'96, Oslo, Postdeadline paper.

Zyskind, John, "Optical amplifiers for optical networking", 2nd international workshop on optical networking, March 1, 1996, SanJose, CA, USA.

Zyskind, J.L., E. Desurvire, J.W. Sulhoff and D. DiGiovanni, "Determination of homogeneous linewidth by spectral gain hole-burning in an erbium-doped fiber amplifier with GeO_2-SiO_2 core", IEEE Photonics Technol. Lett., 2(1990) 869.

Zyskind, J.L., "Advances in Erbium-doped fiber amplifiers for optical communications", in: M.J. Digonnet (Ed.) *Fiber Laser Sources and Amplifiers II*, SPIE Proceedings, No. 1373, Bellingham, WA: SPIE, pp. 80-92.

Zyskind, J.L. and J.W. Sulhoff, "Length dependence of saturation power in erbium-doped fiber amplifiers", in Proc. SPIE, Boston, MA, 1581 (1991) 251.

Zyskind, J.L., Y. Sun, A.K. Srivastava, J.W. Sulhoff, A.J. Lucero, C. Wolf and R.W. Tkach, "Fast power transients in optically amplified multiwavelength optical networks", OFC'96, San Jose, CA, OSA Technical Digest Series, Postdeadline paper PD31.

Zyskind, J.L., E. Desurvire, J.W. Sulhoff, and D.J. DiGiovanni, "Determination of homogeneous linewidth by spectral gain hole burning in an Erbium-Doped Fibre Amplifier with GeO2:SiO2 core", IEEE, Photon. Technol. Lett., 1990, 2, P.869.

Zyskind, J.L., "Performance issues in optically amplified systems and networks", OFC'97, Dallas, Texas, OSA Technical Digest Series, 6 (1997) 81, TuP1.